ISSN 0366-5542
CODEN : CCHHAQ

REPORT No. 277
GEOLOGICAL SURVEY OF JAPAN

HIGH-TEMPERATURE ACID FLUIDS AND ASSOCIATED ALTERATION AND MINERALIZATION

Extended Abstracts of the 3rd Symposium on Deep-crust Fluids "High-temperature Acid Fluids and Associated Alteration and Mineralization", held at Tsukuba, October, 1990.

Edited by

Yukihiro MATSUHISA, Masahiro AOKI and Jeffrey W. HEDENQUIST

GEOLOGICAL SURVEY OF JAPAN

Higashi 1-1-3, Tsukuba-shi, Ibaraki-ken, 305 Japan

1991

REPORT No. 277
GEOLOGICAL SURVEY OF JAPAN

Katsuro OGAWA, Director

HIGH-TEMPERATURE ACID FLUIDS AND ASSOCIATED ALTERATION AND MINERALIZATION

Extended Abstracts of the 3rd Symposium on Deep-crust Fluids "High-temperature Acid Fluids and Associated Alteration and Mineralization", held at Tsukuba, October, 1990.

Edited by

Yukihiro MATSUHISA, Masahiro AOKI and Jeffrey W. HEDENQUIST

November 1991
Geological Survey of Japan

CONTENTS

Preface

Over the last several years, gold-copper mineralization associated with acid alteration and acid-leached residual silica in volcanic rocks has become a topic of interest, both for exploration geologists and researchers alike, throughout the Circum Pacific. In addition to their academic interest, some deposits of this style are known to contain up to 150 t Au. These ore deposits are commonly referred to as Nansatsu type (after the district in southern Kyushu), acid-sulfate type (after the chemistry of the fluids inferred to be responsible for the leaching), kaolinite-alunite type (after the common alteration minerals which develop in the halo to mineralization), or high sulfidation type (which refers to the fluid having a high sulfur oxidation state, an intrinsic characteristic of the acid fluids responsible for alteration and mineralization).

A genetic model for this style of mineralization is evolving in which highly acid and oxidizing fluids exsolved from a magma (probably intruded to shallow levels) are of critical importance in the formation of the high sulfidation deposits. These fluids become highly reactive in the near-surface environment due to the dissociation of magmatic HCl and HF (at temperatures less than about 350°C); furthermore, magmatic SO_2 disproportionates to H_2SO_4 and H_2S in the presence of water at about 300°C, with the sulfuric acid then dissociating and also contributing to the reactive nature of the fluid. The highly acid nature of these fluids ($pH < 2$), which often discharge around volcanoes, accounts for the rocks which have been leached of all components, including Fe and Al, leaving only a residue of silica; the alteration haloes of kaolinite, alunite, diaspore and pyrophyllite are simply the reaction zones between the most acid fluid and fresh wallrock. In many cases, the gold and associated minerals appear have been deposited slightly later than leaching, suggesting an evolution of the fluid to a situation where metals can be precipitated rather than only rocks being leached; the actual precipitating mechanism is still not well understood, in contrast to the low sulfidation epithermal deposits where geothermal studies have identified boiling as the principal cause of high grade gold mineralization. The few stable isotope and fluid inclusion studies from high sulfidation deposits indicate that at some time a meteoric water of low salinity was involved, raising the question of whether there was a magmatic to meteoric evolution in systems that have been mineralized. In addition, the source of the metals is not clear, though the obvious association with magmatic fluids at some stage in the history of the system tempts one to invoke a magmatic contribution.

These and other questions concerning the high sulfidation environment and related alteration and mineralization were the subject of a two day symposium, held at the Geological Survey of Japan, Tsukuba, on 15 and 16 October, 1990. This symposium was the third annual meeting in the series on Deep-crust Fluids, partially sponsored by the Tsukuba Expo 85 Fund. Our goal in this symposium was not necessarily to provide answers, but to ensure that we are asking the right questions; we hoped that by bringing together people of many different interests and fields of study, we would be able to integrate the several disciplines necessary to better understand the geochemically complex environment of high sulfidation mineralization.

Geological and geochemical case studies on the high sulfidation style of mineralization in North America and the western Pacific were presented, with occurrence models discussed. Following the ore deposit coverage of the first day, studies of acid

fluids and related alteration in active geothermal and volcanic systems in Japan, the Philippines and Iceland were presented, as well as the results of related experimental study. During the closing session, we discussed the interaction between shallow magmatic fluids, meteoric waters and their host rocks, and examined the relationship of this interaction to mineralization in the proximal volcanic environment. The interaction of a magmatic fluid, probably degassed from a shallow intrusive, with meteoric water was identified to be of critical importance in understanding how these systems develop, and eventually lead to mineralization. Careful mineralogic and isotopic study, particularly using alunite and clays, is one avenue of further research to clarify the hydrothermal evolution in this environment. Other areas of study include magmatic contamination of geothermal systems (particularly those in the Philippines and Japan), and further examination of the chemical and isotopic composition of high temperature discharge of volcanoes of varying composition and stages of degassing. In the latter environment, study of acid hot springs around a degassing volcano, particularly their metal contents, will improve our understanding of the reactions taking place between a condensed magmatic fluid and host rock, its interaction with meteoric waters, and the conditions favoring mineralization.

Yukihiro Matsuhisa
Masahiro Aoki
Jeffrey W. Hedenquist

Opening Remarks: Necessity of Ore Deposit Research for Mineral Exploration

Shunso ISHIHARA*

Director General, Geological Survey of Japan
Higashi 1-1-3, Tsukuba, Ibaraki, 305 Japan

The discovery of ore deposits and the development of mining industry in Japan are becoming more difficult than ever before, as the targets of mineral exploration are progressively located deeper in the earth's crust. We need a more complete understanding of the interaction between magma and fluids, and between fluids and the wall rocks, to improve our ability to disc over new deposits.

The Japanese islands are richer in metallic mineralization than most people think. The metals produced per kilometer of volcanic front are of the same order as in the Philippines and Chile (Table 1). That is, the Japanese islands are not poor in metallic resources, but rather have had an excessive consumption in recent years. Most Japanese production is mined from 3 types of ore deposits, Kuroko and Besshi type massive sulfides, veins and skarns.

If we look back on the discovery history of completely blind ore deposits in Japan, most are of the Kuroko type (Table 2). Uchinotai West orebody of Kosaka mining area was the first blind deposit discovered, in 1959, under 20-50 m of volcano-clastic sediments from the Quaternery Towada volcano. The first "real" blind orebody discovered in a deep formation was the Shakanai No. 1 orebody, in 1962 (Otagaki, 1966). Follow-up exploration in the same area resulted in the discovery of Shakanai Nos. 2-11 orebodies and the Matsumine ore deposit. These discoveries occurred just after the establishment of a new understanding of Kuroko genesis, based on the syngenetic theory of Horikoshi (1960) and others, in contrast to the epigenetic view which previously prevailed.

The discovery of the Fukazawa deposit (Tanimura *et al.*, 1972) was also epoch-making, because it was the first ore deposit discovered not along the margin but in the center of the Hokuroku basin, and led to the discovery of the Ezuri deposit.

Table 1 Ore metals produced per kilometer of magmatic front (Ishihara, 1980, unpublished data).

Arc	Cu (t)	Pb (t)	Zn (t)	Sn (t)	W (t)
Chile	30,000	none	trace	none	trace
Philippines	15,000	130	270	none	none
Northeast Japan (Neogene)	3,400	2,100	6,600	trace	none
Sumatra-Java	some	trace	some	trace	none
Outer Zone, SW Japan (Miocene)	170	10	30	50	21*

* Late Cretaceous Sanyo Province, SW Japan.

* Presently, Director General of Agency of Industrial Science and Technology.
Keywords : blind ore deposit, Kuroko type deposit, epithermal gold deposit, Hishikari gold deposit

Table 2 Major discovery of blind ore deposits in Japan. Most are Kuroko type which were found after proposal of the new syngenetic theory.

Year	Kuroko Deposits	Vein-type Deposits	Skarn Deposits
1959	Uchinotai (including Uwamuki), 12×10^6 t (0.8 g/t Au, 93 g/t Ag, 1.84% Cu, 1.78% Pb, 4.93% Zn, 17.5% Py-S)[*1] 20–50 m below surface		
·····	Horikoshi's (1960) syngenetic theory ·····		
1962	Shakanai, 7×10^6 t (0.6 g/t Au, 66 g/t Ag, 2.18% Cu, 1.44% Pb, 4.46% Zn)[*3] 170–600 m below surface		
1963	Matsumine, 11×10^6 t (0.6 g/t Au, 54 g/t Ag, 2.52% Cu, 0.84% Pb, 2.94% Zn)[*1] 180–360 m below surface		
1969	Fukazawa, 5×10^6 t (0.6 g/t Au, 107 g/t Ag,1.2% Cu, 3.2% Pb, 12.0% Zn, 7.1 % Py-S, 10.6% $BaSO_4$)[*2] 340–410 m below surface		
1976	Ezuri, 3×10^6 t (1.2 g/t Au, 180 g/t Ag, 0.89 % Cu, 3.32%Pb, 10.1% Zn)[*2] 270–350 m below surface		
1981		Hishikari, 250 t Au 140–180 m below surface	
1984	Nurukawa, 1×10^6 t[*2] Au-Ag-rich Kuroko deposits (200×10^3 t, 5.7 g/t Au, 123 g/t Ag, 0.70% Cu, 3.76% Pb, 7.11% Zn[*1]) 100–300 m below surface		
1990s	····· We need a break-through idea here for vein and skarn type deposits ·····		

[*1] Production up to 1990 given by Dowa Mining Co. Ltd.
[*2] From Dowa Mining Co. Ltd. (1981, 1990) and Ishihara (1989).
[*3] Tonnage and ore grade are from Nippon Mining Group (1981).

These great successes in the exploration for Kuroko deposits were very much dependent upon the progress in genetic studies, as well as in exploration techniques.

Among the other types of ore deposits, the discovery of the Hishikari Au-Ag quartz vein deposit in March, 1981, is noteworthy in the past decade. The discovery was made possible after an epithermal gold vein model for Hokusatsu (northern Kagoshima)-type mineralization was established. Besides this model, gravity anomalies indicating "basement relief", electromagnetic anomalies implying argillized zones, and high-grade assay values in minor mineralized fractures were all considered important keys (Sato, 1991).

Exploration for epithermal gold deposits, after all, has an advantage in that the deposits are formed at high levels. Other meso- and hypothermal vein and skarn deposits are generally formed much deeper than the epithermal veins; however, natural erosion often brings these deep deposits closer to the surface. In addition, we have many data available on granitoids, host rocks, etc. In the Chugoku district,

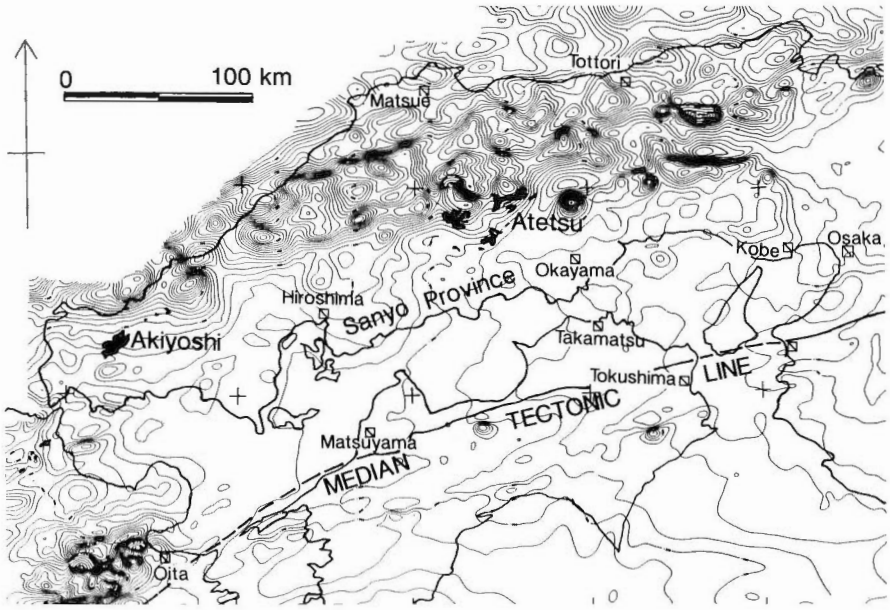

Fig. 1. Residual magnetic intensity of the Chugoku district (after Okubo *et al.*, 1985) and major limestone masses (solid areas). The intensity here generally reflects the distribution of magnetite-series relatively magnetic and ilmenite-series granitoids, because there is no overlapping of younger magnetic bodies in the district. Major limestone masses are located in the northern part of the Sanyo province in general. However, limestones of the Atetsu Plateau are intruded by magnetite-series granitoids, and are thus favorable sites for skarn-type mineralization.

e.g., magnetite-series granitoids (which have a higher potential than ilmenite-series granitoids to be related to the formation of sulfide deposits) intrude into many limestone masses at Atetsu Plateau, Okayama Prefecture (Fig. 1), and many ore deposits may be still hidden in the region.

Alteration is a key to mineralization. I would hope that this small, highly specialized meeting will deepen our understanding on the processes of fluid-rock interaction, not only of the acid fluid type but also other types of alteration and mineralization, which will give us clues for new exploration strategies to discover blind ore deposits of vein, skarn and even porphyry types.

Acknowledgements : Jeff Hedenquist of GSJ kindly reviewed this manuscript.

References

Dowa Mining Co. Ltd. (1981) Exploration history of ore deposits. *Exploration of Ore Deposits in Japan.* Soc. Mining Geol. Japan. vol. 1, p. 113-169,

Horikoshi, E. (1960) The stratigraphic horizon of the "Kuroko" deposits in Hanaoka-Kosaka area, Green Tuff district of Japan. *Mining Geol.*, vol. 10, p. 300-310.

Ishihara, S., editor (1989) Kuroko deposits and geothermal fields in northern Honshu. Guidebook 3, *Soc. Mining Geol. Japan,* 59 p.

Nippon Mining Group (1981) On the exploration of Kuroko mine. *Exploration of Ore Deposits in Japan.* Soc. Mining Geol. Japan. vol. 1, p. 171-218.

Okubo, T., Tsu, H., Horikawa, Y., Ogawa, K. and Takagi, S. (1985) Aeromagnetic map of Japan. *Chishitsu News,* no. 374, p. 48-57.

Otagaki, T. (1966) Development of prospecting at the Shakanai mine. *Mining Geol.*, vol. 16, p. 237–240.

Sato, T. (1991) Discovery history of the Hishikari gold deposits. *J. Geography, Centennial Issue*, vol. 100, p. 132.

Tanimura, S., Shimoda, T. and Sawaguchi, T. (1972) On the Fukazawa black ore-type deposits in the Hokuroku district.—A history of its discovery and geologic setting. *Mining Geol.*, vol. 22, p. 108–120.

Acid-Sulfate Alteration and Vein Alunite Formation in Volcanic Terrains : Stable Isotope Systematics

Robert O. RYE[1] and Philip M. BETHKE[2]

1) *Branch of Isotope Geology, U.S. Geological Survey, Denver, CO U.S.A*
2) *Branch of Resource Analysis, U.S. Geological Survey, Reston, VA U.S.A.*

Introduction

Acid-sulfate alteration characterized by the assemblage alunite + kaolinite + quartz ± pyrite ± pyrophyllite ± diaspore develops in two distinct hydrothermal environments in volcanic terrains, and vein alunite, having only minor argillic alteration selvages, forms by vapor transport in a third environment. In addition, acid-sulfate alteration is a common product of supergene weathering of sulfide-rich rocks. Stable isotope analyses of $\delta^{34}S$ and $\delta^{18}O$ in the sulfate site and δD and $\delta^{18}O$ in the OH site in alunite, in conjunction with similar analyses of coexisting minerals, particularly sulfide and kaolinite group minerals, provide useful criteria for distinguishing between the different origins. Of greater importance, such analyses can provide much useful information on the thermal, hydrologic, and chemical evolution of hydrothermal systems.

Environments of Acid-Sulfate Alteration and Alunite Formation

In *Magmatic-hydrothermal* environments, the requisite amount of sulfuric acid to produce acid-sulfate alteration is formed from the disproportionation of magmatic SO_2 to H_2S and H_2SO_4. In the shallow, epithermal environment disproportionation appears to occur in a magmatic vapor plume, and acid-sulfate alteration commences as the vapor plume condenses.

In *Steam-heated* enviromments, such as the surficial parts of many active geothermal systems, the requisite sulfuric acid is produced by the oxidation, at and above the water table, of H_2S distilled off an underlying, near-neutral hydrothermal system. Such steam-heated environments may occur over Adularia-Sericite type base- and precious-metal ore-depositing systems, such as those as that at Cactus, California and Buckskin, Nevada.

In *Magmatic steam* environments, vein-filling alunite is deposited directly from an SO_2-dominated (with respect to sulfur species) vapor phase. Such an oxidized vapor phase may result from the release of a high-temperature magmatic vapor at low pressures, or from the oxidation of a more reduced vapor by entrained atmospheric oxygen in the carapace of a volcanic edifice.

Supergene acid-sulfate alteration is important to the subject of this symposium only in that it may be mistaken for that produced by the above mechanisms. Its stable isotopic characteristics, determined by the low-temperature, surficial oxidation of pre-exisiting sulfide minerals, serve to make the distinction. Although not germane to the theme of this conference, the stable isotope systematics of supergene alunite are very interesting, and may provide powerful insights into the hydrogeochemical environment of supergene oxidation.

Keywords : Acid-sulfate alteration, alunite, stable isotopes, magmatic hydrothermal, steam-heated, magmatic steam, supergene

Principles of Stable Isotope Geochemistry of Alunite and Acid-Sulfate Alteration

Alunite contains four stable isotope sites, more than any other common mineral except the crystallographically similar jarosite. Kinetic factors governing the rate of isotopic exchange between each of the four stable isotope sites in alunite (δD, $\delta^{18}O_{SO4}$, $\delta^{18}O_{OH}$, and $\delta^{34}S$) and fluid play the determining role in the stable isotope systematics of alunite and acid-sulfate alteration. To a very large extent they form the isotopic basis for distinguishing between environments of acid-sulfate alteration, and they provide important insights into attendant processes. Exchange rates for sulfur isotopes between aqueous sulfur species and for oxygen isosopes between sulfate and H_2O are kinetically inhibited but reach a maximum for a given temperature at the low pH of alunite formation. Sulfur and oxygen isotopic equilibrium between sulfate and fluids is probably readily obtained in most magmatic-hydrothermal environments, and at least oxygen isotopic equilibrium is obtained in most steam-heated environments. However, complete kinetic control of isotopic compositions is likely for sulfate in the supergene environment. Hydrogen and oxygen isotopic equilibrium for OH between alunite and fluids is likely in all environments during the precipitation of the mineral.

Most low- to moderate-temperature hydrothermal minerals retain their stable isotopic compositions after deposition unless they are recrystallized. Our data suggest that retrograde stable isotope exchange between alunite and later fluids does not normally occur except for the OH site. Recent experimental studies indicate that nearly complete D exchange between fine-grained alunite ($<$ 2-5 microns) and water will occur in less than 10^4 years at 25°C. Since hydrogen occurs in the OH site, post-depositional exchange probably modifies most original $\delta^{18}O_{OH}$ values in such alunite as well. However, because the fractionation between alunite and water is very small at all temperatures, significant changes in δD occur only if water with a different δD is involved. Alunite from supergene and some steam-heated environments, are typically very fine-grained, and current studies indicate that later isotope exchange may complicate the interpretation of data from some areas. Fine-grained steam-heated alunites from Rodalquilar, Spain have undergone post-depositional oxygen isotope exchange and yield K/Ar ages approximately 7 My too young, suggesting that argon loss may also be a problem in fine-grained alunite. Our studies indicate that alunites from magmatic-hydrothermal systems are also subject to post-depositional exchange in the OH site even though their grain size may exceed 100 microns, but we have seen no evidence of such exchange in magmatic steam alunites whose grain size ranges from millimeters to centimeters.

Stable Isotope Systematics of the Magmatic-Hydrothermal Environment

Theoretical considerations and relatively detailed studies of magmatic-hydrothermal systems at Julcani, Peru; Summitville, Colorado, USA; Red Mountain near Lake City, Colorado, USA; and Rodalquilar, Spain, and two samples from El Salvador, Chile, indicate that initial stable isotope compositions of alunite and associated sulfide and kaolinite minerals reflect isotopic equilibrium. Values of $\delta^{34}S_{alunite}$ are large relative to coeval pyrite, supporting the conclusion that the sulfuric acid was produced by disproportionation of SO_2. Isotopic temperatures calculated from $\Delta^{34}S_{pyrite-alunite}$ range from 200-390°C, in agreement with available fluid inclusion homogenization temperature measurements. The $\delta^{34}S$ values of coexisting alunite-pyrite pairs reflect the H_2S/SO_2 ratio of the fluid. $\delta^{18}O_{SO4}$ and δD values of alunite indicate that the SO_2 was derived from a magma and that the

acid-sulfate altering fluids were dominated by magmatic water, but at some deposits, such as Summitville, variable amounts of mixing with exchanged meteoric water is evidenced. Variations in pyrite-alunite isotopic temperatures with depth at Summitville document a geothermal gradient, and suggest a transition from lithostatic to hydrostatic pressure regimes between 1 and 1.5 km below the paleosurface. In all deposits studied, $\Delta^{18}O_{quartz-alunite(SO4)}$ values approach equilibrium but are unsuitable for geothermometry because of the low temperature dependence of the fractionation. $\Delta^{18}O_{SO4-OH}$ values in alunite yield unreasonably high temperatures, probably because of retrograde exchange in the OH site. In all cases studied, the δD and $\delta^{18}O$ values of kaolinite formed during acid-sulfate alteration reflect mixing with exchanged meteoric waters and/or some retrograde exchange with such waters. In all deposits studied from areas having low δD meteoric waters, kaolinites associated with later Cu-Au-Ag ore formation have substantially lower δD values reflecting deposition from waters dominated by exchanged meteoric water.

Stable Isotope Systematics of the Steam-Heated Environment

Stable isotope data from Tolfa, Italy, and from the replacement alunite deposits at Marysvale, Utah show that the steam-heated environment is characterized by both equilibrium and kinetic stable isotope fractionation and that the stable isotope systematics vary from deposit to deposit. At Tolfa the $\delta^{34}S$ values for alunite are within range for pyrite and marcasite in the underlying volcanics indicating lack of significant sulfur isotope exchange between SO_4 and H_2S during oxidation of the H_2S. Temperatures calculated from $\Delta^{18}O_{OH-SO4}$ range from 80 to 180°C, and δC and $\delta^{18}O$ values of waters calculated using these temperatures lie close to the meteoric water line, indicating that oxygen in both the OH and SO_4 sites in alunite was close to isotopic equilibrium with the fluid. δD values of alunites and kaolinites from Tolfa overlap, and are consistent with values for local spring water. δD-$\delta^{18}O$ values for kaolinite are substantially removed from the kaolinite line as expected. Alunite from the replacement deposis at Marysvale, Utah yields $\delta^{34}S$ values that are much larger than those for pyrite in the underlying propylitic zone. It is probable, but not certain, that the source of sulfur was the same for both the pyrite and the alunite. If true, the sulfate must have undergone substantial sulfur isotope exchange with H_2S during or following oxidation of the H_2S, in contrast to the lack of exchange at Tolfa. Isotope temperatures calculated from $\Delta^{18}O_{OH-SO4}$ range from 90 to 160°C, but $\delta^{18}O_{H2O}$ values of fluids calculated using these temperatures indicate that the fluids underwent substantial isotopic exchange with wall rock. The stable isotope data suggest that the high-temperature residence time of the fluids at Marysvale may have been longer than that at Tolfa and/or that the Marysvale system was more rock dominated.

Stable Isotope Systematics of the Magmatic Steam Environment

Stable isotope studies on alunite from the type deposit of a magmatic steam system, the vein alunite deposits on Alunite Ridge near Marysvale, Utah, USA, are difficult to interpret completely. The alunite occurs as coarse crystals in wide, tight veins containing only trace amounts of quartz and hematite. Pyrite is not found. Fluid inclusions in the alunite are vapor filled. δD values are nearly constant and are substantially larger than those of alunites and kaolinites from nearby replacement alunites formed in a steam-heated environment, indicating a

large magmatic component in the fluids. $\delta^{18}O_{SO4}$ values are also tightly clustered and typical of magmatic sulfates. In contrast to alunites from the magmatic-hydrothermal environment, the $\delta^{34}S$ values are tightly clustered near 0 ‰, the same as the presumed value for bulk sulfur in fluids, believed to have been derived from an underlying stock. Sulfides from the nearby, and coeval, Deer Trail Mountain base-metal manto deposits, believed to have formed from fluids derived from the same stock, have $\delta^{34}S$ values near 0 ‰. These observations indicate that the vein alunite formed from a vapor phase dominated by magmatic fluids whose sulfur had been quantitatively oxidized. The veins occur deep enough in the system that oxidation by entrainment of atmospheric oxygen in the vapor can be ruled out, and the most probable interpretation is that the vapor was released from the magma at high temperature and low pressure where SO_2 was the dominant sulfur species. The $\delta^{18}O_{OH}$ values are reasonably consistent, but are too low by 3 to 4 ‰ to represent equilibrium with $\delta^{18}O_{SO4}$. The large grain size of the alunite and the tightness of the veins effectively rule out post-depositional exchange. It seems most likely that the $\delta^{18}O_{SO4}$ and $\delta^{34}S$ were fixed at a higher temperatue and preserved due to the rapid transport and deposition inferred for such an environment. However, much more detailed study of this and other similar systems and a better understanding of transport and precipitation mechanism of alunite in magmatic vapor are required to interpret the stable isotope data with confidence.

Relationships Between Environments

Although discussed above as end-member situations, the several environments can and do overlap in time and space in volcanic terrains. Thus, at Rodalquilar the steam-heated environment overprints the magmatic-hydrothermal environment; at Red Mountain near Lake City alunite formed in a magmatic-hydrothermal environment is cut by veins of magmatic-steam alunite; and at the Cactus gold mine, located in a volcanic dome field, steam-heated acid-sulfate alteration appears to be cut by magmatic-steam alunite veinlets. Magmatic-hydrothermal deposits frequently contain large amounts of sulfide minerals, particularly pyrite, and are, therefore, subject to acid-sulfate alteration resulting from supergene oxidation.

Conclusions

Stable isotope systematics provide useful criteria for distinguishing between the several acid-sulfate alteration, or alunite-forming environments, but, more importantly, they may also provide such useful process information as temperatures of precipitation, geothermal gradients, transition from lithostatic to hydrostatic gradients, fluid fluxes and residence times, degree of mixing of magmatic and meteoric water, degree of isotopic exchange with wall rock, isotopic composition and redox state of magmas and evolved fluids, and the thermal, hydrologic, and chemical evolution of the hydrothermal system. The common overprinting of the environments and the potential problems of post-depositional exchange require that application of stable isotope studies to alunite and acid-sulfate alteration be approached carefully through geologically well-controlled sampling. Although stable isotope data can be very powerful tools in the study of acid-sulfate alteration, their full value can only be obtained when applied in combination with careful geologic and mineralogic studies.

Geological Survey of Japan Report, No. 277, 1991, p. 9-20

High Sulfidation Epithermal Gold Deposits: Characteristics and a Model for Their Origin

Noel C. WHITE

BHP Minerals, PO Box 619 Hawthorn, Vic 3122, Australia

Introduction

It is now 83 years since the high sulfidation (or acid-sulfate, or alunite-kaolinite) deposits were first recognised as a distinct class of the epithermal precious metal deposits (Ransome, 1907). As knowledge of the characteristics and origin of low and high sulfidation deposits grows, so it becomes increasingly apparent that the two classes are distinctly different deposit types, rather than sub-types of one class of deposit (Table 1).

Table 1 Characteristics of low and high sulfidation deposits.

	Low Sulfidation	High Sulfidation
Form of Deposits	Open space veins dominate Disseminated mostly minor Replacement minor Vein breccias common	Veins mostly subordinate Disseminated common Replacement dominates Vein breccias uncommon
Ore Mineralogy	pyrite, sphalerite, galena, electrum, gold, realgar, orpiment, cinnabar, arsenopyrite, chalcopyrite, argentite, proustite, pyrargyrite.	pyrite, enargite, luzonite, covellite, chalcopyrite, galena, tetrahedrite-tennantite, sphalerite, gold, arsenopyrite.
Gangue Mineralogy	quartz, chalcedony, calcite, rhodochrosite, adularia, barite, clays.	quartz, clays, alunite, barite.
Common Textures	veins, cavity filling, banded textures, vein breccias, drusy cavities, colloform structures, lattice texture, comb, cockade, cockscomb textures.	wallrock replacement textures, drusy cavities, hydrothermal breccias, veins.
Minor Textures	wallrock replacement textures.	banded textures.
Dominant Chemistry	Ag, Au, As, Hg.	Cu, Ag, Au, As.
Minor Chemistry	Zn, Pb, Sb, Se.	Zn, Pb, Hg, Sb, Te, Sn, Mo, W.

Keywords : high sulfidation deposit, epithermal gold deposit, Nansatsu type deposit, El Indio type deposit, Temora type deposit, acid hydrothermal alteration, copper mineralization

The terms high and low sulfidation are favoured over the alternatives as they refer to the oxidation state of the parent fluids (Hedenquist, 1987), a fundamental characteristic that determines their behaviour and products (see White and Hedenquist, 1990, for discussion). High sulfidation deposits form from fluids with a

Table 2 Characteristics of high sulfidation deposit types.

	Nansatsu type	El Indio type	Temora type
Form of deposit	disseminated, local veins	veins	disseminated
Geometry of deposit	cone or irregular, flaring upwards	planar veins	large irregular shoots
Deformation	undeformed	undeformed	deformed or undeformed
Alteration	leached silica core, narrow clay-alunite margin, regional propylite	clay around veins, widespread sericitic	pyrophyllite-silica, sericite-silica, regional propylite
Gold in	silica core	veins sulfide-rich and sulfide-poor	pyrophyllite-silica zone
Gold grade	low, locally high	low and high	low, locally high
Sulfide mineralogy	pyrite>enargite>luzonite, minor covellite, chalcopyrite, tennantite-tetrahedrite, galena, arsenopyrite, cinnabar	enargite>luzonite>pyrite	pyrite>>enargite
Gangue mineralogy	quartz, alunite, barite, clays	quartz	quartz, pyrophyllite, sericite, alunite, barite
Age of deposits	Tertiary to Quaternary	Tertiary	Palaeozoic to Mesozoic
Examples	Akeshi, Iwato, Kasuga (Japan) Chinkuashih (Taiwan) La Coipa (Chile) Motomboto (Indonesia) Summitville (USA)	El Indio (Chile)	Temora, Peak Hill, Rhyolite Creek (Australia) various minor in Geongsang Basin (Korea) various minor (Japan) ? Pueblo Viejo (Dominica)

high oxidation state for their contained sulfur.

The aim of this paper is to focus on some characteristics of high sulfidation epithermal deposits which I believe are giving important clues to their origin, and to offer an empirical model which goes some way to explaining these features. I have been privileged to visit many high sulfidation deposits in the circum-Pacific region, and what follows arises mostly from my observations.

Types of High Sulfidation Deposits

As with every other class of ore deposit there is considerable variation between different deposits of the high sulfidation class. Table 2 classifies high sulfidation deposits into three sub-types named for their best-known example. The classification is based on deposit form and alteration mineralogy and zoning. It is believed these three types reflect differences in the depth and pressure of formation as well as the hydrology of the systems involved.

Most known high sulfidation deposits are of the Nansatsu type, named after the deposits in the Nansatsu district of southern Kyushu, Japan, and this type is the best understood (Urashima *et al.*, 1987; Hedenquist *et al.*, 1988). Their distinguishing feature is the vuggy and in some cases partly massive silica core, with a narrow zone of clay alteration enveloping it on the margins, expanding above (Figure 1). The overlying clay is commonly not preserved ; one of the most completely preserved examples is La Coipa in Chile, where the extensive clay alteration overlying the orebodies is preserved by a post-ore andesite. In Nansatsu type deposits the gold is found irregularly disseminated in the silica core. Depth of formation appears to be shallow (top of the silica zone at 200-300 m), and they may have vertical extents of

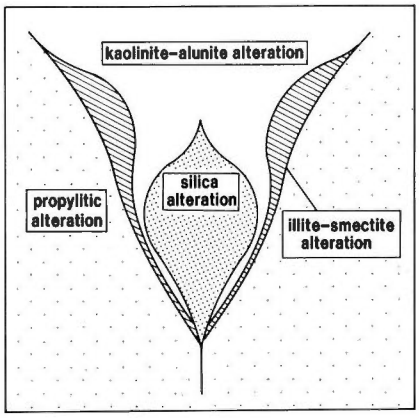

Fig. 1. Idealised alteration patterns for a Nansatsu type high sulfidation deposit. The central silica alteration zone consists of both leached vuggy silica and more massive silicified rock. Pyrite, kaolinite, alunite and barite commonly also occur in this zone, which typically has knife-sharp contacts with the kaolinite-alunite zone. This grades into the illite-smectite zone, which grades into the propylitic zone. Ore occurs in the silica zone only. The top of the silica zone was probably formed about 200-300 m below the surface; its vertical extent can be up to 1000 m. The shape of zones is typically distorted by variations in permeability of the host rocks, and they are commonly cut by hydrothermal eruption breccias (Izawa and Cunningham, 1989). The overall shape of the alteration body may be conical or wedge-shaped, expanding upwards.

up to 1000 m. Nansatsu type deposits may have associated with them massive sulfide veins (pyrite–enargite–luzonite), which are also characteristic of the El Indio type, suggesting some overlap in characteristics.

The El Indio type is characterised by occurrence as veins within a pervasive clay and sericitic alteration zone. The El Indio deposit in Chile (Walthier *et al.*, 1985; Siddeley and Araneda, 1986; Jannas *et al.*, 1990) has two types of veins (massive sulfide and silica); the richest gold grades are associated with the silica veins which have characteristics more consistent with (or tending towards) a low sulfidation origin.

The Temora type is named after the mine at Temora, Australia (Thompson *et al.*, 1986). It is characterised by disseminated mineralization within an envelope of pyrophyllite–sericite–silica alteration. The best known examples are preserved in ancient deformed volcanic sequences (e.g. Temora: Thompson *et al.*, 1986; Peak Hill: Cordery, 1986; Harbon, 1988; Rhyolite Creek: Raetz and Parrington, 1988 a, b), but minor undeformed deposits of otherwise similar character are known in the Cretaceous of Korea (M.E. Park, pers. commun., 1987) and Japan (Utada, 1980). The possibility of interpreting these deposits as buried deformed Nansatsu type deposits is excluded by the difference in alteration mineralogy and zoning, and the location of the gold (Table 2). It is suggested that their characteristics are best explained by formation at substantial depths (>1.5 km) at temperatures around 300°C. The silica–rich rocks found in these deposits may have formed from silica released during pyrophyllite and sericite alteration, and so do not require any major introduction or removal of silica.

Characteristics of High Sulfidation Deposits

General characteristics of high sulfidation deposits are noted in Tables 1 and 2; some specific characteristics which are thought to have a bearing on the origin of the deposits are discussed here.

Associated Hydrothermal Alteration

High sulfidation deposits are typically associated with major zones of intense acid hydrothermal alteration which grades out into less acid alteration styles. Clearly, neutralisation of an acid fluid by wall rock reactions is characteristic. In the Nansatsu type deposits there is a very narrow (typically 1–3 metres) alteration zone between acid leached silica zones and regionally propylitically altered host rocks. This narrow zone consists of kaolinite–alunite–(pyrophyllite–diaspore) close to the silica zone, and grades out to illite–smectite assemblages (Urashima *et al.*, 1987; Heald *et al.*, 1987). This sharp gradient in hydrothermal alteration implies a sharp gradient in fluid chemistry and possibly temperature.

Zones of hydrothermal alteration typically show strong structural control, especially by faults, but any other structures may also be important to provide secondary permeability (Huang, 1963). Primary permeability controls are very important, with alteration diverted along permeable units, or units which were highly reactive to the hydrothermal fluids. The gross cross–sectional shape of the alteration zones associated with Nansatsu type deposits is commonly funnel shaped, flaring upwards (Figure 1).

Distribution of Mineralization

From a large amount of data I have collected to characterise the geochemistry of high sulfidation deposits it is clear that there is a pronounced association of gold with copper in ore zones, a variably weak to strong association with lead and no

association with zinc, which is commonly depleted in ore zones (cf. low sulfidation deposits). At the Penshan orebody at Chinkuashih, Taiwan, metal zoning is from a central zone of copper with subordinate gold, laterally and vertically to a zone of gold with subordinate copper (Huang, 1963; Sakazaki *et al.*, 1964 a, b).

In high sulfidation deposits gold (and copper) is found only in zones of acid alteration (cf. low sulfidation deposits). In Nansatsu type deposits gold occurs within silica alteration only. Gold can occupy limited zones within the silica alteration, or may occupy the whole zone, or be absent (Figure 2). The gold is typically associated with sulfide minerals and quartz, kaolinite, alunite, and barite, which can also occur outside the gold mineralized zones.

The association between gold mineralisation and the most acid hydrothermal alteration is so strong that it seems clear that they are closely related. But the

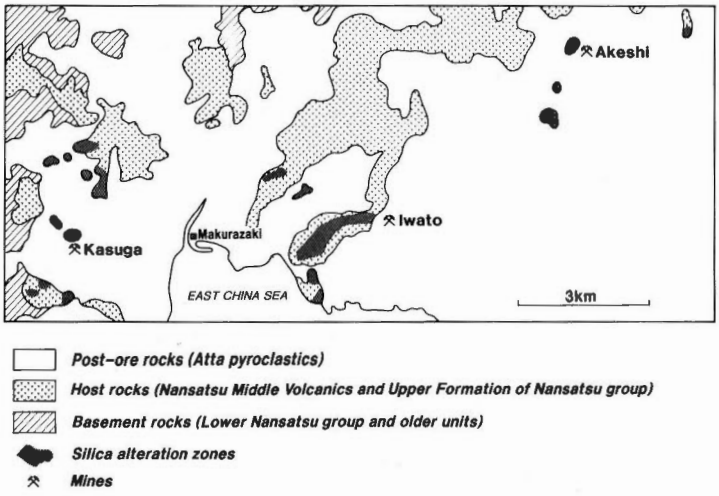

Fig. 2-A. Zones of silica alteration in the Nansatsu district, Japan. Note the widespread occurrence of silica alteration. The ore deposits make up only a small part of these zones.

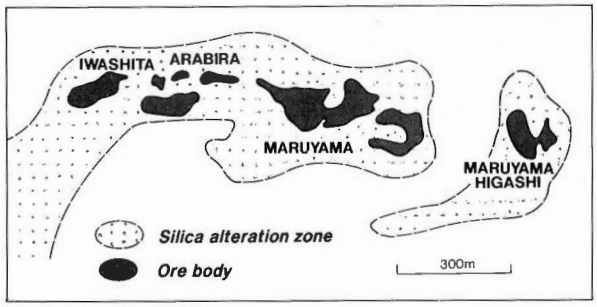

Fig. 2-B. Detail showing the distribution of ore bodies within the silica alteration at the Iwato Mine, which from Figure 2 A can be seen to occur at the end of a very extensive belt of silica alteration. Non-ore silica typically contains >0.2 g/t Au (Urashima *et al.*, 1987). Figure redrawn from Urashima *et al.*, 1987.

relation is not simple; Au (with or without Cu) mineralisation typically occupies only part of the acid alteration zone, though it may occupy all, and it may be completely absent (e.g. Iwato, see Figure 2). This suggests that the metals are related to the fluids that produced the acid alteration, but are not necessarily in the same fluids. The main base metal association with gold is copper, in striking contrast to the low sulfidation deposits, which typically contain mostly zinc and lead, and little copper. This suggests formation by fluids which were higher temperature, more saline and more acid than is typical for low sulfidation deposits. The critical observation though, is that the strong and persistent association between Cu and Au is indicative that they were introduced in the same fluid. Copper and gold are readily transported together in high temperature, saline, oxidised acid fluids (Large *et al.*, 1988). They are not readily transported together in the fluids that are characteristic of low sulfidation systems, i.e. moderate to low temperature, reduced, neutral pH, and low salinity.

The features of different Nansatsu type deposits are strikingly similar wherever they occur, and it seems inescapable that the fluids that caused the intense acid alteration and the fluids that introduced the metals, while not necessarily the same, must have been very closely related in origin, time, and space. In the following section an attempt will be made to explain how this might happen.

Genetic Models

Although a few high sulfidation deposits show some overlap in characteristics with deposits of low sulfidation type, most show no typical low sulfidation features, and the vast majority of low sulfidation deposits show no high sulfidation characteristics. Notwithstanding this, recent studies (e.g. Stoffregen, 1987; Berger and Henley, 1990) have explained the precious metal mineralization in high sulfidation deposits as having been introduced by later incursion of low sulfidation geothermal fluids into previously formed high sulfidation alteration zones of magmatic origin. In this model the acid alteration (vuggy silica, etc.) is regarded as forming from wall rock neutralisation of acid magmatic volatiles. Low sulfidation geothermal fluids are interpreted to have invaded the previously-formed acid alteration, and introduced metals which deposited in response to the pH changes consequent on reaction with the acid alteration products (Berger and Henley, 1990). If this were true we should expect to see gold concentrated in the zone of sharp pH change, i.e., outside the margins of the silica zone; we do not. We would also not expect to see the marked gold-copper association. This model requires the coincidence of two distinctly different styles of mineralization, and does not explain the metal associations, the restriction of gold to acid alteration zones, its distribution within the acid alteration zones, and the general absence of the minerals and textures which typify low sulfidation deposits.

An alternative model presented here aims to show that the observed characteristics of high sulfidation deposits all result from one system responsible for producing the extensive advanced argillic alteration and the metalliferous mineralization that may occur within it. What follows is described as it applies to Nansatsu type deposits; similar processes also apply to the other types of high sulfidation deposits.

Genetic Model for High Sulfidation Deposits

It has been widely accepted that the fluids responsible for the alteration systems associated with high sulfidation deposits resemble those inferred to be responsible for

porphyry copper deposits. The behaviour of such fluids has been modelled by Henley and McNabb (1978), and Fournier (1987). To understand the behaviour of these fluids in a high sulfidation environment we must consider the different setting. Henley and McNabb (1978) modelled the release of magmatic fluids into an essentially homogeneous environment (an intensely fractured carapace of a porphyry intrusion). While this is appropriate to understand porphyry copper deposits, it is not relevant to high sulfidation deposits which regionally and locally show strong structural control. It is believed that porphyry copper deposits form when fluid overpressuring causes explosive rupturing of the carapace of the largely crystallised intrusion, and fluids are released into the resulting mesh-fractured volume of rock. By contrast, high sulfidation deposits are thought to result from episodic

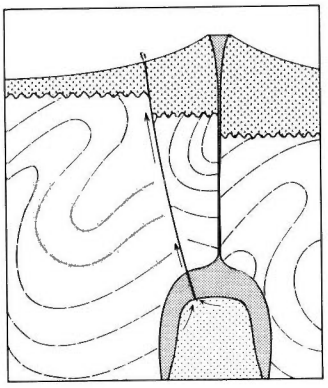

Fig. 3a. A saline hydrous magmatic fluid accumulates in a subvolcanic magma chamber. Faulting causes violent rupturing of the carapace, and releases the magmatic fluids into a localised fracture. Because the fluids are confined to the fracture they may travel for a considerable distance to be vented at the surface, or they may mix with groundwater along their path.

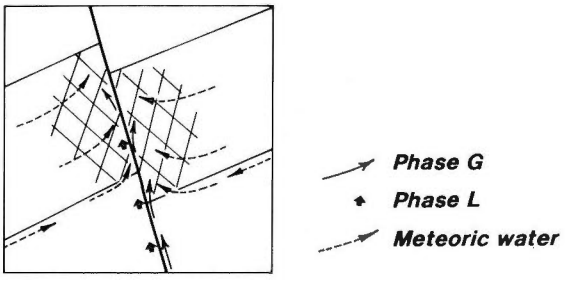

Fig. 3b. When a zone of increased permeability is reached (e.g. where there is a major fracture zone), the magmatic fluids may mix with groundwater. Dissociation of the acid magmatic gasses produces an extremely corrosive fluid that reacts strongly with the wall rocks, thus enhancing permeability, and encouraging the influx of more groundwater. An upwardly expanding alteration zone strongly controlled by host rock permeability results.

fracturing by faulting of the carapace of the crystallising porphyry magma chamber, and the release of the fluids up a confined fracture.

The proposed model is illustrated by Figure 3 (a-d), and explained below:

1. A saline hydrous magmatic fluid accumulates in a sub-volcanic magma chamber at depths of 2-6? km. At the prevailing pressures and temperatures the wall rocks adjacent to the intrusion will be plastic, and so will not form conduits for fluids without some form of violent rupturing, and then they will be short-lived.

2. Episodic fracturing releases the magmatic fluids into a localised fracture. The fluids are confined to the fracture, and as it is the most permeable path (at least at depth), there may be a considerable path length along which the fluids flow. The fluids may flow through to be vented at the surface, or may mix with groundwater (Figure 3a).

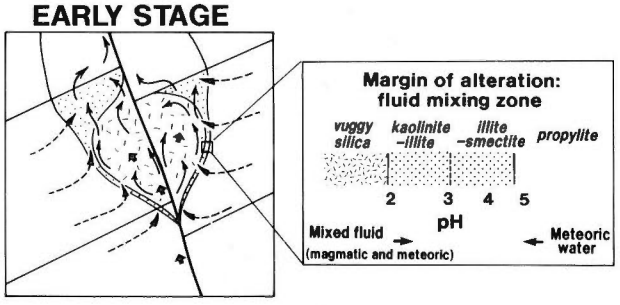

Fig. 3ci. Interaction of the acid mixed magmatic-meteoric fluid with wall rocks produces an upward-expanding zone of alteration. The central part is leached vuggy silica produced by fluids with pH about 2 or less (Stoffregen, 1987). Adjacent to this is a localised zone of intense fluid mixing in which the pH drops from >5 to about 2, typically over a distance of about 3 metres (inset). At this early stage the magmatic fluid input is dominantly phase G, so little or no metals are introduced.

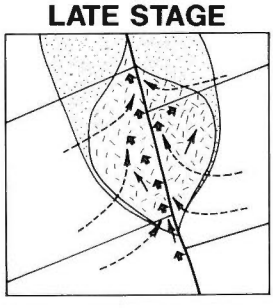

Fig. 3cii. In the late stages the acid alteration zone may be increasingly invaded by phase L, which is transporting most of the metals. Mixing of phase L with meteoric water will occur in the permeable acid leached alteration zone. Cu and Au will deposit in the zones of most active fluid mixing. Differences in the hydrology within these zones determine where phase L flows, and where sufficient mixing with groundwaters occurs to allow deposition, producing localised zones of mineralization within the more extensive alteration zone.

3. The fluid released from the magma will expand and cool, and will form low and high density phases (phases G and L respectively). The composition of phases G and L depends on the pressure, and will change constantly during ascent, so the two fluids will continue to re-equilibrate as conditions change.

4. Low density phase G will contain most of the gas components of the parent fluid, especially CO_2, SO_2, HCl and HF. It will contain little or no Au, Cu or other metals. Phase L will contain a relatively minor part of the CO_2, SO_2, HCl and HF, but it will contain most or all the Au and Cu, and the other non-volatile components such as NaCl. Partitioning of volatile and non-volatile components between the two phases, and their relative volumes depend on temperature and pressure, and will change as these change.

5. Phases G and L travel at high velocity up the fracture conduit as a result of the pressure in the parent magma chamber that expelled them, the pressure of the 'second boiling' (Burnham and Ohmoto, 1980) that results from the pressure release on fracturing, and the volume increase that results from pressure drop as the fluids pass up the conduit. As a consequence, the tendency for the two phases to separate is inhibited, but still the more mobile (less dense) phase G travels faster than phase L, which will tend to lag behind, especially if the fluid path is long. The result of this is that the fluids that first arrive at any distant point along the fluid path will be relatively enriched in phase G; during the life of the pulse the proportion of phase G will drop, and of phase L will increase (Figure 3d). Consequently the waning stage of a mineralising pulse will be dominated by phase L.

6. When a zone of increased permeability is reached (e.g. where there is a major fracture zone), the magmatic fluids may mix with groundwater (Figure 3b). Depending on the temperatures of the mixing magmatic and meteoric fluids and their proportions this may cause the groundwater to be heated above its boiling point for depth, causing boiling, or if sufficiently high pressures are attained it may cause hydrothermal brecciation, thus increasing permeability.

7. Mixing of phase G with groundwater, together with the effects of cooling will produce a mixed magmatic-meteoric fluid with extremely low pH (from dissociation of HCl and HF, and disproportionation of SO_2, with dissociation of the resulting

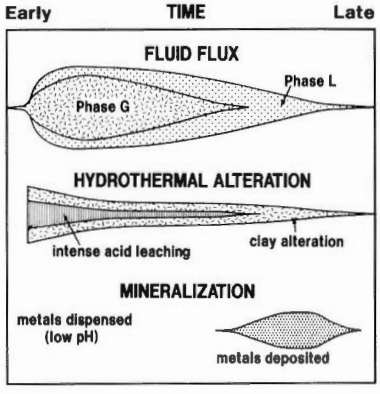

Fig. 3d. Evolution of the system with time. Early stages are dominated by the effects of interaction between phase G and ground water. Late stages are dominated by the interaction of phase L with ground water; in this stage metal deposition occurs. See text for further explanation.

H_2SO_4). Wallrock reactions will attempt to neutralise the acid fluid, producing intense acid hydrothermal alteration, so enhancing permeability, and encouraging the influx of more groundwater. An upwardly expanding alteration zone strongly controlled by host rock permeability results (Figure 3ci). Phase L is likely to be absent or very minor at this stage, and what little is present will be dispersed by mixing, without any localised metal deposition occurring (because of the very acid conditions).

8. As it forms, the acid alteration zone may be invaded by an increasing proportion of the slower moving (more dense) phase L, which is transporting the metals. As the system wanes the ratio of phase L to phase G will sharply rise, while the overall fluid pressure will drop. Neutral pH meteoric water will invade the alteration zone of leached silica, mixing with the phase L. The acidity within this complex mixing region will decrease, allowing deposition of Au and Cu to occur as a result of dilution (lowering $[Cl^-]$ and increasing pH), cooling, and lowering of fo_2(because of SO_2 disproportionation). Differing responses to these factors, as well as differing pH stability fields and rates of deposition will result in zoning of metals and late stage gangue minerals (Figure 3cii). Lower acidity will allow silica deposition locally, producing zones of massive silica from silicification of the vuggy silica. Kaolinite may deposit from pH rise allowing dissolved Al to precipitate. Barite may also deposit.

9. Because metal deposition results chiefly from the effects of mixing with groundwater, the metals are confined to the zones of most active fluid mixing (i.e., the greatest permeability), which coincide with the zones of most intense acid alteration. The extent of metal deposition within the acid alteration zone depends on the extent to which phase L invaded the alteration produced by phase G. Every stage from complete invasion to none is possible. Differences in the hydrology within this zone will determine where phase L flows, and where sufficient mixing with groundwaters occurs to allow deposition, producing localised zones of mineralization within the more extensive alteration zone. Dilution factors of several orders of magnitude are probably required to allow ore mineral deposition, thus explaining the elusiveness of isotopic or fluid inclusion evidence for a magmatic fluid contribution (e.g, Hedenquist, 1987; Hedenquist *et al.*, 1988).

Conclusions

High sulfidation epithermal deposits occur in generally similar geologic settings to low sulfidation deposits; there are differences in mineralogy, but there is also substantial overlap; both types show generally similar styles of hydrothermal alteration, but their zoning differs significantly. The major difference between high sulfidation and low sulfidation deposits is the fluids that produce them; they differ in origin, chemistry, and consequently behaviour, resulting in differences in the form, mineralogy, and zoning of deposits.

It is proposed that high sulfidation deposits are produced from magmatic fluids which segregate into two phases during transport. The spectacular acid hydrothermal alteration that characterises most high sulfidation deposits is produced mostly by interaction of the more volatile magmatic fluid whith groundwater. The metalliferous mineralization results from the second, slower moving, denser magmatic fluid, which invades the zone of alteration formed ahead of it by the faster moving magmatic volatiles, and there deposits metals as a result of groundwater dilution (lowering $[Cl^-]$ and pH), cooling and lowering of fo_2. The

presence of mineralization depends on availability of the dense fluid phase; if it is not available or insufficient, then a barren alteration zone may result. The distribution of mineralization within the alteration zone depends on the quantity of the dense fluid phase available, and on local hydrology during the waning stages of the system, which determines the sites and extent of mixing of the metal-bearing dense fluid with groundwater. The high degree of dilution required for deposition is consistent with the scarcity of magmatic isotopic signatures and very saline fluid inclusions.

This model differs from previous models in that two genetically closely related magmatic fluids are invoked, and the metals are regarded as being derived from a magmatic source and transported in a dense saline magmatic fluid. The acid alteration and metal deposition are seen as closely related aspects of an evolving magmatic-hydrothermal system, rather than as two genetically unrelated superimposed events. This is justified by studies of porphyry copper deposits, and more satisfactorily explains metal associations, and the location of gold deposition in the system.

This model contains many variable factors such as the composition of the magmatic source, and consequently the composition of the primary magmatic fluid; temperature and pressure of fluid release; the length of the fluid path and extent of separation of the two phases G and L; and the temperature and pressure at which mixing with groundwater occurred. These will affect the products formed, and explain much of the variability seen in high sulfidation deposits.

Acknowledgements

Jeff Hedenquist and Stuart Simmons have long acted as mostly uncomplaining sounding boards for my ideas. Many geologists in many mines and prospects around the world have generously given time to show me their deposits. My colleagues have encouraged my enthusiasm with their interest. My employers have given unflinching support. To all, my thanks. Published with permission of BHP-Utah Minerals International.

References

Berger, B.R. and Henley, R.A. (1990) Advances in the understanding of epithermal gold-silver deposits, with special reference to the western United States. In Keays, R.R., Ramsay W.R.H. and Groves, D.I., eds. *The Geology of Gold Deposits: The Perspective in 1988. Economic Geology Monograph,* 6, p. 405-423.

Burnham, C.W. and Ohmoto, H. (1980) Late-stage processes of felsic magmatism. *Mining Geology, Special Issue,* 8, p. 1-11.

Cordery, G. (1986) Epithermal alteration zonation at Peak Hill. *Geol. Soc. Australia, Abstracts* no. 18, p. 1-8.

Fournier, R.O. (1987) Conceptual models of brine evolution in magmatic-hydrothermal systems. In *Volcanism in Hawaii. USGS Prof. Pap.* 1350, p. 1487-1505.

Harbon, P.(1988) Peak Hill project, Peak Hill, New South Wales. In Bloom, M.S. and Parrington, P.J., eds., *Bicentennial Gold 88 Core Shed Guidebook.* Geol. Soc. Australia, p. 38.

Heald, P., Hayba, D.O. and Foley, N.K. (1987) Comparative anatomy of volcanic-hosted epithermal deposits: acid-sulfate and adularia-sericite types. *Econ. Geol,* vol. 82, p. 1-26.

Hedenquist, J.W. (1987) Mineralization associated with volcanic-related hydrothermal systems in the circum-Pacific basin. In Horn, M.K., ed., *Transactions of the Fourth Circum-Pacific Energy and Mineral Resources Conference, Singapore.* Am. Assoc. Pet. Geol. p. 513-524.

———, Matsuhisa, Y., Izawa, E., Marumo, K., Aoki, M. and Sasaki, A. (1988) Epithermal gold mineralisation of acid-leached rocks in the Nansatsu district of southern Kyushu, Japan. *Bicentennial Gold 88, Geol. Soc. Australia, Abstracts* no. 22, p. 183–190.

Henley, R.W. and McNabb, A. (1978) Magmatic vapour plumes and ground-water interaction in porphyry copper emplacement. *Econ. Geol.*, vol. 73, p. 1–20.

Huang, C.K. (1963) Factors controlling the gold-copper deposits of the Chinkuashih mine, Taiwan. *Acta Geologica Taiwanica,* vol. 10, p. 1–9.

Izawa, E. and Cunningham, C.G. (1989) Hydrothermal breccia pipes and gold mineralization in the Iwashita orebody, Iwato deposit, Kyushu, Japan. *Econ. Geol.*, vol. 84, p. 715–724.

Jannas, R.R., Beane, R.E., Ahler, B.A. and Brosnahan, D.R. (1990) Gold and copper mineralization at the El Indio deposit, Chile. In Hedenquist, J.W., White, N.C. and Siddeley, G., eds. *Epithermal Gold Mineralization of the Circum-Pacific: Geology, Geochemistry, Origin and Exploration, II. J. Geochem. Expl.*, vol. 36, p. 233–266.

Large, R., Huston, D., McGoldrick, P., McArthur, G. and Ruxton, P. (1988) Gold distribution and genesis in Palaeozoic volcanogenic massive sulphide systems, eastern Australia. *Bicentennial Gold 88, Geol. Soc. Australia, Abstracts* no. 22, p. 121–126.

Raetz, M.C. and Parrington, P.J. (1988 a) Rhyolite Creek, Victoria, a Lower Palaeozoic epithermal gold prospect. *Bicentennial Gold 88, Geol. Soc. Australia, Abstracts* no. 23, p. 291–294.

——— and ——— (1988 b) Rhyolite Creek project, Jamieson, Victoria. In Bloom, M.S. and Parrington, P.J., eds., *Bicentennial Gold 88 Core Shed Guidebook, Geol. Soc. Australia,* p. 42.

Ransome, F.L. (1907) The association of alunite with gold in the Goldfield district, Nevada. *Econ. Geol.*, vol. 2, p. 667–692.

Sakazaki, H., Ohtagaki, T. and Chin, W. (1964 a) Geology and ore depositions of the Chin-qua-shih mine district (2)-Characteristics of mineralization. *Mining Geology,* vol. 14, p. 274–285 (in Japanese with English abstract).

———, ——— and ——— (1964 b) Geology and ore depositions in the area of the Chin-qua-shih mine (3)-Zonal mineralization. *Mining Geology,* vol. 14, p. 350–355 (in Japanese with English abstract).

Siddeley, G. and Araneda, R. (1986) The El Indio-Tambo gold deposits, Chile. In Macdonald, A.J., ed., *Proceedings of Gold '86 Symposium,* Toronto, Canada, p. 445–456.

Stoffregen, R. (1987) Genesis of acid sulfate alteration and Au-Cu mineralization at Summitville. *Econ. Geol.*, vol. 82, p. 1575–1591.

Thompson, J.F.H., Lessman, J. and Thompson, A.J.B. (1986) The Temora gold-silver deposit: A newly recognized style of high sulfur mineralization in the Lower Paleozoic of Australia. *Econ. Geol.*, vol. 81, p. 732–738.

Utada, M. (1980) Hydrothermal alterations related to igneous activity in Cretaceous and Neogene formations of Japan. *Mining Geology, Special Issue* 8, p. 67–83.

Urashima, Y., Izawa, E. and Hedenquist, J.W. (1987) Nansatsu-type gold deposits in the Makurazaki district. In Urashima, Y., ed., *Gold deposits and Geothermal Fields in Kyushu, Soc. Mining Geologists of Japan, Guidebook* 2, p. 13–22.

Walthier, T.N., Sirvas, E. and Araneda, R. (1985) The El Indio gold-silver-copper deposit. *Eng. Min. J.*, vol. 186 (10), p. 38–42.

White, N.C. and Hedenquist, J.W. (1990) Epithermal environments and styles of mineralization: variations and their causes, and guidelines for exploration. In Hedenquist, J.W., White, N.C. and Siddeley, G., eds., *Epithermal Gold Mineralization of the Circum-Pacific: Geology, Geochemistry, Origin and Exploration, II. J. Geochem. Expl.*, vol. 36, p. 445–474.

Geological Survey of Japan Report, No. 277, 1991, p. 21-30

Geology and Mineralization Characteristics of the Mankayan Mineral District, Benguet, Philippines

Jose S. GARCIA, Jr.

Lepanto Consolidated Mining Company, Mankayan, Benguet 2609, Philippines

Geologic Setting

The Mankayan Mineral District lies near the eastern limb of a broad north-trending anticline. The arch's core is an Early Miocene intrusive complex of gabbroic to tonalitic composition while its eastern flank consists of E-dipping, N to NE-trending volcanics, clastics and volcaniclastics (Fig. 1). In fault-contact with the intrusive complex is a folded pre-Eocene ophiolitic basement consisting of regionally metamorphosed basaltic-diabasic flows which, at the upper section, is intercalated with fine andesitic volcanics and cherts. In the northeastern part of the district, the basement is unconformably overlain by the Late Eocene-Early Oligocene Apaoan Sequence consisting of thin bedded red and green sandstones, shales and fine volcaniclastics. Overlying these older rock units is the Middle Miocene Balili Volcaniclastics consisting of andesitic breccias and tuffs, polymictic conglomerates, wackes and shales (Fig. 2). Late Miocene porphyry copper-related quartz diorite porphyry bodies intrude the Balili Volcaniclastics.

Late Miocene to Early Pliocene Imbanguila Dacite occurs as a blanket of pyroclastics over, and as porphyry intrusions into, the older rock units. Enargite-gold mineralization, subsequently followed by epithermal gold-base metal sulphide veining, were deposited after the Imbanguila Dacite emplacement (Fig. 2). The unmineralized Late Pliocene to Early Pleistocene Bato Dacites occur as tuffaceous diatreme infills and porphyry domes.

Mineralization

Three economically significant mineralization types are known in the district.

Porphyry Copper-Gold Mineralization:

This mineralization is represented by the FSE deposit located at the far southeast (FSE) section of the present enargite mine (Figs. 1 and 3). The deposit is WNW-trending and longitudinally bell-shaped with the top lying 650 m below surface. It is centered on a melanocratic quartz diorite stock which intruded the Balili Volcaniclastics. Preliminary fluid inclusion studies indicate a Th of $529 \pm 80°C$ with salinities ranging from 42-54 wt.% NaCl equivalent. Silicate alteration consists of three zones generally enveloping each other (Fig. 4). At the core, extending roughly 100 m from the intrusive contact, is potassic (biotite) alteration which was subjected to partial retrograde clay-chlorite replacement. Outwards, the potassic core grades into pervasive chlorite-illite alteration which encompasses the bulk of economic mineralization. Fringe alteration is propylitic, characterized by epidote, calcite and chlorite. Sulphide zoning is characterized by bornite-chalcopyrite-magnetite in the

Keywords.: Mankayan mineral district, Lepanto deposit, FSE deposit, porphyry copper-gold mineralization, enargite-gold mineralization, epithermal gold mineralization, hydrothermal breccia

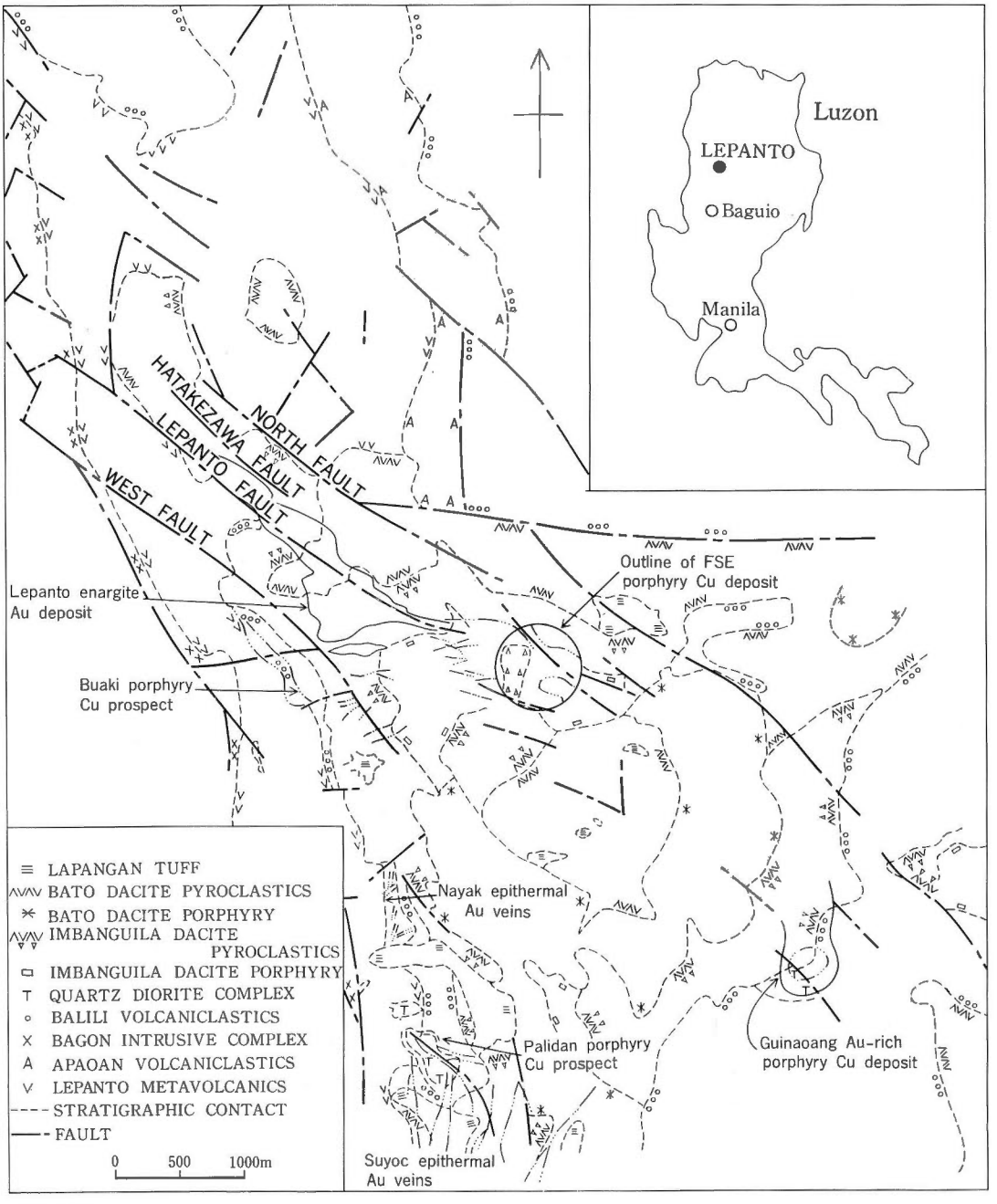

Fig. 1. Surface geologic map of the Mankayan mineral district showing the location of the Lepanto enargite-luzonite-gold mine, the Nayak and Suyoc epithermal gold veins, the FSE and Guinaoang gold-rich porphyry copper deposits and the Palidan-Pacda-Buaki porphyry copper prospects.

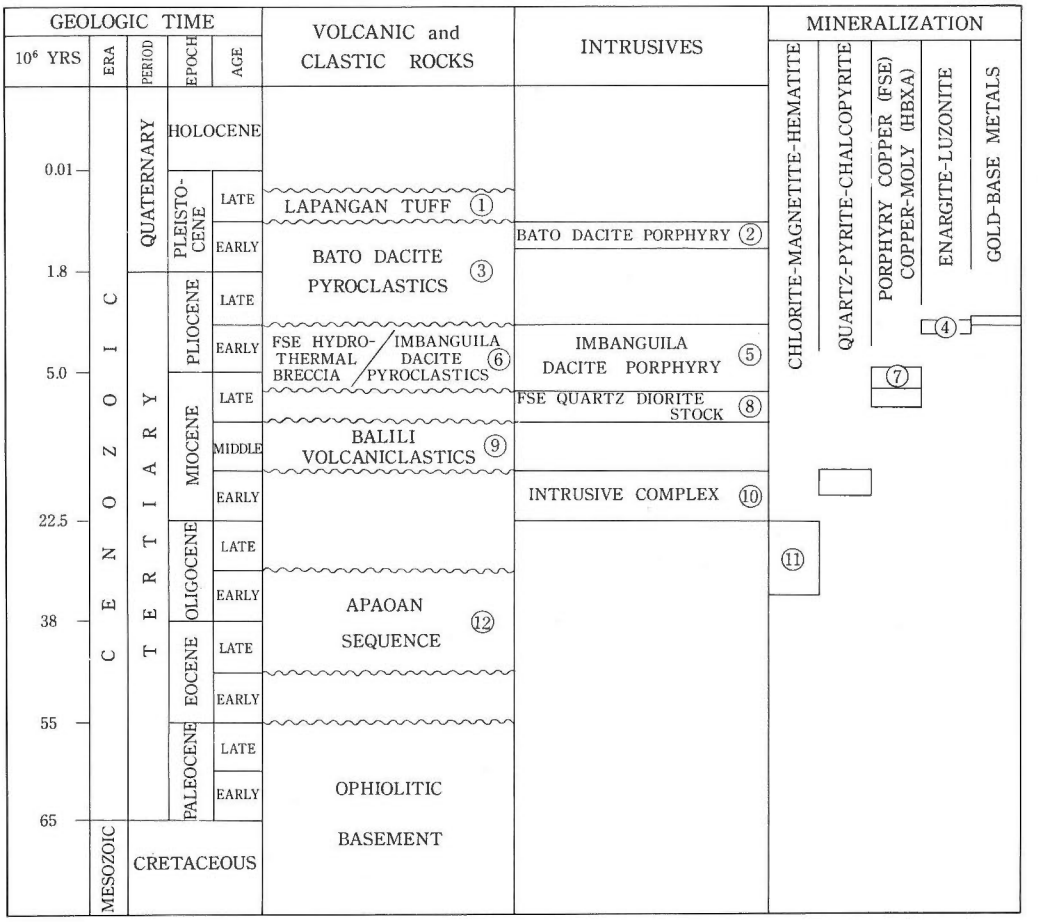

Fig. 2. Stratigraphic-chronologic section of the Mankayan mineral district (Adopted from Concepcion and Cinco, July '88 ; Garcia and Bongolan, Nov. '89).

1. ^{14}C-age on humic soil at Bugias (Bed-Jica) 18,820±670 y.
2. Mt. Pusdo volcanism (Ringenbach *et al.*) 0.5 Ma.
3. K-Ar age on biotite from Bato Diatreme (Sillitoe and Angeles) 2.9±0.4 Ma.
4. K-Ar ages on alunite (Hedenquist)
   at Airstrip 1.4-1.5 Ma,
   at 35 L 1070 L 2.0-2.2 Ma,
   at Mohong Hill 1.6-1.7 Ma.
   K-Ar ages on hydrothermal sericite (Krueger) at FSE 2.5-3.3 Ma,
   (Sillitoe and Angeles) at Guinaoang 3.5±0.9 Ma.
5. K-Ar ages on feldspar from Imbanguila Dacite Porphyry
   (Krueger) 6.9±0.8 Ma.
   Post Klondyke Intrusion
   (Wolfe) 5.6-6.1 Ma ; (BMGS) 7 Ma, east of Abatan.
6. K-Ar ages on Lepanto Dacite (Ringenbach) 5.7-6.1 Ma.
7. K-Ar age on alunite from FSE Hydrothermal Breccia (Hedenquist) 6.9-8.5 Ma.
8. Late Agno Intrusion (Wolfe) 9-10 Ma.
   K-Ar on dacitic/andesitic dikes in Cervantes (Ringenbach *et al.*) 9.9-11.0 Ma.
9. Limestone clast at Tubo (Gutierrez, lower to middle Miocene).
   Limestone clast at base of Balili (Sillitoe and Angeles, late Oligocene to mid Miocene).
10. K-Ar ages on hornblende and biotite from Bagon Tonalite (Sillitoe and Angeles) 12-13 Ma. Early Agno Intrusion (Wolfe) 14-19 Ma, (R.P.-Japan) 18 Ma.
11. Low copper to barren Cordilleran magmatism (Wolfe) 23-32 Ma.
12. Pelagic foraminifer in ss and clay at Cervantes (Ringenbach *et al.*) Late Eocene to early Oligocene.
    Radiolaria from Red Beds at Tubo (Maac) Early Oligocene.

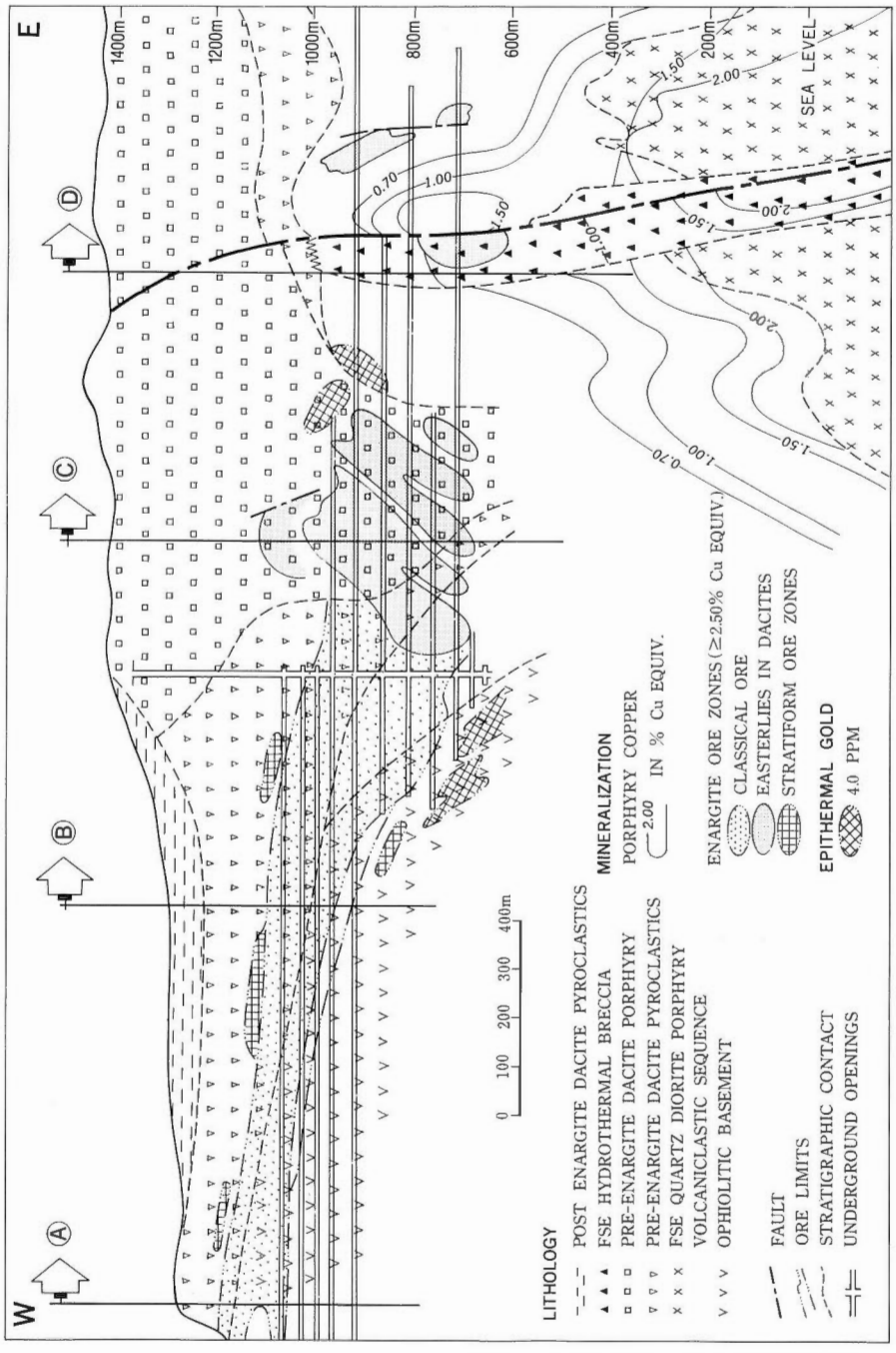

Fig. 3. Idealized longitudinal section showing the FSE gold-rich porphyry copper deposit, the enargite ore bodies, and occurrences of epithermal gold mineralization (after Concepcion and Cinco, Oct. '89).

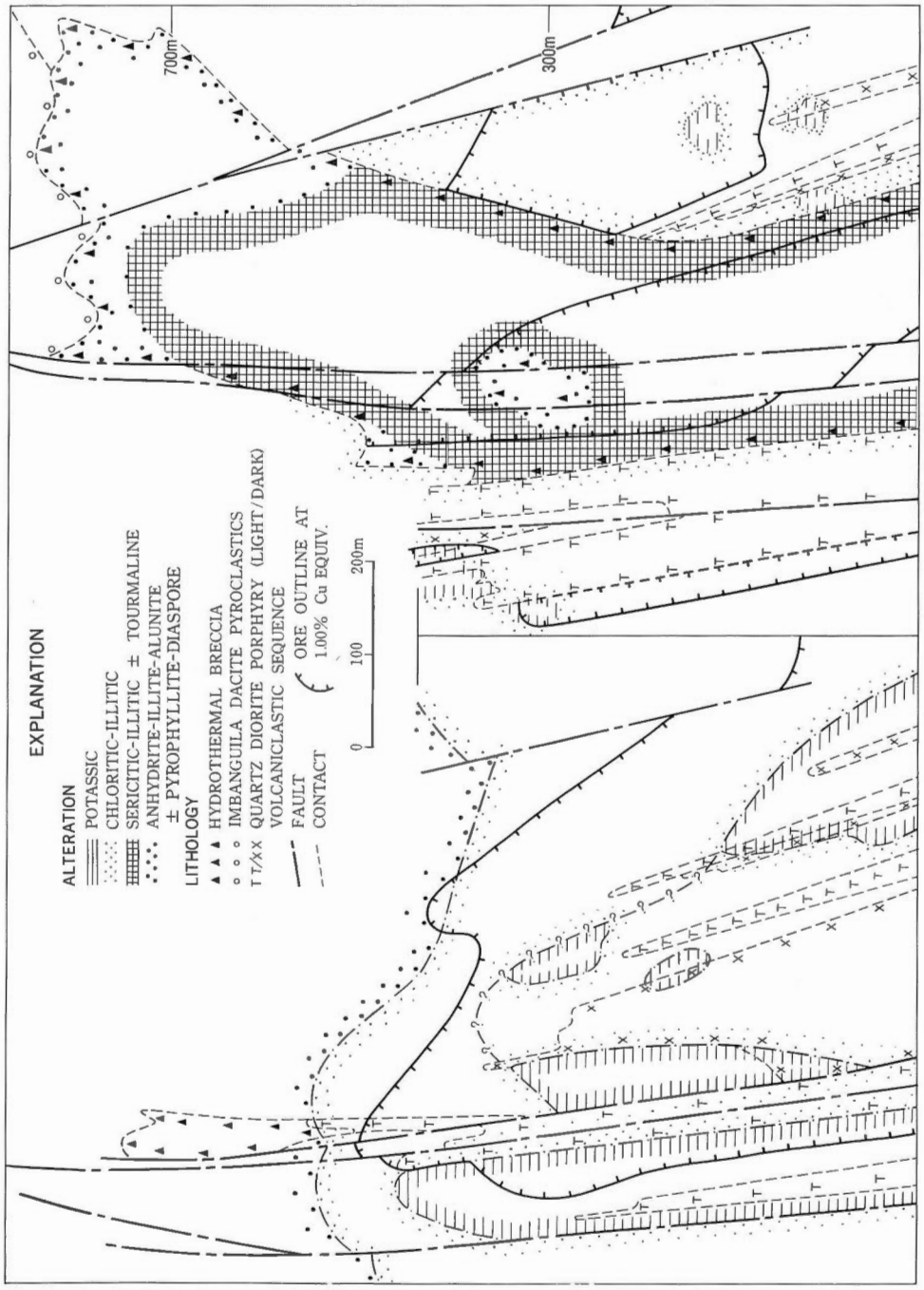

Fig. 4. Cross sections (Fig. 3) along E-250 and E-400 of the FSE porphyry copper deposit with alteration, mineralization, the hydrothermal breccia pipe and other geologic features (after Concepcion and Cinco, Oct. '89).

potassic core grading to chalcopyrite-magnetite-hematie ± pyrite and molybdenite in the chlorite-illite zone, then to chalcopyrite-pyrite-hematite in the propylitic zone. Gold occurs in native form, intimately interlocked and/or attached to chalcopyrite-bornite, and shows a positive correlation with copper and magnetite.

A steep post-porphyry copper hypabyssal breccia pipe centrally truncates the FSE deposit (Fig. 4). The pipe's upper terminus abuts into the Imbanguila Dacite (Figs. 3 and 4) while its bottom is unexplored. Alteration zoning consists of sericite-illite ± tourmaline-chlorite in the lower portion while the upper portion consists of anhydrite-illite-alunite-diaspore-zunyite-pyrophyllite (Fig. 4). This advanced argillic zone extends beyond the breccia as an extensive cap over the FSE porphyry copper alteration. Enargite-bearing advanced argillic bands crosscut the chlorite-illite halo of the FSE deposit. K-Ar dating on the alunite yielded ages of 6.9-8.5 m.y., while isotope studies yielded $\delta^{34}S$ values of 13-16 per mil. Sulphide zoning is characterized by chalcopyrite-magnetite-pyrite ± bornite-molybdenite in the deeper sericitic-illitic zone while chalcopyrite-pyrite-hematite ± enargite, secondary covellite and molybdenite predominate in the upper advanced argillic zone.

Enargite Mineralization:

The enargite-gold deposit consists of a main zone and multiple veinlets that branch off from the main zone at an acute angle. The main zone, an elongated, pipelike, tectonic breccia-filling body, 10-50 m wide (Fig. 5), developed for over 2 km., and about 100 m in height, has an average strike of N55W and steep NE dip. Postmineral oblique slip faulting, sinistrally sliced the main orebody. In the western section of the enargite mine, hosted by the ophiolitic basement, volcaniclastics and Imbanguila dacite pyroclastics, are the branch veins consisting of east-trending, steep dipping, fissure-filling structures (Fig. 6). They rarely exceed 10 cm width individually, but as closely spaced veinlets, form wide mineable zones. In the eastern portion of the mine, where the Balili Volcaniclastics and Imbanguila Dacite Porphyry are the dominant rock units, the Easterlies consist of widely spaced (10-100 m apart), east-trending, steep dipping, narrow but strike and dip persistent enargite zones. Enargite-luzonite also occurs as stratiform lenses with areas of ten to a few hundred square meters and thickness of a few cm to a few meters (Fig. 5). Pyrite, together with the Cu-As sulphides, replace 10-90% volume of the lenses. Localization of the lenses is controlled by (a) the presence of more permeable members of host rocks such as agglomeratic-volcanic breccia member of the dacites, calcareous graywackes and shales of the Balili Volcaniclastics, and laminated sandstones of the Apaoan Sequence and (b) sites of sudden decrease in the slope of the unconformities.

Alteration and mineralization are controlled by the chemistry-permeability of individual rock units and by structures such as NW trending breccia zones, east-trending tension fractures and unconformities. In the branch vein area, wedge-shaped massive to vuggy silica alteration is extensively developed along these structures. The silicified wedges are narrower in the pre-dacite rocks, widest in the unconformity and then extend up to 30 meters into the dacites; they are enveloped by quartz-alunite-kaolinite alteration (Fig. 5). In the pre-dacite rocks, the advanced argillic envelope grades outward into pervasive chloritization while in the dacites, the envelope is abruptly succeeded by 5-20 meter thick blanket of intense kaolinization. Atop the kaolinized blanket is argillization characterized by montmorillonite-illite. Further upwards, the argillization encroaches on unaltered dacites. On the

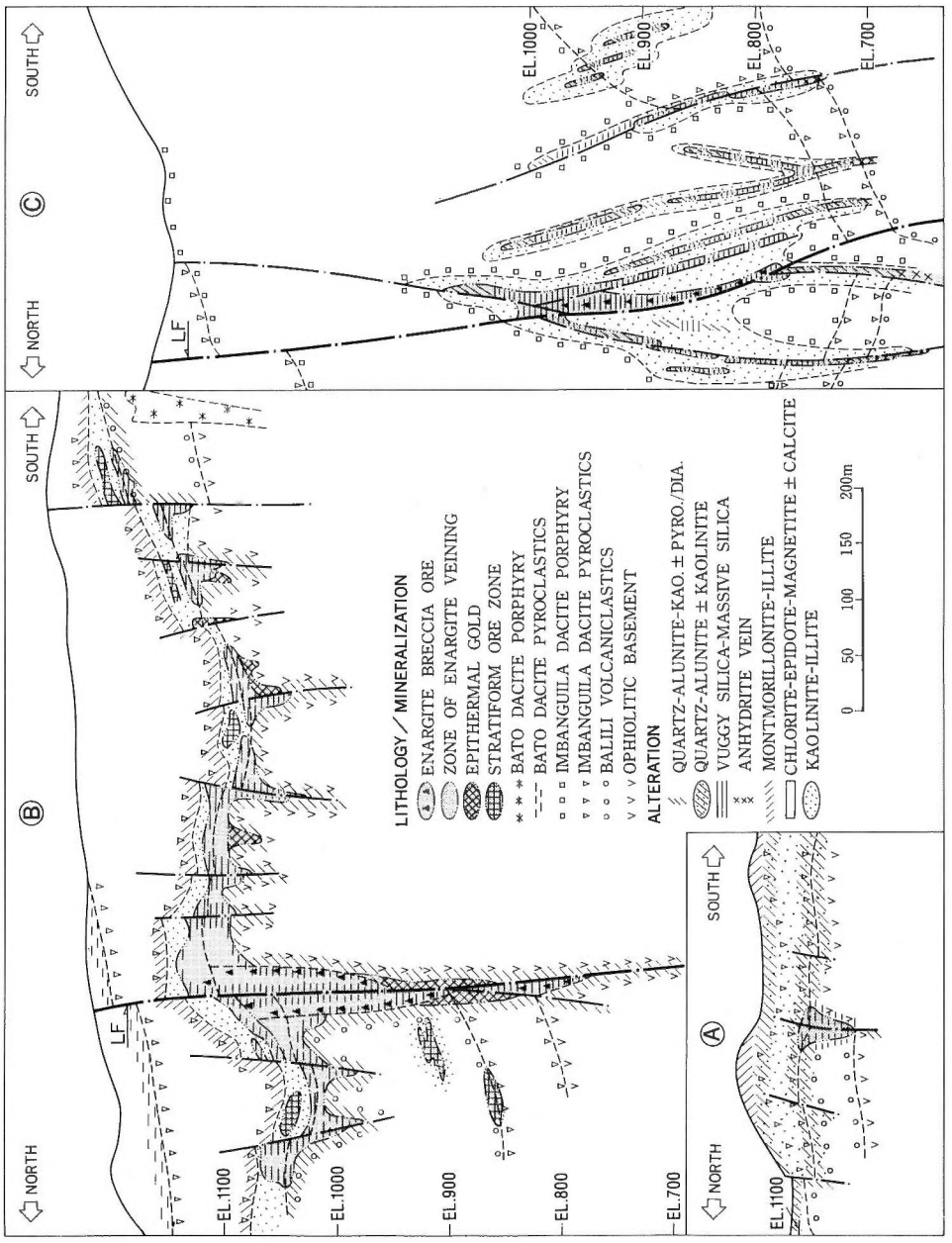

Fig. 5. Sections (Fig. 3) across the enargite ore body showing lithology, alteration and mineralization. A) NW area, B) Main orebody and branch veins, C) Easterlies.

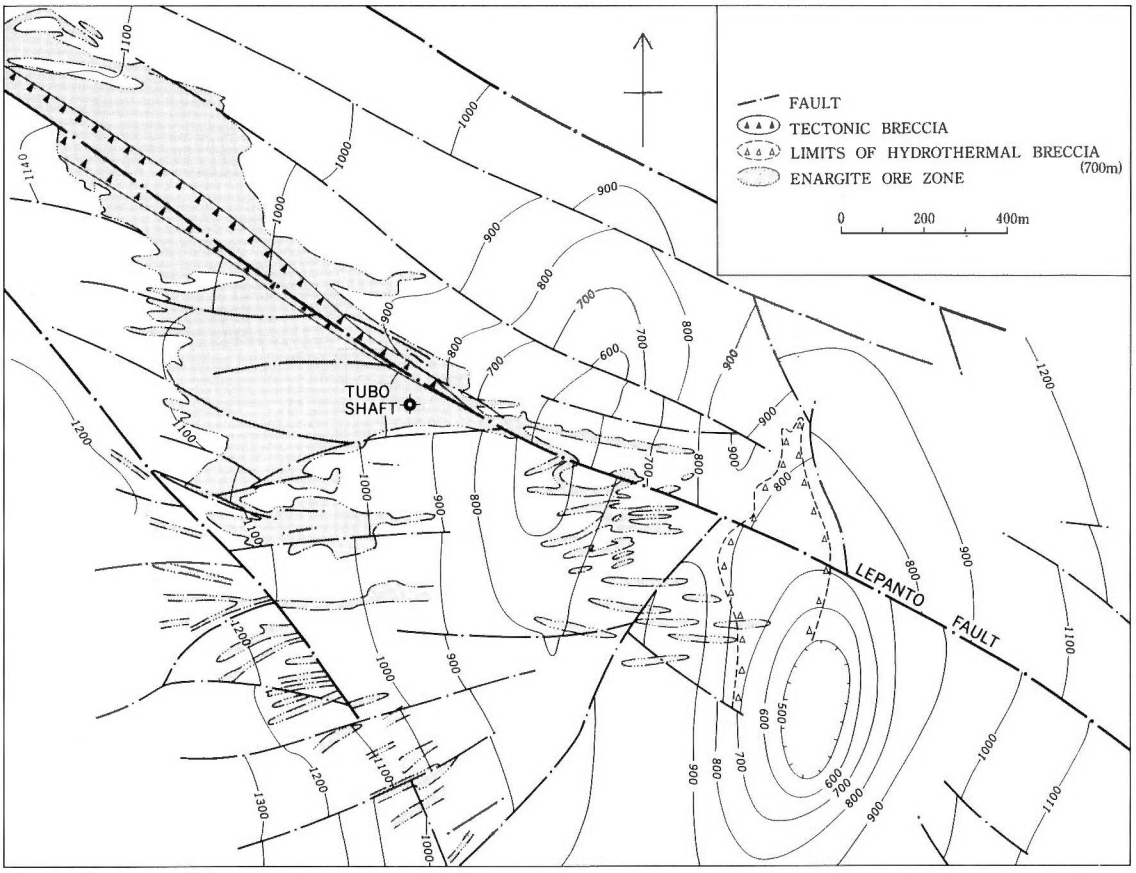

Fig. 6. Structure contours showing the base of Imbanguila Dacite.

western edge of the district, extensive quartz-alunite-kaolinite alteration, with or without the enclosed silicification, occurs as a 6-km long ridge defining the extent of the unconformity between the pre-dacite and the dacitic rock units. K-Ar dating on alunite from this ridge gave ages of 2.0-2.5 m.y. while $\delta^{34}S$ values range from 20-27 per mil. In the Easterlies area, 2-10 meter wide fracture-controlled strips of vuggy to massive silica are sheathed by thin bands of quartz-alunite-kaolinite $\pm$ pyrophyllite-diaspore alteration. Pervasive kaolin-quartz-illite alteration envelops the silicified strips and advanced argillic sheaths. Kaolin replaces the feldspar phenocrysts while quartz and illite replace the rock matrix. The kaolinized envelope grades outwards into chloritized-argillized wallrock. Toward the FSE area, this envelope is hardly distinguishable from the advanced argillic cap above the FSE deposit.

The main orebody, the branch veins and the easterlies are mostly confined within the massive and vuggy silica alteration, while the stratiform ore occurs in the kaolinized zone. More than 90% of the copper in the deposit occurs in the form of enargite and luzonite. Chalcopyrite-tennantite-minor stibnite occur late in the deposit paragenesis while chalcocite-covellite are observed as supergene replacement.

Gold and silver are mainly as tellurides. Gangue minerals are quartz, pyrite, kaolinite, dickite and barite.

Epithermal Gold Mineralization:

Zones of auriferous pyrite-quartz stringers are observed in several areas in the district. Where these zones coincide with roots of enargite ore shoots (Fig. 5), Cu-As sulphide content increases gradually upwards. Pyrite, occupying 60-80% volume of the zone, occurs as very fine, sooty aggregate while quartz occurs as white-milky to yellow-citron linings and bands. Microscopic analyses and metallurgical tests indicase that the gold is occluded in the pyrite grains.

The weakening of Cu-As sulphide mineralization, atop and on the edges of enargite ore shoots, sometimes gives way to localized occurrence of chalcopyrite-tennantite-barite-stibnite-gold mineralization.

In the southern part of the district, in the Nayak area (Fig. 1), north-trending fracture-controlled argillic zones in the ophiolitic basement host quartz veinlets and stockworks. Associated with the quartz is native gold ± marmatitic sphalerite, galena, and pyrite. The argillic zone is characterized by quartz-sericite ± adularia. Fluid inclusion studies on the sphalerite yielded Th of 170-250°C and salinities of 2.06-3.05 wt. % NaCl equivalent.

Localized occurrence of the Nayak-type mineralization is observed in the enargite mine as (1) quartz-Au breccia lenses without Cu-As sulphides situated below and/or peripheral to the main enargite-luzonite breccia body (MOB), (2) NE-trending, steep dipping quartz-sphalerite-galena zones crosscutting the NW-trending MOB, (3) quartz-Au stringers in roots of branch veins, (4) gold-bearing quartz stringers crosscutting enargite related alteration, (5) fine quartz-gold stringers cutting stratiform lenses and (6) centimeter to meters wide gold-bearing argillic zones with gypsum-anhydrite-sphalerite-galena enclosed by chloritized volcaniclastics or dacite porphyry.

Discussion

The FSE deposit is genetically related to the melanocratic quartz diorite porphyry body which is one of at least three porphyry copper related stocks identified in the district. These stocks are interpreted to represent the latest, dated 9-11 m.y., of a three-phase Cordilleran plutonism, in the Luzon magmatic arch. Mineralization is found in all the alteration zones but was probably deposited mainly during the retrograde clay-chlorite and the chlorite-illite alteration. This is evidenced by higher metal content and more extensive quartz-anhydrite-sulphide-magnetite stockworks (up to 40% volume) in these alteration zones, compared to the potassic and propylitic zones. The FSE deposit is pre-hydrothermal breccia and pre-enargite as evidenced by porphyry copper-bearing clasts in the hydrothermal breccia and in the enargite-hosting Imbanguila Dacites. K-Ar dating of feldspar in the Imbanguila Dacites yielded ages of 5.7-6.9 m.y.

Mineralization in the hydrothermal breccia is attributed to post-porphyry copper magmatic fluids partly diluted by meteoric waters. The enargite-bearing advanced argillic alteration characterized by abundant anhydrite and alunite, both as stockworks and as filling of interclast spaces at the pipe's upper portion, may be due to the reaction of the lime-rich Balili Volcaniclastics with sulphuric acid generated from disproportionation of magmatic SO_2. K-Ar dating on alunite gives the age of mineralization at 6.9-8.5 m.y. Mineralogical assemblage distinguishes this breccia-

related advanced argillic alteration from the younger quartz-alunite ± kaolinite envelope of enargite ore shoots. The chalcopyrite-gold mineralization in the deeper sericitic-illitic zone may be interpreted as a post-main stage porphyry copper deposition below the zone of SO_2 disproportionation.

In the case of enargite mineralization, two scenarios are possible. Clustering of K-Ar age data, viz., on hydrothermal sericite in the FSE area, on biotite in dacite at Guinaoang and on alunites in the western and southern sections of enargite mine, indicates a district-wide heating event that occurred between 2-3 m.y. Enargite mineralization may have been a product of this event, though no mineralized district-wide heat source has yet been chronologically correlated with this period. Alternatively, enargite may have been deposited immediately after the Imbanguila Dacite emplacement (6-7 m.y.). This scenario provides the district-wide mineralized heat source. The cluster of K-Ar dates at 2-3 m.y. may then be attributed to a non-mineralizing reheating event.

Permeable structures confined the flow of a district scale convectively circulating meteoric water cell driven by a heat source, probably centered in one of the diatremes near the FSE deposit. The convective cell was probably contaminated by acid fluids-magmatic vapor emanating from this heat source, thereby developing structurally/stratigraphically-controlled massive and vuggy silica zones bounded by quartz-alunite alteration. The leaching, silica deposition and the subsequent evolution of a magmatic vapor-dominated system into a liquid-dominated system was due to the influx of meteoric waters, which lowered the acidity of the fluids, resulting in the deposition of enargite-gold. The high sulphur and high copper activities in the early stages evolved through time to a decreased sulphur activity and lower concentration of copper, indicating that no additional magmatic components were added into the hydrothermal cell. Increase in iron and antimony activities in the consequent copper and sulphur deficient fluids resulted in the deposition of auriferous pyrite-quartz stringers along fracture zones and of stibnite-tennantite-barite-chalcopyrite-gold near the upflow, relatively cooler zones. Collapse of the cell allowed the descent, thereby dominance, of meteoric fluids producing a neutral pH-low salinity environment. This enviroment was responsible for the deposition of epithermal gold and base metal sulphide veins in several areas in the district. The unaltered Bato Dacites, aged equivocally as either 0.5 or 2.9 m.y., postdate the hydrothermal cell.

Epilogue

The Mankayan Mineral District is host to porphyry copper, high sulphidation enargite and low sulphidation gold mineralization. Continuing studies on the characteristics of and relationships between the types of mineralization provide insights to the genesis of these and similar ore deposits. The district is currently the subject of a joint study and research program between the Geological Survey of Japan, Mineral Resources Department and the Lepanto Consolidated Mining Company and, shortly, between the National Taiwan University and Lepanto.

Geological Survey of Japan Report, No. 277, 1991, p. 31-33

Stable Isotope Systematics of Alunite

Roger E. STOFFREGEN

Dept. of Geological Sciences, Southern Methodist University
Dallas, Texas, 75275, U.S.A.

Alunite ($KAl_3(SO_4)_2(OH)_6$) is unique among common alteration minerals in containing hydrogen, sulfur, and both hydroxyl and sulfate oxygen. Stable isotope data on these four sites can potentially be used to determine (1) the temperature of alunite formation based on ^{18}O fractionation between the two oxygen sites; (2) the isotopic composition of the coexisting water; and (3) the redox state of the system based on the ^{34}S value (Pickthorn and O'Neil, 1985; Rye *et al.*, 1989). In addition, alunite can be used for K/Ar age dating. This paper discusses the experimental determination of alunite-water D and ^{18}O fractionations as a function of temperature, along with the calibration of the alunite OH-SO_4 ^{18}O geothermometer. It also presents data on rates of alkali and isotope exchange between alunite and water, and considers their implications for interpretation of alunite isotope data and K/Ar ages.

Experimental determination of isotope fractionations at temperatures below 500°C is made difficult in most minerals by slow reaction rates. Several techniques have been developed to circumvent this problem, including the use of coupled alkali exchange reactions to enhance rates of dissolution-reprecipitation, which also enchances isotope exchange (e.g. O'Neil and Taylor, 1967). Alunite is ideally suited to this approach because its Na-K exchange properties are well known and rates of alkali exchange are sufficiently rapid above 250°C to produce >90% exchange in runs of less than 9 months duration.

The alkali exchange reaction used in these experiments was

$$NaAl_3(SO_4)_2(OH)_6 + K^+ = KAl_3(SO_4)_2(OH)_6 + Na^+.$$

The maximum amount of alkali exchange, defined as the measured mol% potassium in the run product alunite divided by the predicted equilibrium value based on data from Stoffregen and Cygan (1990), was 98%, with most runs showing between 90 and 95% exchange. Because the reactions did not attain complete equilibrium, the partial equilibrium technique was used to compute isotope fractionation factors. The % isotope exchange on the three sites computed with this technique are generally within 5% of the observed alkali exchange.

Least squares fits of the exchange data at 200-450°C, weighted by the reciprocal of estimated error squared, give $10^3 \ln\alpha_{\text{alunite(SO4-site)-water}} = 3.09\ (10^6/T^2) - 2.94\ (R^2 = 0.99)$. The slope of this curve is essentially identical to the bisulfate-water fractionation of Mizutani and Rafter (1969) and is similar to barite-water (Kusakabe and Robinson, 1977) and anhydrite-water (Chiba *et al.*, 1981) ^{18}O fractionations. The hydroxyl-water curve shows more scatter than the sulfate site curve, but still gives a good linear correlation with $10^3 \ln\alpha_{\text{alunite(OH site)-water}} = 2.29\ (10^6/T^2) - 5.74\ (R^2 = 0.96)$. The fractionation between the sulfate and hydroxyl

Keywords: alunite, hydrogen isotopes, oxygen isotopes, sulfur isotopes, isotope fractionation, geothermometer

sites is given by 0.8 ($10^6/T^2$) + 2.80 and ranges from 4.3 at 450°C to a predicted value of 11.8 at 25°C. Although this large range suggests that ^{18}O fractionation within alunite should make an excellent geothermometer, the predicted variation from 400–200°C, which is of most interest in the study of the hydrothermal ore deposits, is only 1.8. Fractionation of ^{18}O in alunite is thus a relatively insensitive geothermometer over this temperature range.

The alunite–water D fractionations are −19 at 450°C, −18 at 400°C, −11 at 350°C, −1 at 300°C, −6 at 250°C and −9 (based on only 10% exchange) at 200°C. These data indicate that from 350°C to 200°C the alunite–water D fractionation is relatively constant, which indicates that the alunite D value can be used to obtain a reliable estimate of D for the coexisting water even if temperature is poorly constrained. The alunite–water D fractionation has some similarity to the boehmite–water D curve of Grahman *et al.* (1980), which may reflect the chemical and structural similarity between the two minerals.

In order to test the effect of mol% Na on the alunite–water D and ^{18}O fractionations a limited number of isotope exchange experiments were conducted with the coupled alkali exchange reaction

$$KAl_3(SO_4)_2(OH)_6 + Na^+ = NaAl_3(SO_4)_2(OH)_6 + K^+.$$

These experiments indicate that mol% Na has minimal effect on the alunite isotope fractionations, at least above 350°C.

In addition to providing equilibrium fractionations, the experimental results have been used to obtain information about the rates of alkali and isotope exchange between alunite and water. The amount of alkali exchange as a function of time can be represented with a second order rate law, which probably reflects an Ostwald ripening mechanism. Regression of the experimentally determined rate constants gives log k (sec^{-1}) = −7.4 (1000/T) + 8.1 ($R^2 = 0.99$), which implies an activation energy for the alkali exchange reaction of 33.8 kcal/mol. When extrapolated to 25°C, this equation suggests that alkali exchange between alunite and solutions will not occur at surficial conditions, except perhaps for the fine grained (<1 micron) alunites characteristic of low temperature settings.

Rates of D and ^{18}O exchange were studied in reconnaissance runs without coupled alkali exchange. The % D exchange was substantially greater than ^{18}O exchange in most of these runs, suggesting that "proton diffusion" was an important exchange mechanism for D. This was best displayed in experiments at 150°C with fine grained natural natroalunite which produced negligible ^{18}O and alkali exchange but 58% D exchange. Calculated log hydrogen diffusion coefficients ($cm^2\,sec^{-1}$) based on SEM observations of grain size are −14.1 to −13.8 at 400°C and −16.8 at 150°C. Although an activation energy for hydrogen diffusion could not be computed with these data, the results suggest that D exchange between fine grain alunite and water should occur within a few thousand years even at surficial temperatures. However, D exchange should not occur between coarse (>1 mm) hydrothermal alunite and water under these conditions.

The amounts of ^{18}O exchange below 400°C on both the sulfate and hydroxyl sites were too small to allow accurate estimates of reaction rates. As a result, conclusions about the amount of reequilibration that may occur on these sites, and its effect on the intramineral ^{18}O geothermometer, will have to be drawn from data on natural samples.

References

Chiba, H., Kusakabe, M., Hirano, S-I., and Somiya, S., (1981) Oxygen isotope fractionation factors between anhydrite and water from 100 to 550°C. *Earth Planet. Sci. Lett.*, vol. 53, p. 55-62.

Graham, C.M., Sheppard, S.M.F. and Heaton, T.H.E. (1980) Experimental hydrogen isotope studies -I. Systematics of hydrogen isotope frationation in the systems epidote-H_2O, zoisite-H_2O and AlO(OH)-H_2O. *Geochim. Cosmochim. Acta,* vol. 44, p. 353-364.

Kusakabe, M. and Robinson, B.W. (1977) Oxygen and sulfur isotope equilibria in the $BaSO_4$-HSO_4^--H_2O system from 110 to 350°C and applications. *Geochim. Cosmochim. Acta,* vol. 41, p. 1033-1040.

Mizutani, Y. and Rafter, T.A. (1969) Oxygen isotopic fractionation in the bisulphate ion-water system. *N.Z.J. Sci.*, vol. 12, p. 54-59.

O'Neil, J.R. and Taylor, H.P., Jr. (1967) The oxygen isotope and cation exchange chemistry of feldspars. *Am. Mineral.*, vol. 52, p. 1414-1437.

Pickthorn, W.J. and O'Neil, J.R. (1985) ^{18}O relations in alunite minerals: potential single-mineral geothermometer. *GSA Abstracts with Programs,* vol. 17, p. 689.

Rye, R.O., Bethke, P.M., and Wasserman, M. (1989) Diverse origins of alunite and acid-sulfate alteration: stable isotope systematics. *U.S.G.S. Open-File Report* 89-5, 33 p.

Stoffregen, R.E. and Cygan, G.L. (1990) An experimental study of Na-K exchange between alunite and aqueous sulfate solutions. *Am. Mineral.*, vol. 75, p. 209-220.

Mineralogical Features and Genesis of Alunite Solid Solution in High Temperature Magmatic Hydrothermal Systems

Masahiro Aoki

Geological Survey of Japan, Higashi 1-1-3, Tsukuba, Ibaraki, 305 Japan

Formation Process and Texture of Alunite

Alunite solid solution (hereafter abbreviated as alunite s.s) forms over a wide temperature and pH ranges from volcanic to weathering environments. The compositional variation in crystals of alunite s.s. sometimes indicates that the physical and chemical conditions fluctuated considerably during crystal growth. In high temperature acid sulphate-chloride hydrothermal systems, boiling of the fluid, mixing of ascending hot water with cooler meteoric water, intermittent input of high temperature acid components from a deep source, etc., commonly occur, followed by mineral-fluid reequilibration. These processes cause changes in temperature, pH, cation and anion ratios, salinity and so on, leading to variation in the chemistry of alunite s.s. Along the fluid conduits the changes tend to happen in quick response to the triggering events. On the other hand, in the wall rocks away from the conduit, any changes that occur in the channel tend to be propagated with considerable retardation and modification through the process of dissolution and precipitation of minerals, since the limited permeability prevents a rapid flow of fluid. In this situation, an insufficient rate of mass transfer relative to the rate of crystal growth may lead to an oscillation of chemistry in both fluid and crystal. Thus, compositional heterogeneity is an inevitable feature of hydrothermal alunite s.s. Usually it is rather difficult to recognize the compositional heterogeneity in alunite s.s. under the optical microscope and it can easily be overlooked. By using a back scattered electron image under the scanning electron microscope, a very weak compositional contrast can easily be detected.

It is necessary to apply an analytical technique with resolution comparable to the fineness of the texture in order to obtain accurate chemical and isotopic compositions on which we may construct models of hydrothermal activity. In practice, too finely banded textures often oblige us to determine only an average composition. Even so, it is a basic requirement to determine the growth texture and nature of heterogeneity, to understand the physical and chemical cause of it, and to deduce the geological processes responsible for such changes to allow a better explanation of the "average" value.

A Case Study on a Typical Magmatic Hydrothermal Alunite from Kusatsushirane

As a typical example of alunite s.s in a high temperature hydrothermal system, the occurrence, compositional heterogeneity and texture is described here for a specimen from Kusatsushirane volcano, Japan. An extensive acid sulfate alteration halo crops out on the western flank of the active Kusatsushirane andesite volcano; pyrophyllite and alunite zones have been identified, together with some zones of hydrothermal brecciation. The first occurrence of minamiite, the calcium analog of

Keywords : alunite, solid solution, magmatic hydrothermal system, growth banding, back scattered electron image, minamiite, Kusatsushirane

alunite, was also recorded (Ossaka *et al.*, 1982) from the alunite zone. Judging from the close spatial relationship with recent volcanic activity, and the high temperature suggested by stable isotope data, it is likely that acid volcanic fluids have been responsible for the alteration. Alunite s.s. is in close association with pyrite, with $\delta^{34}S$ of + 20.8‰ for alunite s.s. and − 0.2‰ for pyrite. Assuming isotopic equilibrium, the formation temperature is estimated to be about 290°C. Alunite s.s . shows coaxial overgrowth texture (Fig. 1) with sporadic dissolution and fragmentation. The chemical composition changes systematically from REE-and Sr-bearing crandallite through REE-free Sr-bearing crandallite, Sr-bearing woodhauseite to relatively random alternations of Na-K-Ca alunite s.s (Aoki, 1984). The PO_4/SO_4 ratio decreases outward to the boundary between woodhouseite and alunite s.s. The volume of phosphate-bearing core is less than 5% of the whole crystal.

Apatite contained as a primary mineral in the host andesite possibly released phosphate ion during the initial stage of acid leaching. The depletion of phosphate source mineral in the alteration halo along with the sustained supply of sulfate from a deep source could account for the PO_4/SO_4 ratio in the solution decreasing over a short period. REE concentration in the early formed phosphate-rich core can be explained as a derivative result from the high fractionation coefficient for trivalent cations of the crandallite structure. The major part of the crystal is composed of finely banded Na-K-Ca alunite s.s. containing no phosphate or REE elements. The irregular variation in the thickness of each band, and in the compositional contrast between adjacent bands, together with the relative homogeneity in each band, indicates some discontinuous process rather than gradual changes in temperature, pH and chemistry of the ambient fluid. During the cooling period of the hydrothermal system, early formed anhydrite likely dissolves to form a calcium-rich fluid because of the inverse temperature dependence of its solubility, and the progressive decrease of pH by dissociation of sulfuric and hydrochloric acid. The sporadic input of high

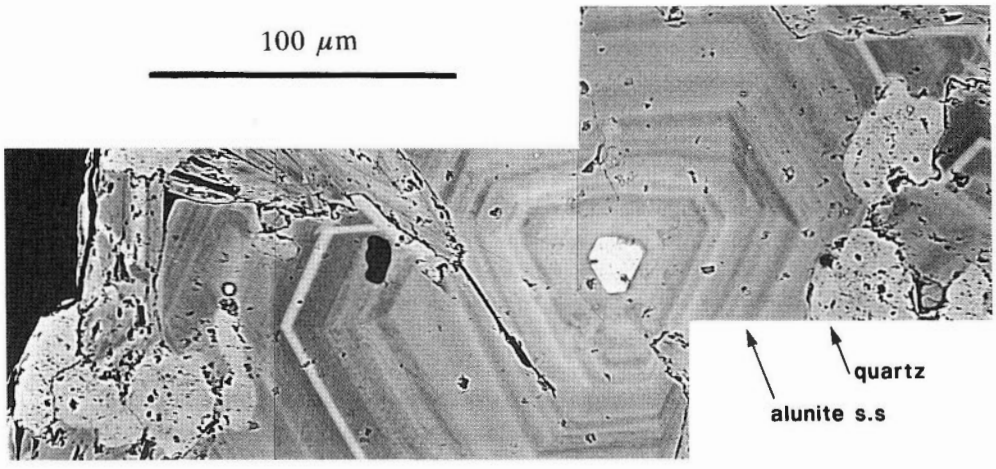

Fig. 1. Back scattered electron composition image showing typical growth banding texture in alunite s.s. Bright part with hexagonal outline is the core of crandallite and woodhouseite. Concentric hexagonal bands alternating randomly from dark gray to light gray around the bright core are natroalunite, minamiite, and alunite. Sample was collected from Okumanza, on the western flank of Kusatsushirane volcano, central Honshu, Japan.

temperature volcanic gas followed by the disproportionation of SO_2 could raise the temperature and sulfate concentration of ambient fluid, leading to the precipitation of anhydrite and reduction of calcium concentration in the solution again. In the higher temperature solution, sodium tends to be incorporated into the alunite structure, assuming a constant K/Na ratio in the solution (Stoffregen and Cygan, 1989). The observation that the sodium-rich alunite with rapid growth texture overgrowing on the broken surface of finely banded crystals supports the speculation of sporadic destruction of the fluid channel by the input of high temperature fluid. Thus the fluctuation of temperature and sulfate concentration and subsequent change in calcium concentration induced by the intermittent input of high temperature magmatic components have probably been responsible for the complex texture of the alunite s.s. crystal.

It is not surprising that some crystals lack a phosphate-rich core and contain a very small amount of calcium, and that some crystals are relatively homogeneous and show a gradual compositional change, even if the samples were collected from the same hydrothermal system. The relation between the growth texture in alunite crystals and the whole hydrothermal system can be compared to that of annual rings of tree to a forest in a mountainous district. There are various ages of trees in a wide variety of growing conditions in such a forest. Annual rings in each tree can record the only events which happened in the vicinity of the tree after its coming into the world. The wide spectrum in texture and chemistry itself is a characteristic feature of the alunite s.s. in the forest of the high temperature magmatic hydrothermal system.

References

Aoki, M. (1984) Occurrence of crandallite-florencite solid solution from the hydrothermal alteration halo at Okumanza, Gunma pref. *Proceedings of the Joint Meeting of the Mineral. Soc. Japan, the Soc. Mining Geol. Japan, and the Japanese Assoc. Miner. Petrol. Econ. Geol.* p. 16 (in Japanese).

Ossaka, J., Hirabayashi, J., Okada, K., Kobayashi, R. and Hayashi, T. (1982) Crystal structure of minamiite, a new mineral of alunite group. *Amer. Mineral.*, vol. 67, p. 114-119.

Stoffregen, R.E., and Cygan, G.L. (1989) An experimental study of Na-K exchange between alunite and aqueous sulfate solutions. *Amer. Mineral.*, vol. 75, p. 209-220.

Geological Survey of Japan Report, No. 277, 1991, p. 39-48

Hydrothermal Alteration Related to Kuroko Mineralization in the Kamikita Area, Northern Honshu, Japan, with Special Reference to the Acid-sulfate Alteration

Atsuyuki INOUE[1] and Minoru UTADA[2]

1) *Geological Institute, College of Arts and Sciences, Chiba University, Chiba, 260 Japan.*
2) *The University Museum, The University of Tokyo, Tokyo, 113 Japan.*

Introduction

The study of wall rock alteration contributes to the evaluation of processes of ore deposition (Meyer and Hemley, 1967). If we consider a hypothetical simple case of alteration, as exemplified by Meyer and Hemley (1967), the sequence of alteration may be easily understood on the basis of cross-cutting relation of veins and mineral paragenesis in the mineral zones. In actual cases, however, the distribution of alteration minerals is usually more complicated owing to the superimposition of alteration zones and the tectonic modification of early formed alteration at later stages. Therefore, determining the sequence of alteration is not always easy except in some specific cases.

We have examined the mineralogy of hydrothermal alteration products in the Kamikita Kuroko mineralization area, where acid-sulfate, propylitic, and other types of alteration are intricately distributed over a total area of about 100 km^2. The aim of this paper is to clarify the spatial and temporal relations of each type of alteration, in particular the relationships between the acid alteration and the other types of alteration, on the basis of field and laboratory investigations, including X-ray powder diffraction and microprobe analyses of secondary minerals and K-Ar age determination. We also attempt to clarify the differences in physicochemical conditions of each alteration on the basis of compositional variation of secondary minerals.

Outline of Geology and Ore Deposits

A simplified geologic map of the Kamikita area and the location of drill holes studied here are shown in Fig. 1. According to previous studies (Miyajima and Mizumoto, 1965; 1968; Lee, 1970; Lee *et al.*, 1974), marine sediments and volcanic rocks of Miocene to Quaternary age are distributed in the area. Rocks of Miocene age constitute the Kanegasawa, Yotsuzawa, and Wadagawa formations, in ascending order. The Kanegasawa formation is composed of massive and brecciated basaltic to andesitic lava flows. The Yotsuzawa and Wadagawa formations are composed mainly of andesitic to dacitic lava flows and volcaniclastic rocks; these rocks are intercalated with layers of mudstones. The three Miocene formations dip moderately (10-30°) at both sides of an anticlinorium with N-S trend in the studied area. They are intruded by several small quartz diorite bodies and by dacite and andesite intrusive rocks. A small diorite intrusive mass is found below 400 m in No. 15 drill hole. Hornfelsic rocks are not observed in the field and drill holes. The zones of

Keywords: Kuroko mineralization, Kamikita area, hydrothermal alteration, acid-sulfate alteration, propylitic alteration, alunite

volcanic activities at Kamikita appear to display a N–S trend.

The Quaternary group is divided into three formations: the Tashirodai welded tuffs, andesite lava flows, and lake deposits. They unconformably overlie the Miocene sediments.

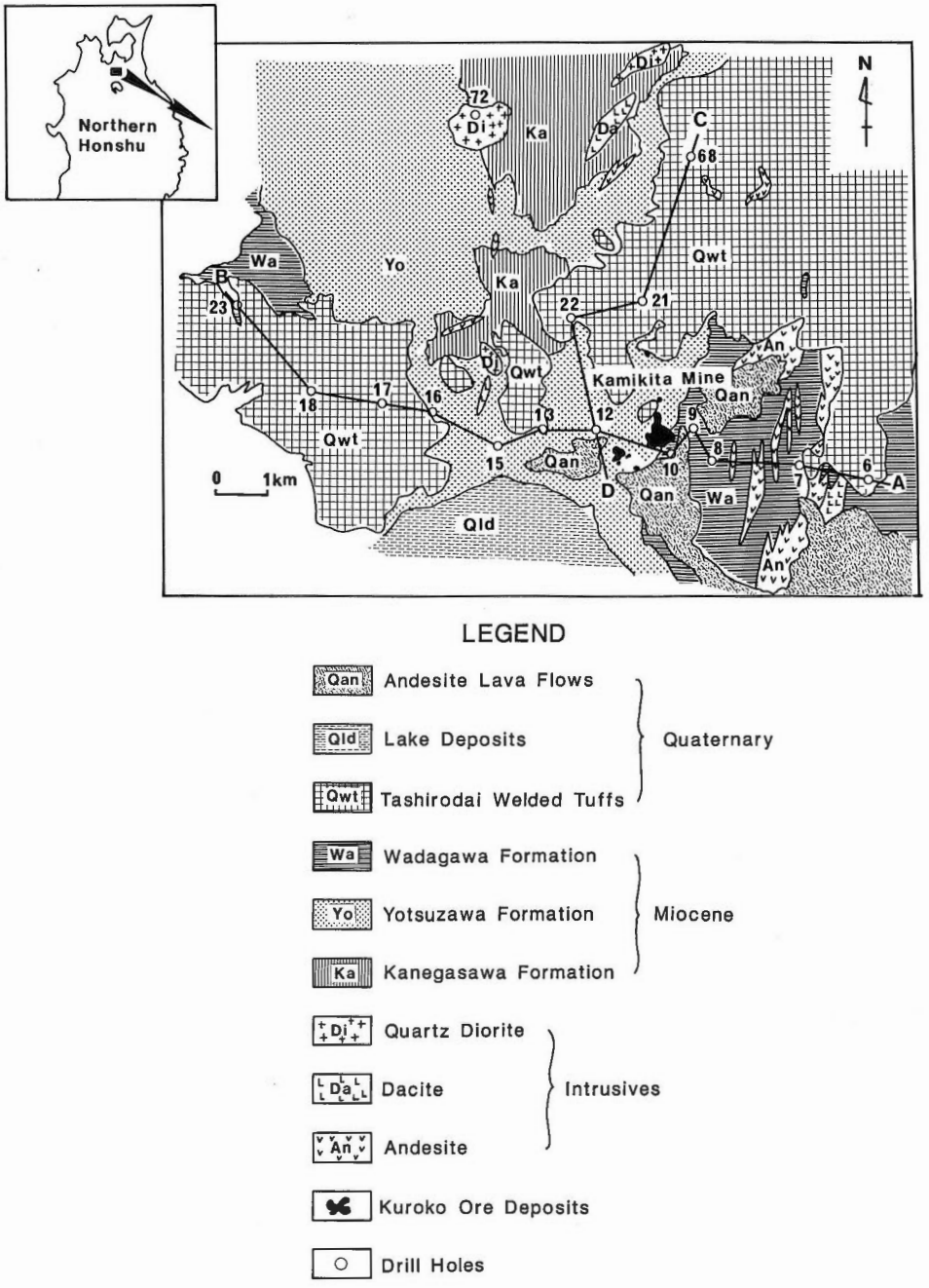

Fig. 1. Geologic map of the Kamikita area indicating locations of drill holes used in this study.

The Kuroko deposits are embedded just below a relatively thick mudstone of the lowermost horizon of the Wadagawa formation. Five deposits at Kamikita are localized along a N–S trend (Miyajima and Mizumoto, 1965; 1968). The deposits are characterized by fragmental ores poor in lead content (Lee *et al.*, 1974). Mining of all deposits has ceased.

Spatial Distribution of Alteration

More than one thousand samples were collected from 16 drill holes and outcrops (Fig. 1). The distribution and textural variation of secondary minerals were determined by X-ray powder diffraction and optical microscopy. Four types of alteration are distinguished in the Kamikita area, and each type of alteration can be divided into several mineral zones (Table 1). The distribution of alteration zones is illustrated in Figs. 2 and 3.

Alteration type I is found in the western part of the studied area (Figs. 2 and 3). The mineral zones are arranged concentrically from a small mass of diorite intrusion in No. 15 drill hole (center) to the periphery (approximately 6 km radius) in the following order: a biotite–actinolite zone, a chlorite–epidote zone, a corrensite–laumontite zone, a smectite–zeolite zone, and a smectite zone. The entire alteration extends from the Kanegasawa to the Wadagawa formations. Petrographic descriptions of the secondary products in alteration group I are given by Inoue and Utada (1991a). It is noteworthy that hematite and calcite are abundant over the whole range of alteration zones.

Alteration type II is found in the central part of the studied area (Figs. 2 and 3). The mineral zones are arranged from a K–feldspar zone in the stratigraphically lower part to a mixed layer mineral zone in the upper part, separated by an illite–chlorite zone in the middle part. The mixed layer mineral is usual illite/smectite, having various amounts of smectite layer. Abundant barite was identified in rocks from the Kuroko horizon of No.10 drill hole (Fig. 3). The mineral assemblage of alteration type II is nearly equivalent to those typical of the Kuroko-related hydrothermal alteration (Utada, 1980; 1988).

Table 1 Types and zones of hydrothermal alteration in the Kamikita area.

Types of alteration	Mineral zones
Alteration I	smectite zone smectite–zeolite zone corrensite–laumontite zone chlorite–epidote zone biotite–actinolite zone
Alteration II	mixed layer mineral zone illite–chlorite zone K–feldspar zone
Alteration III	laumontite zone wairakite zone
Alteration IV	mixed layer mineral zone pyrophyllite–diaspore zone alunite zone

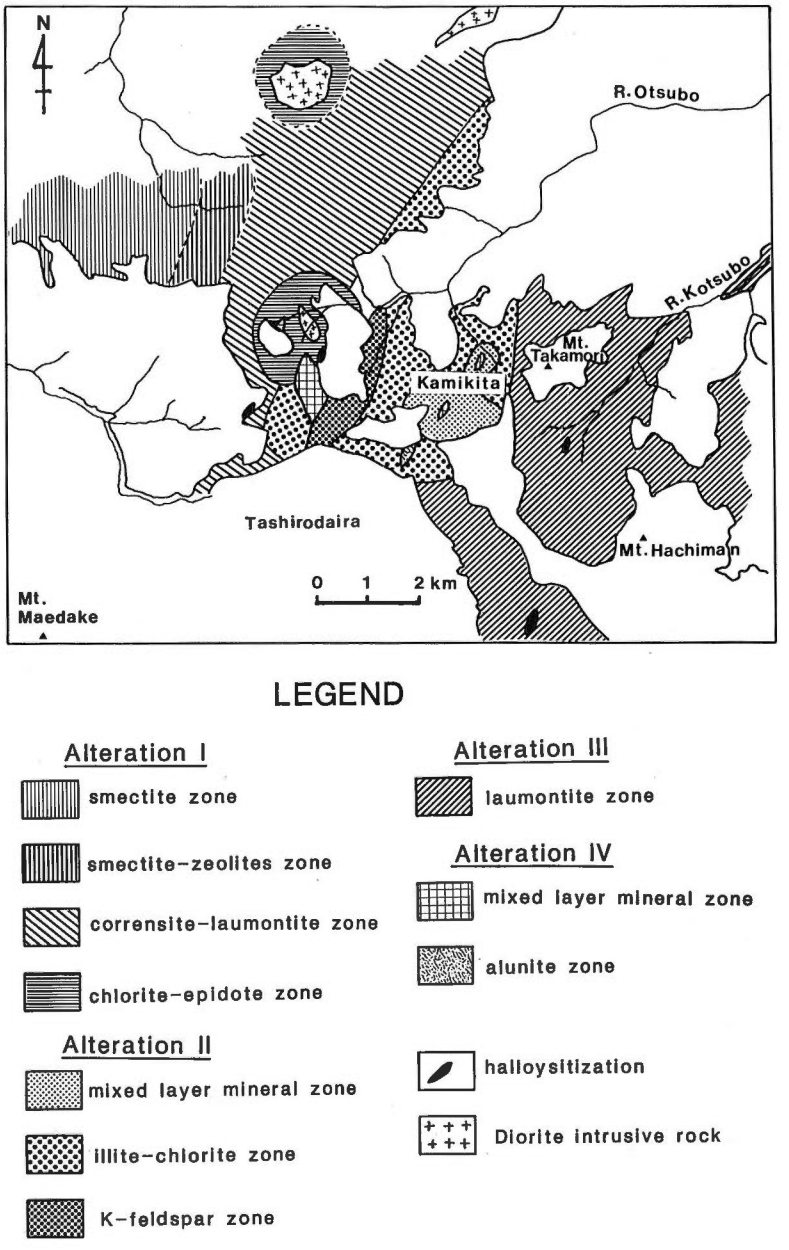

Fig. 2. Distribution of alteration zones in the Kamikita area.

Alteration type III is found in the eastern part of the studied area (Figs. 2 and 3). The alteration is confined to the upper part of the Yotsuzawa formation and the Wadagawa formation. This type of alteration, which is composed of laumontite and wairakite zones, is essentially characterized by the mineral assemblage of propylitic alteration (Meyer and Hemley, 1967), but is distinguished from alteration type I by the abundant occurrence of prehnite, pumpellyite, hedenbergite, and almandine–spessartine garnet (Inoue and Utada, 1991b). Calcite and hematite are rare in

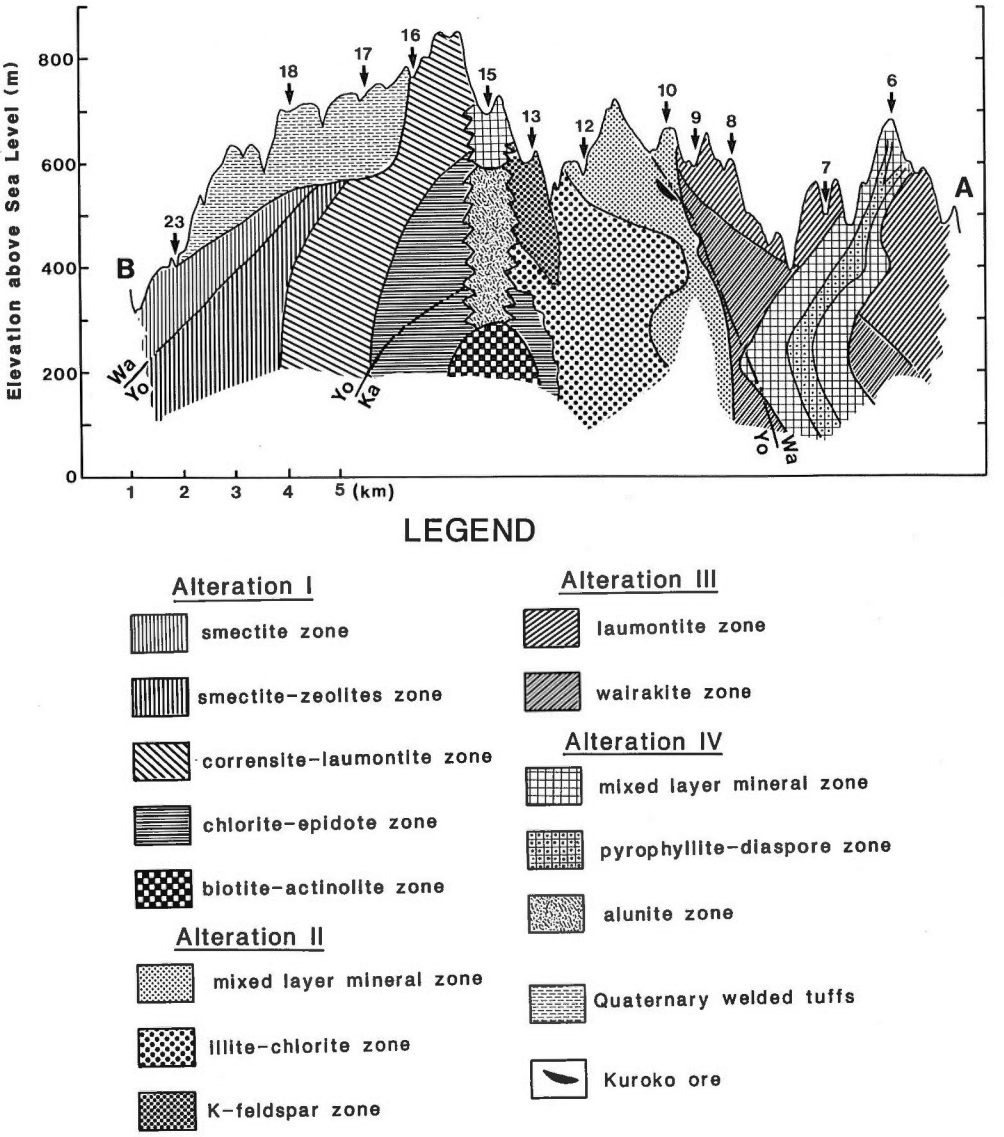

Fig. 3. Cross-section showing the distribution of alteration zones along the A–B line in Figure 1.

alteration type III, especially in rocks containing the above CaAl-silicates.

Alteration type IV is distributed locally in the central part of the studied area (Fig. 2). The alteration is characterized by the acid minerals. Among the three mineral zones included (Table 1), the pyrophyllite-diaspore and mixed layer mineral zones occur from the center to the margin, respectively (Fig. 3). The mixed layer minerals are mainly aluminous varieties such as tosudite and rectorite. The alunite zone, on the other hand, appears to be spatially discriminated from the above two zones. The alunite zone observed in No. 15 drill hole is comprised mainly of alunite, quartz, dickite, topaz, zunyite, and pyrite. The alunite zone, which outcrops on the surface, does not contain pyrite, topaz, and zunyite, and kaolinite instead of dickite

is the major polymorph.

In the Kamikita area, local halloysitization is found in the field (Fig. 2) and in drill hole (400–420 m depth in No. 15 drill hole). It affects both the Quaternary welded tuffs and the Miocene rocks.

Compositional Variations of Secondary Minerals

Illite, chlorite, and epidote occur commonly in the higher-grade zones of the alteration types I–IV. They show compositional variations characteristic of each type of alteration (Inoue and Utada, 1991c), and thereby it is possible to classify the type of alteration. The compositional variations of the unique minerals observed in each alteration zone, i. e., pumpellyite, prehnite, biotite, actinolite, etc., are discussed by Inoue and Utada (1989; 1991a; 1991b; 1991c). Here we refer only to the compositional variation in alunite.

The composition of alunite which was collected from drill holes and outcrops was determined with an energy-dispersive microprobe (EDS). The alunite usually shows very complicated compositional zoning within a single grain. When all of the point-analyses are plotted in a K–Na–2Ca diagram (Fig. 4), the K/(K + Na) ratio ranges from 0.1 to 0.9 and the Ca content is less than 0.3. The Fe content was negligible. Such compositional variations are common regardless of different occurrence.

Figure 5 shows variations in composition and amount of alunite as a function of depth in No. 15 drill hole. Based on the microprobe analyses, the alunite shows a large compositional variation from grain to grain within thin section, as well as within a single grain. The average composition, determined by the alunite 113 X-ray peak position, varies between 0.4 and 0.6 in K atomic proportion. The amount of alunite is also variable with depth; the variation is proportional to that of quartz and inversely proportional to that of dickite. The vertical variation in amount of pyrite coincides nearly to that of alunite. The amounts of topaz and zunyite vary nearly parallel to that of dickite.

The fluorine content in topaz ranges from 14.7 to 7.7 wt.%, determined by X-ray diffraction method (Ribbe and Rosenberg, 1971), which corresponds to a F/(F + OH) ratio of 0.7 to 0.85. The ratio tends to increase with depth.

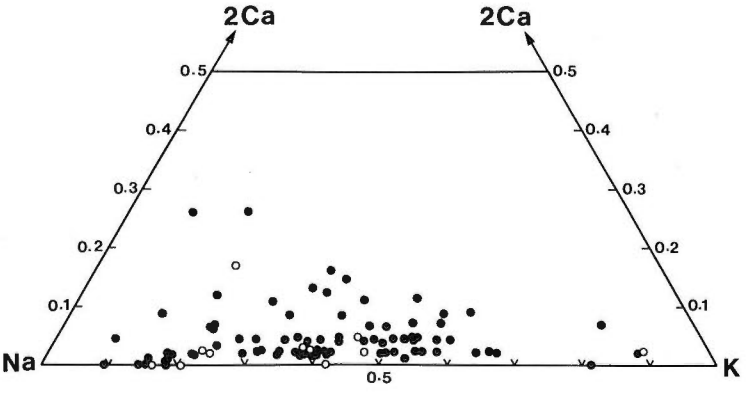

Fig. 4. Plot of atomic proportions of K, Na, and 2 Ca in alunite. Solid and open circles indicate alunite samples from drill holes and outcrops, respectively.

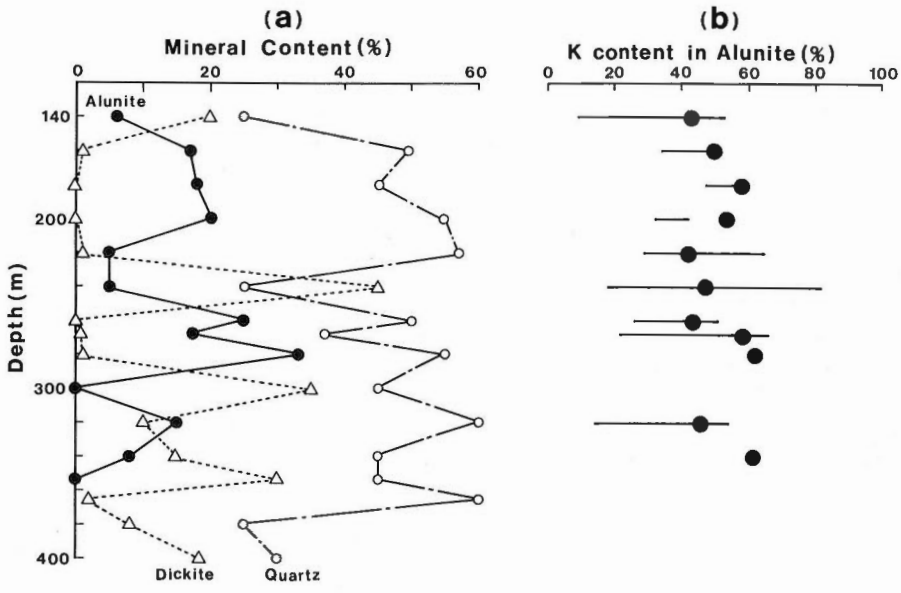

Fig. 5. (a) Variation of mineral content (wt.%) with depth in No. 15 drill hole. (b) Variation of K content (atomic proportion) in alunite with depth. Bars indicate the range of 10 points analyzed by microprobe. Solid circles indicate the average composition determined by X-ray diffraction method.

Physicochemical Conditions

The precise temperature and pressure conditions for the Kamikita hydrothermal alteration have not been defined, but an approximate range of temperature can be estimated from the mineral paragenesis by analogy with laboratory experiments and information on low-grade metamorphic terranes and active geothermal fields. The alteration type I is thought to form over a temperature range from $>300°C$ in the biotite-actinolite zone to $<100°C$ in the smectite zone (Inoue and Utada, 1991a). The transformation from smectite to chlorite through corrensite occurred between 100–200°C during alteration of type I (Inoue and Utada, 1991a). The maximum amount of smectite layers in illite/smectite of alteration type II is 40% (Inoue and Utada, 1991c); the value indicates the temperature to be around 100°C (Srodon and Eberl, 1984). The whole range of alteration type II took place at approximately 100–300°C, taking into account the formation temperature of Kuroko deposits. The formation of pumpellyite, prehnite, and hedenbergite probably took place at temperatures of 200–300°C in alteration type III (Inoue and Utada, 1991b). The temperature of formation of acid alteration IV was also in the range of 200–300°C.

From the above estimates, we took the temperature range to be 200° to 300°C and assumed vapor-saturation pressure of water at those temperatures. Based upon these assumptions and the compositional data of secondary minerals, we estimated the differences in fugacities of CO_2 and O_2 between the alteration types I and III.

The log $f(CO_2)$ of alteration type III is estimated to range from -2 to 0 (Inoue and Utada, 1991b). Prehnite, pumpellyite, and hedenbergite, characteristic of alteration type III, are absent from alteration type I, and calcite is more abundant in the latter. The log $f(CO_2)$ of alteration type I is estimated to range from -1 to 1, using the compositional data of epidote and illite. It is inferred that the low $f(CO_2)$ condition

facilitated the local formation of pumpellyite and prehnite in alteration of type III.

The log $f(O_2)$ of alteration type III is estimated to range from −47 to −34, using the compositional data of hedenbergite, prehnite, and epidote (Inoue and Utada, 1991b). The log $f(O_2)$ value for alteration type I was probably higher than that of alteration type III, perhaps between −40 and −30, because hematite is very abundant in alteration type I. Stoffregen (1987) estimated the log $f(O_2)$ value to be -31 ± 1 at 250°C for the formation of the quartz-alunite zone in the Summitville gold deposit. The $f(O_2)$ condition for the formation of the alunite zone at Kamikita may be similar to that at Summitville.

The pH value of solution related to the formation of the alunite zone at Kamikita is estimated to range from 2 to 4 at 200–300°C and an appropriate sulfur concentration, according to the experimental and theoretical studies of alunite by Hemley *et al.* (1969), Knight (1977), and Stoffregen (1987). As mentioned before, the alunite shows a repeated variation in amount over about 200 m interval in No. 15 drill hole, with the variation strongly correlated to the occurrence of dickite and quartz. The variation in amount among the three minerals can be represented by the reaction, 2(K, Na)-alunite + 6quartz + 3water = 3dickite + $2(K, Na)^+ + 4(SO_4)^{2-} + 6H^+$. In other words, the repeated variation in amount of alunite may reflect the pH fluctuation in reacting solution: lower-pH solution favors precipitation of alunite and alunite reacts with quartz to form dickite in higher-pH solution. Furthermore, the pH fluctuation in solution probably governed the average K content in alunite. As shown in Fig. 5, alunite apparently contains more K at lower pH values. There are many causes for a fluctuation of the pH of a solution moving upwards, but no reliable cause can yet be defined.

Temporal Relation of Alteration

Based upon the K–Ar ages of altered rocks, the temporal relation of the four types of alteration in the Kamikita area can be summarized as follows (Fig. 6); the intrusion of quartz diorite took place at 13 Ma and it caused the formation of alteration type I along its periphery. At 10–20 Ma, the Kuroko mineralization precipitated on the seafloor and concomitantly alteration type II was developed around the Kuroko deposits. Alteration type III began at nearly the same time as or slightly later in age than the Kuroko stage. Afterwards, alteration type IV locally superimposed upon the previous alteration; the formation of the pyrophyllite-diaspore zone was active at 6 Ma and then the alunitization followed at 3 to 4 Ma. In the Kamikita area, local halloysitization took place at the latest stage during the long hydrothermal activity.

In summary, the present study of alteration at Kamikita indicates that the different types of alteration observed within the total area of about 100 km^2 area resulted from reactions of rocks with different types of solutions ascending at different stages over a period of about 13 My. The acid alteration, including pyrophyllite, diaspore, and alunite, occurred in the later stages of the long history of the Kamikita hydrothermal system.

There remain many unsolved problems concerning the Kamikita hydrothermal system, for instance, (1) the geochemical relation of hydrothermal solutions which formed different types of alteration at different stages, (2) the relation between magmatism and hydrothermal activities, (3) the geological causes for the spatial restriction of distribution of alteration, and (4) the relation between the fossil and active hydrothermal systems, since the Hakkoda district (including the Kamikita

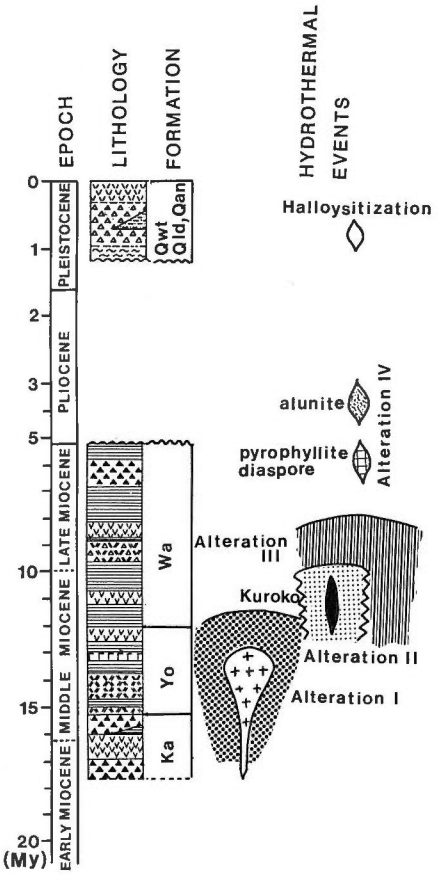

Fig. 6. Schematic represention of the temporal relationship of hydrothermal alteration at Kamikita.

area) is one of the regions of geothermal potential in Japan.

References

Hemley, J.J., Hostetler, P.B., Gude, A.J. and Mountjoy, W.T. (1969) Some stability relations of alunite. *Econ. Geol.*, vol. 64, p. 599–612.

Inoue, A. and Utada, M. (1989) Mineralogy and genesis of hydrothermal aluminous clays containing sudoite, tosudite, and rectorite in a drill hole near the Kamikita Kuroko ore deposit, northern Honshu, Japan. *Clay Sci.*, vol. 7, p. 193–217.

——— and ——— (1991a) Smectite-to-chlorite transformation inthermal metamorphism of volcaniclastic rocks at Kamikita area, northern Honshu, Japan. *Am. Mineral,* vol. 76, p. 628–640.

——— and ——— (1991b) Pumpellyite and related minerals from hydrothermally altered rocks at the Kamikita area, northern Honshu, Japan. *Can. Mineral,* vol. 29, p. 255–270.

——— and ——— (1991c) Hydrothermal alteration in the Kamikita Kuroko mineralization area, northern Honshu, Japan. *Mining Geol,* vol. 41, p.203–218.

Knight, J.E. (1977) A thermochemical study of alunite, enargite, luzonite, and tennantite deposits. *Econ. Geol.*, vol. 72, p. 1321–1336.

Lee, M.S. (1970) Genesis of the lower ore bodies, Kaminosawa ore deposit, Kamikita mine, Aomori Prefecture. *Mining Geol.*, vol. 20, p. 378–393 (in Japanese)

———, Miyajima, T. and Mizumoto, H. (1965) Geology of the Kamikita mine, Aomori Prefecture, with special reference to genesis of fragmental ores. *Mining Geol., Supecial Issue,* no. 6, p. 53–66.

Meyer, C. and Hemley, J.J. (1967) Wall rock alteration. In H.L. Barnes, ed., *Geochemistry of Hydrothermal Ore Deposits* Holt, Rinehart, and Winston, Inc., p. 166–235.

Miyajima, T. and Mizumoto, H. (1965) Geology and ore deposits of the Kamikita mine (I). *Mining Geol.*, vol. 15, p. 142–156 (in Japanese).

——— and ——— (1968) Geology and ore deposits of the Kamikita mine (II), with special reference to the volcanism and mineralization in the Okunosawa formation. *Mining Geol.*, vol. 18, p. 185–199 (in Japanese).

Ribbe, P.H. and Rosenberg, P.E. (1971) Optical and X-ray determinative methods for fluorine in topaz. *Am. Mineral.*, vol. 56, p. 1812–1821.

Srodon, J. and Eberl, D.D. (1984) Illite. In S.W. Bailey, ed., *Micas, Rev. Mineral.*, vol. 13, Mineral. Soc. Am. p. 495–544.

Stoffregen, R. (1987) Genesis of acid-sulfate alteration and Au-Cu-Ag mineralization at Summitville, Colorado. *Econ. Geol.*, vol. 82, p. 1575–1591.

Utada, M. (1980) Hydrothermal alteration related to igneous activity in Cretaceous and Neogene formations of Japan. *Mining Geol., Special Issue,* no. 8, p. 67–83.

——— (1988) Hydrothermal alteration envelope relating to Kuroko-type mineralization: A review. *Mining Geol., Special Issue,* no. 12, p. 79–92.

Hydrothermal Alteration Associated with Nansatsu-type Gold Mineralization in the Kasuga Area, Kagoshima Prefecture, Japan

Eiji IZAWA

Department of Mining, Kyushu University, Fukuoka, 812 Japan

Introduction

The Nansatsu-type gold deposits are characteristically associated with acid sulfate-type alteration. Tokunaga (1955) first recognized and described the acid nature of alteration at the Kasuga deposit. As formation temperatures of these deposits are rather high (200-240°C; Takenouchi, 1983; Izawa and Cunningham, 1989), they can not be formed by activity of near surface waters but rather are due to deep hydrothermal fluids.

The origin of deep, high temperature and acid fluids in the Nansatsu system is not fully understood. However, recent progress of exploration in the Nansatsu area by the Metal Mining Agency of Japan (MMAJ) provides new information about geologic structures and regional distribution of alteration around the deposits. In

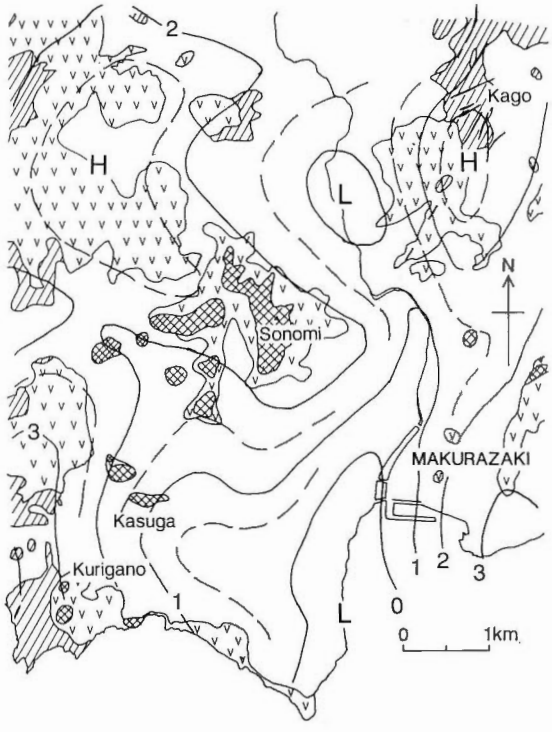

Fig. 1. Bouguer anomaly map of the Nansatsu district superimposed on geology. Contour interval is 1 (and 0.5-dashed) mGal for reduction density = 2.4g/cm^3. Legend for the geologic map is the same as in Figure 3.

Keywords : Nansatsu-type gold deposit, acid-sulfate alteration, Kasuga deposit, caldera, pyroclastic flow deposit, gravity anomaly, Shimanto Supergroup

this paper I describe a caldera-like structure in the Kasuga area and zonation of hydrothermal alteration from deep to shallow levels.

Materials used and procedures

Regional geologic and gravity data of the study area (Fig. 1) are based on the maps of MITI (Ministry of International Trade and Industry, 1985). Several drill hole data with some XRD results from the Kasuga mine area are reported by MITI (1988, 1989 and 1990). In addition, unpublished drill hole data of the Kasuga Mining Co., Ltd. were referred to.

Elevation data of the boundary between basement and overlying volcanic rocks of the Nansatsu Group were obtained from surface outcrops and several drill holes. On the basis of the elevation data the contour lines of the top of the basement were constructed (Fig. 2).

More than 200 samples from surface outcrops and drill cores were examined using XRD in our laboratory and assemblages of alteration minerals were obtained. The zonal distribution of the hydrothermal alteration of the area was characterized with this information.

Discussion and conclusion

It is considered that gravity data primarily reflect the depth of the basement. Hydrothermal alteration, especially silicification (high density), probably modifies the gravity pattern. In Figure 1 the high anomaly of Sonomi-dake is probably due

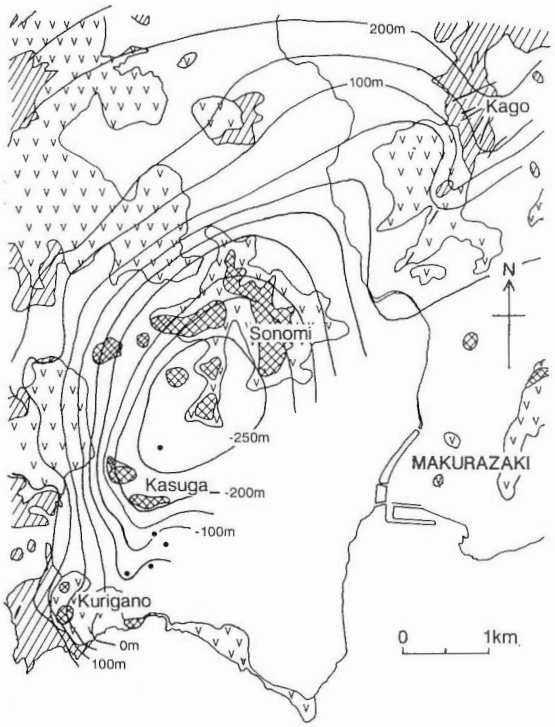

Fig. 2. Elevation of the top of the Shimanto Supergroup basement. Legend for the geologic map is the same as in Figure 3. Location of drill holes also shown as dots.

to the existence of a large, high density silica body near the surface. The cause of the low anomaly near Makurazaki city area is unknown.

Figure 2 shows a semi-circular depression in the basement rocks. Steep slopes are clearly recognized in the southern, western and northwestern parts of the depression. If the topography of the top of the basement represents a caldera collapse, major silica bodies (Kasuga and Sonomi) lie on the inner margin of the caldera wall, while the Kago vein system occurs outside the caldera. Figure 3 shows a NE-SW cross section through Sonomi and Kasuga.

Caldera forming activity in the Kasuga area is inferred from the existence of pyroclastic flow deposits which erupted shortly before (5.9-6.4 Ma) the mineralization event (4.5-5.5 Ma). Younger pyroclastic flow deposits are also recognized in the Iwato and Akeshi areas. These areas, however, have no indication of gravity lows or structural depressions of the basement.

The regional distribution of hydrothermal alteration was examined and Figure 4 constructed. Deep alteration beneath the silica body is characterized by abundant pyrite. Alunite is typically Na-rich and sometimes contains Ca. Dickite dominates over kaolinite. White Mg-rich chlorite occurs sporadically in the alunite-dickite zone (Hashizume and Izawa, 1983).

At depth the dickite-sericite assemblage changes to a sericite-chlorite assemblage.

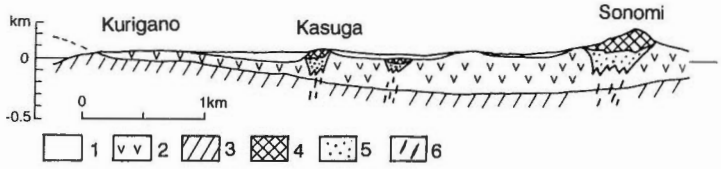

Fig. 3. NE-SW cross section of the Kasuga area. 1, Quaternary pyroclastic flow deposits; 2, Nansatsu Group; 3, Shimanto Supergroup; 4, silica body; 5, argillic zone; and 6, quartz vein.

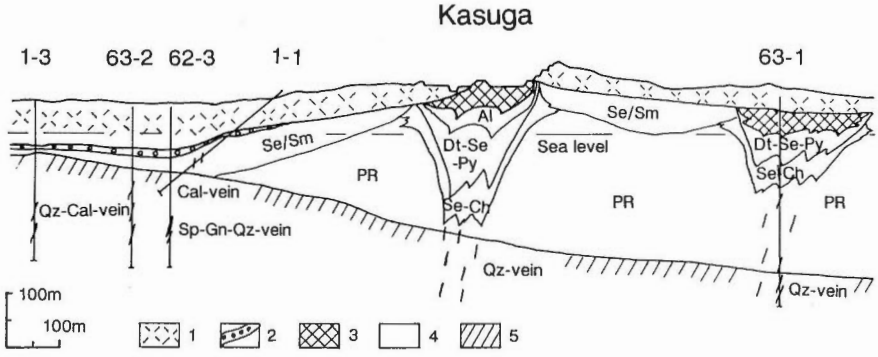

Fig. 4. Zonal distribution of hydrothermal alteration shown on a N-S cross section through the Kasuga deposit. Recent MMAJ drill holes are also shown (Fig. 2). 1, Quaternary pyroclastic flow deposits; 2, Gravels (Quaternary); 3, silica body; 4, altered volcanic rocks of the Nansatsu Group; and 5, Shimanto Supergroup. Al, alunite; Dt, dickite; Se, sericite; Py, pyrite; Ch, chlorite; Se/Sm, interstratified sericite-smectite; Qz, quartz; Cal, calcite; Sp, sphalerite; Gn, galena; and PR, propylitic alteration (quartz-chlorite-albite).

Both alteration assemblages are plagioclase destructive (argillic nature). Beneath the argillic zone narrow veins occur in propylitically-altered volcanic rocks and basement sedimentary rocks. Quartz, calcite, and sulfides (pyrite, sphalerite and galena) are common vein materials and the wall rock is characterized by sericitic alteration.

It is concluded that the ascending water was not highly reactive at depth to account for the lack of deeper acid alteration, though it became acid in the pyroclastic rocks of the Nansatsu Group. If mineralization took place in a caldera environment, the acid sulfate solution was formed by disproportionation of SO_2 gas that was added to the deep high temparature fluids during degassing of magma.

References

Hashizume, M. and Izawa, E. (1983) Hydrothermal alteration of the Nansatsu-type gold deposits, especially the Kasuga deposit (abstract). *Mining Geol,*, vol. 33, p. 49-50 (in Japanese).

Izawa, E. and Cunningham, C.G. (1989) Hydrothermal breccia pipes and gold mineralization in the Iwashita orebody, Iwato deposit, Kyushu, Japan. *Econ. Geol.*, vol. 84, p. 715-724.

MITI (1985) Report of regional geological survey; Nansatsu area, 1984 fiscal year. MITI, 180 p. (in Japanese).

——— (1988) Report of regional geological and structural survey; Nansatsu area, 1987 fiscal year. MITI, 23 p. (in Japanese).

——— (1988) Report of regional geological and structural survey; Nansatsu area, 1988 fiscal year. MITI, 39 p. (in Japanese).

——— (1990) Report of regional geological and structural survey; Nansatsu area, 1989 fiscal year. MITI, 130 p. (in Japanese).

Takenouchi, S. (1983) Fluid inclusion study of the Nansatsu-type gold deposits, southern Kyushu. *Mining Geol.*, vol. 33, p. 237-245 (in Japanese).

Tokunaga, M. (1955) Fundamental studies of the hydrothermal alteration at the Kasuga mine, Kagoshima Prefecture, Japan. *Mining Geol.*, vol. 5, p. 1-8 (in Japanese).

Isotopic Evidence for the Origin of Nansatsu Fluids

Yukihiro MATSUHISA, Jeffrey W. HEDENQUIST and Masahiro AOKI

Geological Survey of Japan
Higashi 1-1-3, Tsukuba, Ibaraki, 305 Japan

Introduction

Gold deposits in the Nansatsu district, southern Kyushu, Japan, are one of the typical examples of high-sulfidation or acid-sulfate type mineralization, which is believed to be a product of high-temperature acid fluids genetically related to magmatic activity at shallow depths. Gold mineralization, which is associated with copper mineralization (enargite) and pyrite, is spatially confined within an intensively silicified zone (>95% SiO_2) of host rocks. The silicified zone progresses outward into regional propylitic alteration through a very narrow (typically 1 to 3 m) zone of kaolinite (including dickite, alunite and minor pyrophyllite and diaspore). The details of geology, alteration and mineralization of the Nansatsu type deposits were described by Urashima *et al.* (1981), Hedenquist *et al.* (1988), Izawa and Cunningham (1989) and Izawa (1991, this volume), and compared with other types of high-sulfidation epithermal gold deposits by White (1991, this volume).

If the hydrothermal fluids responsible for the Nansatsu-type alteration and mineralization are high-temperature acid fluids directly originated from magmatic discharges, a magmatic signature may be present in the isotopic and chemical compositions of minerals and inclusion fluids. In a preliminary study (Hedenquist *et al.*, 1988), we found that the sulfur isotopic ratios ($^{34}S/^{32}S$) of sulfides and sulfate

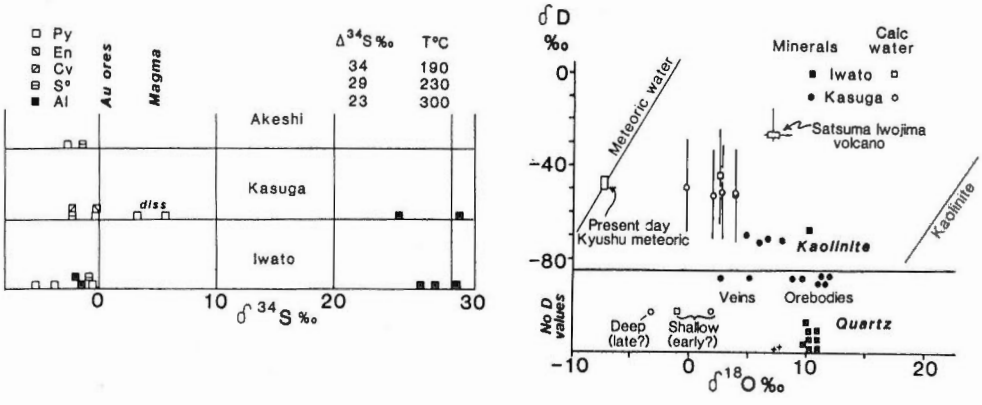

Fig. 1. Summary of (a) sulfur and (b) hydrogen and oxygen isotopic data by Hedenquist *et al.* (1988).

Keywords: Nansatsu-type gold deposit, high-sulfidation mineralization, hydrothermal fluid, magmatic fluid, sulfur isotopes, hydrogen isotopes, oxygen isotopes

(alunite) and their fractionation are suggestive of their origin from the disproportionation of magmatic SO_2 (Fig. 1a). However, the hydrogen (D/H) and oxygen ($^{18}O/^{16}O$) isotopic ratios of clays and quartz are somewhat ambiguous with respect to the fluid origin (Fig. 1 b). Although the $\delta^{18}O$ value of water estimated from the quartz composition is close to 0 per mil, which could be consistent with a contribution of magmatic water, its δD value based on the clay composition favors an ^{18}O-enrichment of meteoric water by reaction with heated rocks.

Fluid inclusion data of the Nansatsu quartz indicate dilute solutions of <1 wt% NaCl equivalent and homogenization temperatures of 190 to 240°C (Hedenquist *et al.*, 1988). If gold is transported by a low-pH acid fluid, the chloride concentration of the fluid may be extremely high (Henley, 1990). This does not appear to be the case in the Nansatsu deposits. To avoid this conflict, Berger and Henley (1989) suggested that in these types of deposits the metals were introduced by a later stage, neutral-pH, low-sulfidation fluid which invaded the previously-formed acid alteration zone following the decline of volcanic activity. White (1991, this volume) proposes a new model in which high sulfidation deposits are produced from a magmatic fluid that segregates into two phases during transport. The acid alteration is produced by interaction of precedent volatile magmatic fluid with groundwater, while the mineralization results from groundwater dilution of the subsequent denser magmatic fluid.

In this paper, we present additional oxygen isotopic data for quartz taken from peripheral vein systems surrounding the Kasuga deposit, western area of the Nansatsu district, and once again look at the isotopic evidence for the sources of fluids.

Oxygen Isotope Ratios of Vein Quartz

In the Kasuga area, western Nansatsu district, more than ten silicified rock bodies are clustered within a caldera structure (about 7 km across), although direct evidence indicating the caldera is fragmentary (Fig. 2). Many quartz veinlet systems radially cut the caldera structure, and are associated with an alteration mineral assemblage of zeolite (chabazite, stilbite, laumontite and wairakite), calcite and pyrite. Although no age data are available (the K-Ar age of the Kasuga deposit is 5.0 Ma), these veinlet systems may represent the peripheral zone of the hydrothermal system which prevailed in the caldera. A NE-trending quartz vein system, which has produced 0.6t Au, is also located in the Kago area northeast of the caldera. The caldera itself appears to lie on the NE-trending regional structure of the basement.

Vein quartz from the peripheral area has uniform $\delta^{18}O$ values of $+12$ to $+13$ per mil, while quartz from the Kago veins has a lower $\delta^{18}O$ value of $+5.6$ per mil (Fig. 2). Vein quartz cutting the silicified rocks of the Kasuga deposit at various depths also has low $\delta^{18}O$ values of $+2.7$ to $+5.8$ per mil (Hedenquist *et al.*, 1988, and this study). Based on zeolite and clay mineralogy, we can make a temperature estimate of 150 to 180°C for the peripheral vein quartz, and 180 to 200°C for the Kago vein quartz; based on these temperatures, $\delta^{18}O$ values of fluids are calculated to be -3.5 to -0.5 per mil for the former, and -7.5 to -6.0 per mil for the latter, respectively. The fluids in the peripheral vein systems are similar to or slightly lighter in isotopic composition than that in the silicified zones of Nansatsu-type alteration, while the hydrothermal system responsible for the Au-bearing quartz veins in the Kago area is much lighter, and is probably meteoric-water dominant. Meteoric-water dominant fluids also invaded the silicified zones in the later stage.

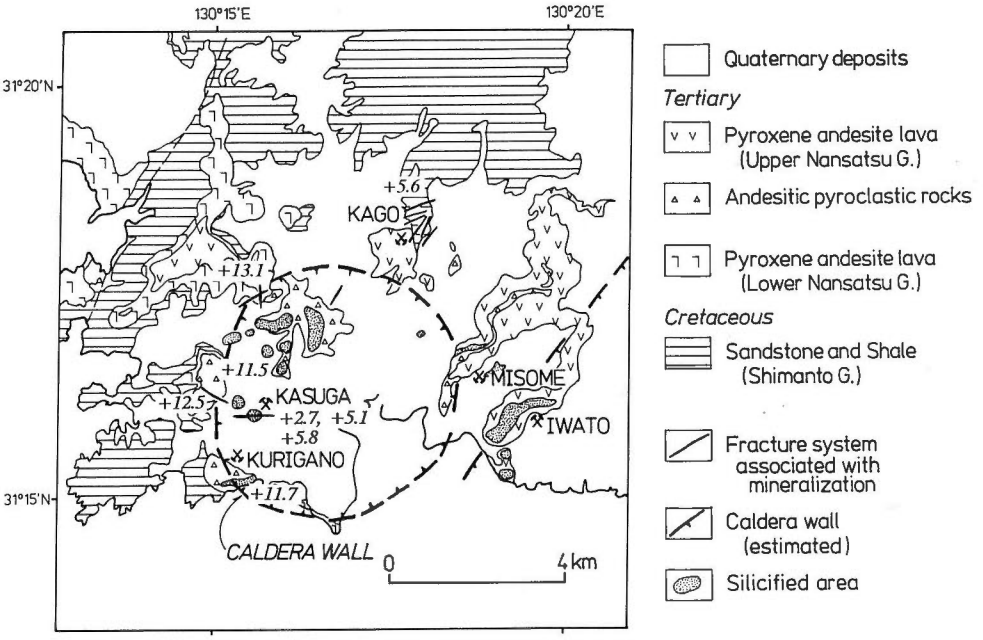

Fig. 2. Geologic map of the Kasuga area, western Nansatsu district, Kyushu. Numbers in italics indicate $\delta^{18}O$ values of vein quartz.

Systematics of Thermal Fluids

Figure 3 summarizes the δD and $\delta^{18}O$ values of quartz, clays and thermal waters. The silicified rocks have uniform $\delta^{18}O$ values of + 8 to + 11 per mil, which indicate $\delta^{18}O$ values of − 2 to + 2 per mil for their host fluids (calculation is based on the isotopic fractionation determined by Matsuhisa *et al.*, 1979). The $\delta^{18}O$ values of fluids become lighter (− 6.0 to − 7.5 per mil) for the Kago veins through the peripheral veins and deep veins. Although this says nothing about hydrogen isotopes, this trend may correspond to the mixing of magmatic and meteoric waters. The initial thermal fluids, which produced acid-leached silicified zones within the caldera, may have been a half-magmatic and half-meteoric mixture. Then, as the hydrothermal system evolved, the fluids became more meteoric-water dominant in the peripheral and later stage vein systems, as well as having been neutralized. This type of a mixing trend of thermal waters is well documented in present-day volcanic hydrothermal systems (e. g. Hedenquist and Aoki, 1991, this volume).

A problem is raised from clay minerals. The clay minerals taken from clay zones enveloping the silicified zones have $\delta^{18}O$ values of + 5 to + 8 per mil, which indicate a fluid composition concordant with that of the silicified rocks (Fig. 3). Although the δD values of clays fall in a narrow range of − 72 to − 69 per mil, the δD values of corresponding fluids are estimated with a large uncertainty to be − 54 to − 50, or − 70 to − 66 per mil, with the two different results due to discrepancy in proposed fractionation factors (Marumo *et al.*, 1980 ; O'Neil, 1986). In either case, the δD values of fluids estimated for the clays are far lower than that expected from the mixing of magmatic and meteoric waters (Fig. 3). The magmatic composition was taken from present-day active volcanic fluids of southern Kyushu, and the meteoric water composition is also for present-day local meteoric waters. We have no other estimate at this moment for 5 Ma meteoric waters in the region, but their δD values

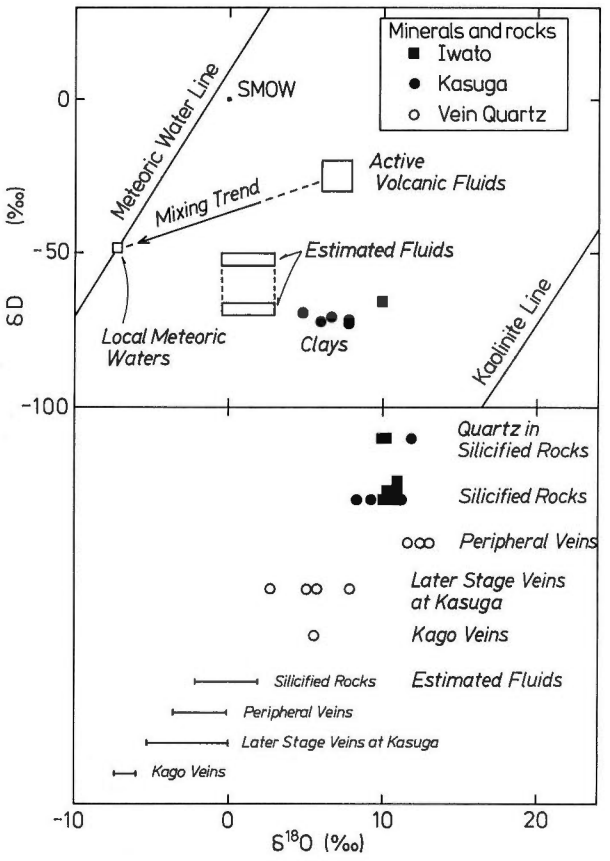

Fig. 3. δ D–δ^{18}O plot for rocks, minerals and the calculated Nansatsu fluids, the latter estimated from mineral data.

could not be lower than − 70 per mil.

Oxygen isotope shift of meteoric waters by reaction with rocks may be a possible way to produce the fluids deduced from clay analyses. However, such fluids would have a neutral pH, which does not agree with the acid alteration of both silicified and clay zones. Furthermore, the clay-related fluids in Fig. 3 seem to be even more depleted in D than present-day meteoric waters.

Steam condensate may be another candidate for low-δD water. Condensation of steam separated from the main thermal fluids at low temperatures (<150°C) could be depleted in D. In order to produce the observed clay alteration, however, the temperature of steam separation must not be lower than 200°C. Hydrogen isotope fractionation in this temperature range is too small to produce the desired shift of δD value by steam separation (fractionation crossover takes place at 220°C). The zonal distribution of clay alteration with respect to the silicified zones argues against a model involving discrete fluids for the two zones.

One possible way to get out of this dilemma may be to extend the experimental uncertainty of hydrogen isotope fractionation between clays and water. Since there is quite a large discrepancy in determining the hydrogen isotope fractionation in the interested temperature range, we tend to lean to the possibility that the fluids equilibrated with clays were on the mixing line of magmatic and meteoric waters

(whose end-member compositions may also have been different from those today). An alternative is that the magmatic water responsible for the mixing might not be represented by the active volcanic fluids in the region (Fig. 3), but may have had a δD range of -40 to -80 per mil, closer to that of the primary magmatic water of Taylor (1974). Further study is necessary to deduce the complete history of these hydrothermal systems, including hydrogen and oxygen isotopic analysis of alunite and other clays, and possibly hydrogen isotopic composition of inclusion fluids within the silicified rocks.

References

Berger, B.R. and Henley, R.W. (1989) Advances in the understanding of epithermal gold-silver deposits, with special reference to the western United States. *Econ. Geol. Monograph,* 6, p. 405–423.

Hedenquist, J.W. and Aoki, M. (1991) Isotopic and metal compositions of volcanic discharges in Japan, and implications for mineralization. In Matsuhisa, Y., Aoki, M. and Hedenquist, J.W., eds., *High-temperature acid fluids and associated alteration and mineralization, Geol. Survey Japan Report,* no. 277, 71–76.

———, Matsuhisa, Y., Izawa, E., Marumo, K., Aoki, M. and Sasaki, A. (1988) Epithermal gold mineralization of acid-leached rocks in the Nansatsu district of southern Kyushu, Japan. *Geol. Soc. Australia Abstracts,* no. 22, p. 183–190.

Henley, R.W. (1990) Ore transport and deposition in epithermal environments. In Herbert, H.K. and Ho S.E., eds., *Stable isotopes and fluid processes in mineralization, Geol. Dept. & Univ. Extension, Univ. Western Australia,* Pub. no. 23, p. 51–69.

Izawa, E. (1991) Hydrothermal alteration associated with Nansatsu-type gold mineralization in the Kasuga area, Kagoshima Prefecture, Japan. In Matsuhisa, Y., Aoki, M. and Hedenquist, J.W., eds., *High-temperature acid fluids and associated alteration and mineralization, Geol. Survey Japan Report,* no. 277, 49–52.

——— and Cunningham, C.G. (1989) Hydrothermal breccia pipes and gold mineralization in the Iwashita orebody, Iwato deposit, Kyushu, Japan. *Econ. Geol.,* 84, p. 715–724.

Matsuhisa Y., Goldsmith, J.R. and Claytom, R.N. (1979) Oxygen isotopic fractionation in the system quartz-albite-anorthite-water. *Geochim. Cosmochim. Acta,* vol. 43, p. 1131–1140.

Marumo, K., Nagasawa, K. and Kuroda, Y. (1980) Mineralogy and hydrogen isotope geochemistry of clay minerals in the Ohnuma geothermal area, northeastern Japan. *Earth Planet. Sci. Lett.,* vol. 47, p. 255–262.

O'Neil, J.R. (1986) Theoretical and experimental aspects of isotopic fractionation. *Reviews in Mineralogy,* 16, p. 1–40.

Taylor, Jr., H.P. (1974) The application of oxygen and hydrogen isotope studies to problems of hydrothermal alteration and ore deposition. *Econ. Geol.,* vol. 69, p. 843–883.

Urashima Y., Saito, M. and Sato, E. (1981) The Iwato gold ore deposits, Kagoshima Prefecture, Japan. *Mining Geol. Special Issue,* no. 10, p. 1–14 (in Japanese).

White, N.C. (1991) High sulfidation epithermal gold deposits: characteristics and a model for their origin. In Matsuhisa, Y., Aoki, M. and Hedenquist, J.W., eds. *High-temperature acid fluids and associated alteration and mineralization, Geol. Survey Japan Report,* no. 277, 9–20.

Geological Survey of Japan Report, No. 277, 1991, p. 59–65

Mineralogy, Distribution and Origin of Acid Alteration in Philippine Geothermal Systems

Agnes G. REYES

Geothermal Division, Philippine National Oil Company–Energy Development Corporation, Fort Bonifacio, Manila, Phipippines

Introduction

Overview of Philippine Geothermal Systems

Seventeen of the thirty geothermal systems in the Philippines have deep wells (depth > 1500 m), four of which provide 894 MWe or 15.4% of the country's electrical power needs.

Philippine geothermal areas are closely linked with Pleistocene to Recent calc-alkaline volcanic complexes, dominated by andesite; or with smaller silicic andesite to dacitic domes. A cross-section of a typical Philippine geothermal system is shown in Fig. 1.

It is common for Philippine geothermal systems to have had several hydrothermal regimes, one of which is presently active, and the rest extinct or waning. In geothermal systems like Palinpinon, portions of the extinct hydrothermal system/s are exposed on the surface and are sometimes explored for epithermal deposits.

The major sources of permeability in the wells are gravity or normal faults with dips of 70–90°C. However, lithological contacts, breccias, fractures, and joints may also provide permeability (Reyes, 1990).

Objectives of Study

The presence of acid sulfate fluids has a debilitating effect in the development of a geothermal system, and may drastically limit the resource. Thus, detailing the occurrences of acid alteration, and understanding its origins and hydrology, may assist in planning the exploration and development strategy of a geothermal resource. The study of acid alteration in active hydrothermal systems may also contribute to an understanding of certain ore deposits such as the high sulfidation type associated with the enargite group of minerals. This study reviews the occurrences, geochemistry, temperature ranges, and mineral assemblages of acid alteration in Philippine geothermal systems, except for Tiwi and Makban, which are privately developed.

Occurrences

Patches of acid alteration common on the surface of most geothermal areas in the world usually form as products of steam-heated acid sulfate fluids when H_2S-laden steam condenses into surficial water (White, 1957). Reaction of groundwaters with sulfur sublimating from H_2S, or relict acid sulfate minerals may also produce a new generation of acid sulfate fluids and alteration as in Rotokawa, New Zealand (Browne, pers. comm., 1985).

However, the propensity for the formation of deep acid alteration, i.e., $\geq$500 m

Keywords: Philippine geothermal systems, acid alterations, fluid inclusions, fluid chemistry

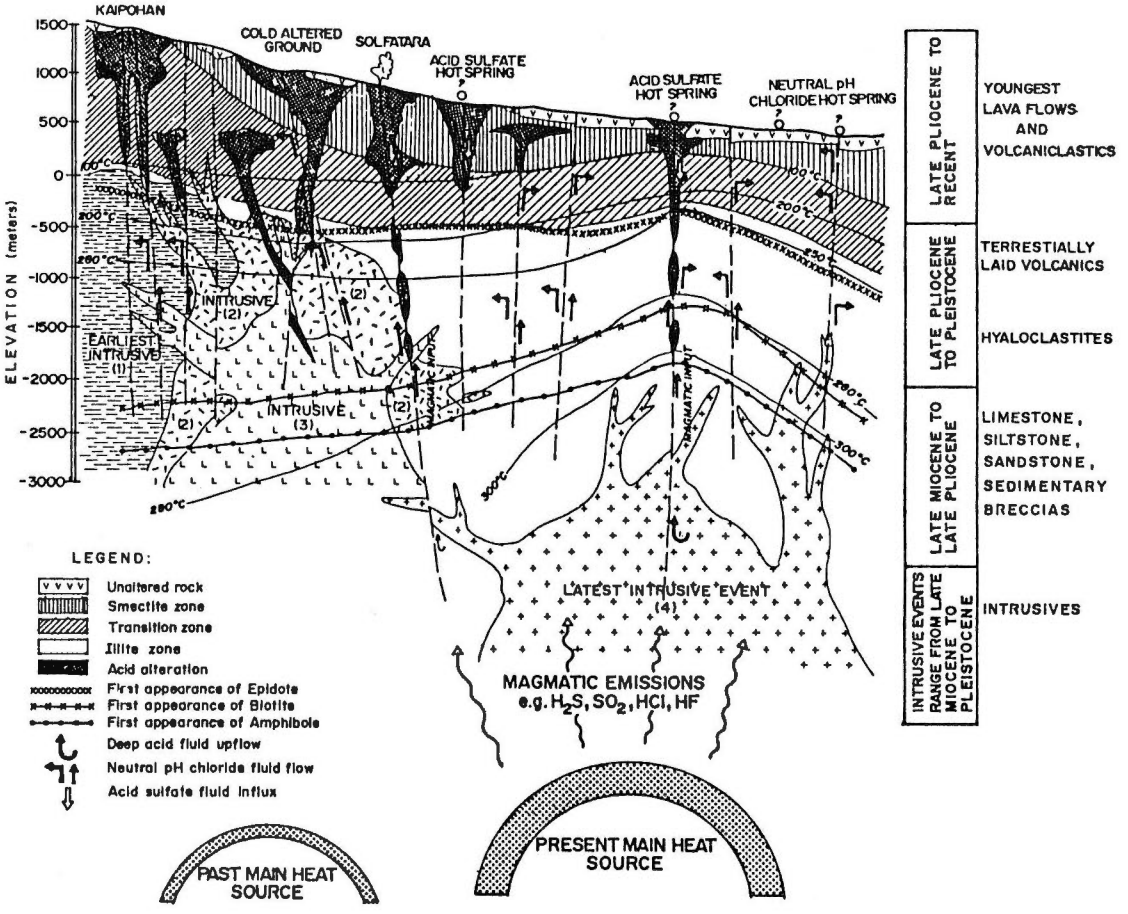

Fig. 1. Geologic model, alteration patterns, and stratigraphy typical of a Philippine geothermal system. The lateral extent of this model is 2–15 km. Note that downflowing acid sulfate fluids may occur throughout the system; but deep acid fluid upflow is associated with young intrusives and deeply-penetrating structures.

depth, and the presence of acid fluid discharging from wells, are common in andesitic to dacitic-hosted geothermal systems (Henley, 1985) e.g., Matsukawa, Otake, Hatchobaru, and Komatsu, in Japan (Sumi, 1969; Sumi and Maeda, 1970; Hayashi, 1973; Browne, 1978; Manabe and Ejima, 1984), Tatun in Taiwan (Chen, 1970), Indonesia (Browne, 1978), Mexico (Cathelineau *et al.*, 1985), Costa Rica (Corrales, pers. comm., 1986), and the Philippines.

Acid alteration in the Philippines occurs in about 90% of the wells reviewed, with about 45% having the potential to discharge acid fluids upon field exploitation. However, to date, only 17 wells are confirmed acid, with some having acid influx occurring only at certain borehole conditions. In general, acid wells have low mass flows and relatively low permeabilities.

Acid alteration in wells may be related to a buried hot spring system or solfatara; or localized along structural zones. These usually form sharp boundaries with the rest of the rock, which is pervaded by neutral pH alteration. Acid altered rocks are

usually only a few tens of centimeters thick. However, thicknesses may be greater in volcaniclastics, as in well OK-11D in Palinpinon, where as much as 750 m is observed. On the average, acid alteration occurs sporadically down to 1600–1800 m, rarely extending down to 2500 m, with thickness and frequency diminishing with depth.

Acid sulfate surface thermal manifestations, whether relict or not, are usually harbingers of subsurface acid alteration, although their absence does not preclude the latter. For example, in the western sector of Palinpinon, ~85% of the surface faults are associated with acid altered ground. Subsequent examination of cuttings confirmed the presence of acid minerals along their subsurface intersections. Since structures are the main avenues for acid fluids deep in the system, study is focussed on structures to determine if the faults channel deep acid fluids (with magmatic input) or merely act as conduits of acidified fluids from the surface.

Mineralogy

About 35 minerals were identified in acid alteration assemblages. Due to extreme depletion in alkali cations, there are little, if any, interlayered clays in this assemblage.

Acid alteration minerals are divided into 5 zones based on the sequential appearance of index clays and associated minerals, with increasing depth, temperature, and distance from the main source of acid fluids (Fig. 2). From the kaolinite to the muscovite zone, there is an increase in the dehydration of the clays, crystallinity, silica content of the clays and aluminosilicates, and the ratio of anhydrite to alunite. Thus, as the acid fluids react with the rock, pH increases, the silica activity of the environment increases and the sulfate activity decreases. Minerals characteristic of acid fluids, e.g., quartz, diaspore, sulfates, sulfides, and iron oxides, are not inert, as suggested by dissolution and reprecipitation textures observed under the SEM.

Types of Acid Alteration

Aside from temperature-based zonations, acid minerals can be divided into two types, based on the virulence and corrosivity of the associated fluids and the propensity of the assemblage to rejuvenate fluid acidity. These are:

1) *Virulent* acid alteration characterized mainly by the presence of sulfur ± alunite ± abundant pyrite/marcasite, and

2) *Deceptively benign* acid alteration characterized by the absence of sulfur and alunite; and the presence of kaolinite, dickite, pyrophyllite, diaspore, anhydrite, and pyrite.

Virulent acid alteration occurs at shallower levels than the other type. In the Bacon-Manito geothermal system, the former persists down to a maximum of 1250 m while the latter can persist to 2500 m. Acid alteration often changes from a virulent to a relatively benign type to neutral pH alteration with depth, along a structure; or laterally, away from the main acid sulfate fluid channel.

When encountered within well aquifers, virulent acid minerals portend immediate acid fluid discharges from a well and intense corrosion of well pipes. Even when relict, the reaction of neutral pH fluids with virulent mineral assemblages rejuvenates fluid acidity- a mechanism that may be aggravated by high temperatures. The second type is deceptively benign as acid fluids may not be apparent during initial well discharges, as in some wells in Tongonan, Palinpinon, and

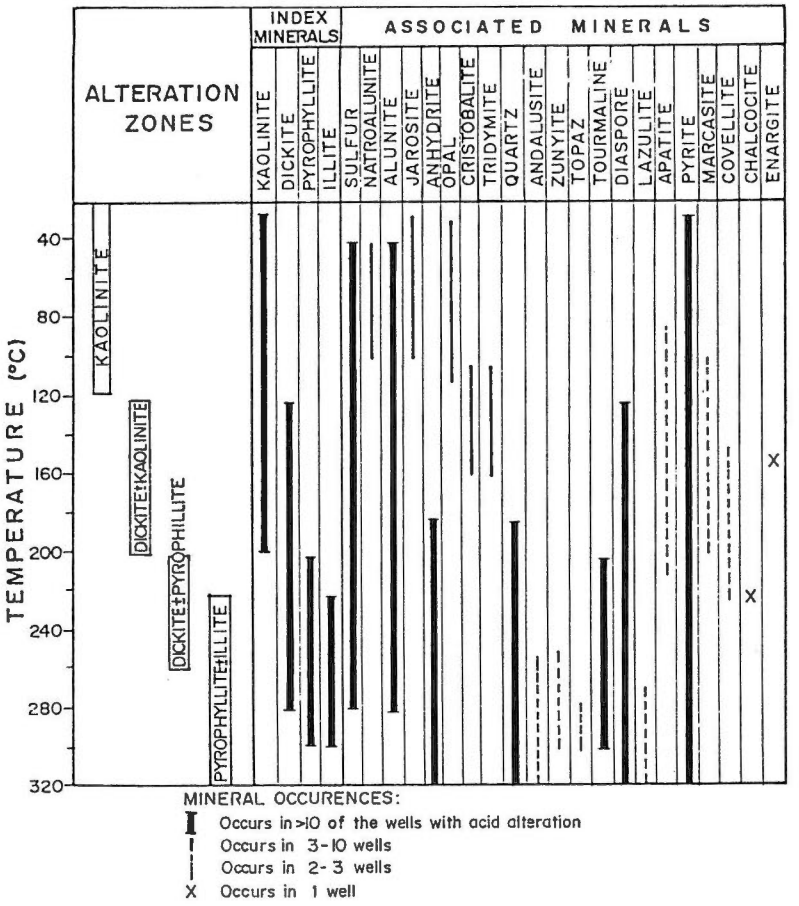

Fig. 2. Acid alteration zones and temperature ranges. Temperatures are based on direct measurement and fluid inclusion homogenization data, as well as temperatures of contiguous neutral pH alteration assemblages.

Bacon-Manito. Exceptions are a well in Mt. Pinatubo, and OK-11D in Palinpinon. The former intersected pyrophyllite + diaspore + anhydrite + abundant pyrite ± lazulite. OK-11D encountered minor acid alteration, but not in the aquifer zones. The Mt. Pinatubo well produced acid fluids upon discharge (Villarosa, pers. comm., 1989), while OK-11D produced molten sulfur nearly two years after drilling (Sarmiento, pers. comm., 1985). Both wells show active magmatic input based on fluid chemistry (Ruaya, pers. comm., 1990) and are adjacent to one of the latest volcanic edifices in each area. In fact, Mt.Pinatubo volcano started to erupt in June 1991.

Rock Chemistry and Mineralogy

Acid sulfate fluid incursion usually results in the complete recrystallization of the rock and mobilization of base cations, leaving hardly any primary minerals. Deep acid assemblages are often closely associated with fractures/faults.

Acid altered rocks are composed largely of residual oxides. Calcium is usually fixed in anhydrite. Potassium forms alunite at low pH, high sulfate activity, and low to moderate temperatures; and illite and muscovite at higher temperatures, pH,

and silica activity. Sodium is rarely partitioned into natroalunite, usually at temperatures below 150°, while magnesium forms hardly any stable mineral in acid zones except for rare lazulite or ralstonite. Mg-rich clays, such as sepiolite, form abundantly at the contact of acid and neutral pH alteration. Total sulfur increases in acid assemblages and occurs in the form of sulfur, sulfides, and sulfates. In Bacon-Manito, there is an increase in arsenic and a depletion in copper and zinc in acid zones. In Palinpinon, arsenopyrite forms as well scales where there is acid sulfate fluid influx.

Fluid Inclusion Studies

Fluid inclusion homogenization and freezing temperatures were measured in anhydrite, quartz, diaspore, and rarely, alunite. Homogenization temperatures usually range from 90° to $\geq$ 420°, similar to those of fluid inclusions in adjacent neutral pH altered rocks. In general, fluid inclusions high in gas are more common in acid assemblages, often forming clathrates that disappear at about 1 to 11°C. Inclusions in diaspore and alunite are often vapor-rich, and in the case of diaspore from Bacon-Manito, homogenize to the vapor-phase. Where clathrates are absent, fluid inclusion equivalent salinities in acid assemblages are similar to those associated with contiguous neutral pH minerals; and when applicable, to well aquifer fluids.

In cases where magmatic input is suspected, based on mineralogy and well fluid chemistry, fluid inclusions show the following characteristics:

1) abundance and variety of isotropic to anisotropic daughter minerals, with

Table 1 A comparison of acid and neutral pH fluids in Tongonan and Palinpinon. These are discharge data from selected wells, analysed at 25°.

FLUID COMPONENT	CHARACTERISTICS
pH	<5.5 for acid fluids
Cl	Generally lower for acid fluid discharges at~3700-13600 ppm
	~8100-25700 ppm for neutral fluids
Ca	Generally lower in acid discharges at~40-200 ppm
	~160-500 ppm for neutral fluids
Mg	May be as much as 50 X greater in acid fluids at~0.5-170 ppm
	~0.01-1.3 ppm in neutral fluids
Fe	May be as much as 400 X greater in acid fluids, at~4.0-445 ppm
	~0.0-9.0 ppm in neutral fluids
SO_4	May be as much as 35 X in acid fluids at~50-3200 ppm
	~15-50 ppm in neutral fluids
H_2 (gas)	Discharge values may be as much as 35 X in acid fluids

some deemed to be copper sulfates,

2) very high salinities ($\geq$ 17 wt% Cl eq., based on melting point of salt crystals),

3) very high temperatures, exceeding 400°, with some inclusions homogenizing at the critical point, and

4) presence of fluid inclusions that form a yellow liquid (sulfur ?) usually starting at~80°, and darkening to deeper yellow with increase in temperature, as in samples from wells in Biliran and Cagua.

Fluid inclusions in acid altered dacitic rocks are richer in daughter minerals than those in andesites.

Fluid Chemistry

Acid fluids from downhole samples and well discharges are often high in sulfate and chloride, and are believed to be a mixture of acid sulfate and neutral pH fluids coming from multi-feed zones in a well. However, the possibility of high chloride coming from HCl associated with magmatic contributions may be present in some wells where Cl is in excess and SO_2 is also detected (Ruaya, pers. comm., 1989). Table 1 shows selected fluid components whose ranges are characteristic of well discharges in Tongonan and Palinpinon. Acid discharges in both systems have higher Ca, Mg, Fe, SO_4 and H_2 gas than neutral fluids. In general, Cl is lower in acid fluids in Tongonan and Palinpinon, probably because acid wells in these areas usually occur at the outflow and/or the acid fluids tapped by the wells originate from the surface. High Mg may suggest the association of some acid fluids with dilute groundwaters.

Origins of Acid Alteration in Philippine Geothermal Systems

There are three major, possibly four, models for the formation of acid alteration and fluids in Philippine geothermal systems:

1) H_2S rising from a boiling aquifer to be oxidized in the vadose zone, and percolation of the resulting acid sulfate fluids along faults. Due to the strong neutralizing effect of the rock, such fluids are limited to shallow levels, perhaps down to 500 m from the surface, at the maximum. A variation of this may occur when extreme drawdown in a system creates a steam cap. Acid fluids are then generated when cooler groundwaters enter the system, react with the gases, and percolate to deeper levels along structures. Fluid acidity may be further aggravated when a virulent acid assemblage is intersected, along its way to deeper levels.

2) Reaction of deep aquifer fluids with magmatic volatiles such as SO_2, H_2S, HF, and HCl. This is supported by the presence of SO_2 and excess Cl in the fluid discharges; minerals like lazulite, topaz, ralstonite, danburite, gadolinite, and zunyite; and fluid inclusion characteristics.

3) Rejuvenation of acidity when neutral pH fluids react with formations enriched in alunite $\pm$ sulfur $\pm$ pyrite. This is corroborated by isotope studies in Palinpinon (Villasenor, pers. comm., 1988).

4) The possibility of deep aquifer acid fluids (not simply acid volatiles), related to Model 2 and exemplified by wells in Mts. Pinatubo and Cagua.

References

Browne, P.R.L. (1978) Hydrothermal alteration in active geothermal systems. *Ann. Rev. Earth Planet. Sci.*, vol. 6, p. 229-250.

Cathelineau, M., Oliver, R. and Nieva, D. (1985) Mineralogy and distribution of

hydrothermal mineral zones in Los Azufres (Mexico) geothermal field. *Geothermics*, vol. 14, p. 49–57.

Chen C. (1970) Exploration of geothermal steam in Tahuangtsui thermal area, Tatun volcanic region, north Taiwan. *Mining Res. Service Org., Min. Econ. Affairs, Republic of China*, p. 1–23.

Hayashi M. (1973) Hydrothermal alteration in the Otake geothermal area, Kyushu. *Jour. Japan Geoth. Ener. Assc.*, vol. 10, p. 9–46.

Henley R.W. (1985) The geothermal framework of epithermal deposits. In Berger B.R. and Bethke P.M. eds. *Geology and geochemistry of epithermal systems. Rev. in Econ. Geol.*, Soc. Econ. Geol. vol. 2, p. 1–24.

Manabe, E. and Ejima, Y. (1984) Tectonic characteristics and hydrothermal system of fractured reservoir at the Hatchobaru geothermal field. *Jour. Japan Geoth. Ener. Assc.*, vol. 21, 13 p.

Reyes, A.G. (1990) Petrology of Philippine geothermal systems and the application of alteration mineralogy to their assessment. *Jour. Volc. and Geotherm. Res.*, vol. 43, p. 279–309.

Sumi, K. (1969) Zonal distribution of clay minerals in the Matsukawa geothermal area, Japan. *Int. Clay Conf. Tokyo*, p. 501–512.

Sumi, K. and Maeda, K. (1970) Hydrothermal alteration of main productive formation of the steam for power at Matsukawa, Japan. *Proc. Symp. Hydrochem. and Biochem.*, vol. 1, p. 211–228.

White, D.E. (1957) Thermal waters of volcanic origin. *Geol. Soc. Amer. Bull.*, vol. 68, p. 1637–1658.

Gold and Base Metal Mineralization in an Evolving Hydrothermal System at Osorezan, Northern Honshu, Japan

Masahiro Aoki

Geological Survey of Japan, Higashi 1-1-3, Tsukuba, Ibaraki, 305 Japan

Introduction

Osorezan is located on the eastern margin of the volcanic front of the northern Honshu arc; it is a long lived composite volcano having a caldera lake, and several post-caldera domes of hornblende dacite. A basaltic andesite strata volcano erupted about 1.0 Ma, followed by andesite to dacite volcanoes around 0.6 Ma, caldera collapse, and then post caldera domes around 0.2 Ma. There have been at least two major stages of associated hydrothermal activity, with the older developed in the main body of the pre-caldera volcano around 0.6 Ma; hypogene acid sulfate fluids predominated. The younger began or was rejuvenated during post-caldera volcanism. The hydrothermal system is still active today, and is characterized by near neutral pH chloride water. Fumaroles and hot springs surround the latest domes, though activity has declined from its peak. Study of the Osorezan hydrothermal system is focusing on how mineralization and surface thermal features are affected by topography and related hydrology.

Osorezan has long been sacred as a place of repose for departed souls. It is believed that communication with the dead is possible at Osorezan through a psychic medium called Itako. Osorezan-Bodaiji temple was build in the center of steaming ground about 1000 years ago, with the monks caring for the surface expression of an extraordinarily interesting hydrothermal system. It is now crowded with many visitors, mainly sightseers but also a few curious geologists. Scientific investigation, with an emphasis on gold mineralization, was recently started by the Geological Survey of Japan, with limitations due to its religious nature.

The recent geological and geochemical studies indicate that the Osorezan hydrothermal system is an active and evolving gold depositing environment. Despite the many visitors, the high grade gold mineralization was only recognized in 1987. The entire mineralized body is still preserved, allowing the study of ore forming processes through geochemical examination of the fluids and precipitates.

Chemistry of the Hydrothermal Fluids

The major hot springs and steaming features are confined inside the pre-dome crater, along fissures trending NNE-SSW and E-W. Though there is wide range of salinity and pH, a consistent B/Cl ratio indicates a common source of fluid, with various modification by boiling and mixing processes.

1) Neutral pH high chloride water with low H_2S

This ascends from the deep reservoir with little dilution. The Na/K, K/Mg and silica geothermometers all indicate a reservoir temperature of 220-230°C; there is substantial loss of dissolved gases by boiling. Occasional precipitation of precious metals in the sinter suggests that this type of water is actively depositing gold below

Keywords : Osorezan, hydrothermal fluid, gold mineralization, base metal mineralization, caldera, acid sulfate alteration, dacite

the surface. The oxygen and hydrogen isotope composition indicates that this fluid is a mixture of about 2 : 1 magmatic water and local meteoric water.

2) Neutral pH intermediate chloride water with high H_2S

This discharges along eruption conduits and precipitates arsenic sulfide and gold where it mixes with low pH surface water. Judging from the stable isotopic composition and chloride concentration, the water is derivated from the deep high chloride water by further dilution with meteoric water. The silica and K/Mg geothermometer temperatures are 120° C to 170°C, while the Na/K geothermometer indicates temperatures higher than 230°C. Cooling by mixing with surficial water prevents shallow boiling and gas loss, allowing gold to be transported to the surface. Despite a large amount of sphalerite in the crater, the present water is undersaturated with respect to sphalerite. Thermodynamic calculation suggests that the water responsible for the previous base metal-rich precipitate contained several times more zinc than the present water; if so, the earlier fluid may have had a significantly higher salinity than at present.

3) Neutral pH low chloride water with high H_2S and HCO_3

This discharges on the eastern margin of the hydrothermal system, precipitating calcium carbonate and/or sulfur around the springs. Judging from the isotope composition, this is a mixing product of steam-heated gas-rich water with a minor amount of deep chloride water.

4) Acid mixed sulfate-chloride water

This water forms from mixing of steam-heated acid sulfate ground water with neutral pH chloride water. This is present near the surface and does not boil; its temperature is less than 80°C. People from the temple use this hot acid water (pH about 2) for bathing.

History of Hydrothermal Activity

The evolution of hydrothermal activity may be inferred from geometrical relationships and radiometric age determinations.

1. Acid sulfate alteration and gold mineralization around 0.6 Ma

Strong silicification and argillization is present on the western and eastern rim of the caldera, and large amounts of fragments of altered rock are interbedded in the intra-caldera sediment and pyroclastic flow deposit around the caldera. The acid sulfate alteration in the main body of the andesite/dacite volcano preceded the caldera collapse. K-Ar ages of alunite in ejected breccias and fresh dacite lava cropping out on the eastern rim of caldera wall range from 0.35 to 0.80 Ma. The $\delta^{34}S$ values of closely associated alunite and pyrite are + 29.7 per mil and − 0.5 per mil, respectively, indicating a high temperature source of sulfate. Gold is present in breccias of vuggy silica rock containing alunite, pyrite and quartz. These data suggest that the hypogene acid sulfate gold mineralization is related to fluids of volcanic origin.

2. Catastrophic eruption and caldera formation

Repeated eruption of pyroclastic flows and associated debris flows destroyed the main body of the andesite/dacite volcano to form a caldera. The structural disruption caused a drastic change in the hydrology, and in the balance between magmatic input and meteoric dilution, with high temperature acid components no longer reaching the surface. The hydrothermal system has evolved to a rock-buffered neutral pH water.

3. Post caldera volcanism of hornblende dacite

Post-caldera volcanism began around 0.23 Ma in the northern part of the caldera lake. After eruption of pumice flows, dacite lavas and repeated phreato-plinian explosions, the 800 m diameter crater was penetrated by several domes of hornblende dacite around 0.17 Ma. The surface expressions of hydrothermal activity would have been destroyed by these explosive events. The water level of the caldera lake was possibly 20 to 25 m higher than at present.

4. Post-dome hydrothermal activity and mineralization

Post-dome hydrothermal activity has been rich in mineralization. Many hydrothermal eruption craters have formed in the lake, ranging from several tens to one hundred meters across. The trigger of these eruptions is not clear. Closely spaced lacustrine terraces (1 to 2 m) suggest lowering of the water level was rather gradual. The craters are aligned in an east-west trend. Since the compressive stress field in northern Honshu is east-west, pressure related to either a magma or hydrothermal fluid will tend to open fractures in this direction. Therefore, a rapid increase of pressure caused by shallow intrusion of high temperature magma may be the most probable triggering mechanism of the hydrothermal eruption. After formation of the hydrothermal eruption conduit, various metals have precipitated, with some temporal and spatial separation: 1) Pb, Zn sulfides, 2) gold and mercury tellurides, lead antimony sulfide, lead arsenic sulfide, 3) arsenic sulfide, 4) mercury sulfide and 5) sulfur (Table 1). With time, precipitation of metals was confined to the remaining crater because of progressive filling by both hydrothermal precipitates and

Table 1 Bulk chemistry of selected metal rich sediments from filled eruption craters in the Osorezan hydrothermal area.

	1.	2.	3.	4.
Au	0.0	6510	151	6.9
Ag	0.0	0.4	0.0	3.6
Hg	1860	5520	1750	54300
Pb	229000	1350	150	21500
Zn	120000	2600	260	46300
Cu	119	71	12	191
Tl	380	393	260	46300
Sb	4300	1040	7440	1210
As	45300	3650	499000	46300
Te	240	10520	1800	2010
Se	2020	270	1960	640
Mn	297	1950	53	1310
Fe	29900	33400	11400	290000

(concentration in ppm)

1. Black to brown sandy sediment containing jordanite, sphalerite, wurtzite and barite.
2. Black muddy sediment containing krennerite, coloradoite, pyrite and marcasite.
3. Orange yellow sandy sediment mainly composed of orpiment.
4. Black sandy sediment containing marcasite, metacinnabar, cinnabar, wurtzite, sphalerite, As-Sb-Pb sulfosalt and magnetite.

clastic sediments ; this has formed a partial overprint of mineralization, especially along the main fluid channel. At the latest stage, the ascending fluid precipitated mainly amorphous silica. Larger craters have abundant gold, mercury and arsenic mineralization relative to base metals. On the other hand, the smaller craters contain mainly base metals with minor overprints of gold and arsenic sulfide. The positive correlation of gold/base metal ratio to the size of crater suggests that the smaller conduit clogged in a short period and failed to record the later stage overprint.

In association with the gradual decrease of the lake level, an oxidizing environment has prevailed around the fluid conduits. Scorodite, jarosite, limonite, and anglesite formed in this period, with possible metal remobilization from earlier sulfides such as orpiment, pyrite, galena, and jordanite. Galena was also formed by secondary conversion from anglesite, due to an occasional input of H_2S along cracks. Stream erosion has removed some surface features except for areas protected by silica cover. The selective erosion of soft sediments surrounding the silica cap have unmasked the original structure of the eruption craters, and show that sediments dip into the craters. Hot water still discharges from some craters, precipitating arsenic sulfide and sulfur with gold. Silica sinter is present on hills above the water level. The sinter shows various textures, from steep chimney forms filled by geyserite to stratification with casts of algae. Silica-cemented pebble and sand beneath some stratified sinter indicates that the sinter formed along the paleo shore line of the lake. Some sinters have been cut by barite veins with a minor association of colloidal antimony-arsenic sulfide. Other sinter has red bands of 1 to 30 mm thickness of colloidal Tl-Sb-As sulfide lining the vent. The distribution of sinter is controlled by the NNE-SSW trending fracture system. Active hot springs in the vicinity of these sinters are oversaturated with silica and form a layered sinter.

Though there are many fragments of quartz vein at the surface, the time relation to the early hypogene acid sulfate mineralization has not been clarified because of the scarcity of associated K-bearing minerals. It is possible that vein mineralization formed before the birth of Osorezan volcano. Quartz veins do not crop out inside the caldera, and fragments occur only on the surface of altered lake sediment in the main hot spring area. This indicates that the fragments of quartz vein were erupted from depth.

Isotopic and Metal Compositions of Volcanic Discharges in Japan, and Implications for Mineralization

Jeffrey W. HEDENQUIST and Masahiro AOKI

Geological Survey of Japan, Higashi 1-1-3, Tsukuba, Ibaraki, 305 Japan

Introduction

In order to directly examine the interaction of magmatic fluids with overlying meteoric waters, we sampled the fumarolic discharges of two recently active volcanoes in Japan, Esan and Kirishima. Representative hot springs associated with each volcano, as well as geothermal wells at Kirishima, were also sampled. The chemical composition, including trace metals of economic interest, and isotopic signatures of all samples were analyzed to identify the degree of magmatic contribution to the hydrothermal systems.

The pioneering studies of stable isotopes in active geothermal systems and extinct epithermal ore deposits indicated that the water reflects both a dominantly meteoric source and reaction with host rocks (e.g., Taylor, 1979). However, magmatic fluids are a major source of fluid components in deep-seated hydrothermal ore systems (e.g., Taylor, 1979). If there is a transition from deep, magmatic-domination to shallow, meteoric-domination in the hydrothermal environment, then there should be some evidence for magmatic contamination of meteoric systems. This study seeks to identify how magmatic fluids degassing from volcanoes interact with meteoric waters and their host rocks, and how this interaction may affect mineralization in this environment.

Geologic Setting and Hydrothermal Activity

Esan volcano rises to an altitude of 618 m only 1 km from the south Hokkaido coast (Fig. 1), and comprises andesitic domes and lava flows of Recent age (Ando, 1974). The youngest magmatic eruption was several hundred years ago, and phreatic eruptions occurred 140 years ago. Kirishima volcano, southern Kyushu, is composed of at least 20 eruptive centers of late Pleistocene to Recent age (Kobayashi *et al.*, 1981). Cones and lavas which erupted up to about 6000 years ago overlie Mesozoic sedimentary basement and older andesites. More than 40 eruptions have occurred since 742 A.D., with the most recent activity at Iwoyama in 1768. The composite andesitic cones form a massif 12 km in radius and with a relief of 1500 m (Fig. 1). The composition of the parent magmas of both andesitic volcanoes is probably similar. Both volcanoes have been recently active, and are now in repose. However, we have no evidence of the depth to, or degassing state of, the underlying magmas.

At Esan, moderate temperature (100 to 225°C), HCl-bearing fumaroles discharge from the highly altered southern flank at an altitude of about 400 m (Fig. 1). An acid sulfate spring discharges at 100 m altitude, and some neutral pH warm springs of low to seawater salinity are present along the coastline. Condensed samples of the fumaroles contain up to 2000 mg/kg chloride, with a pH of 1.5 due to condensed

Keywords: isotopic composition, metal composition, volcanic discharge, Esan, Kirishima

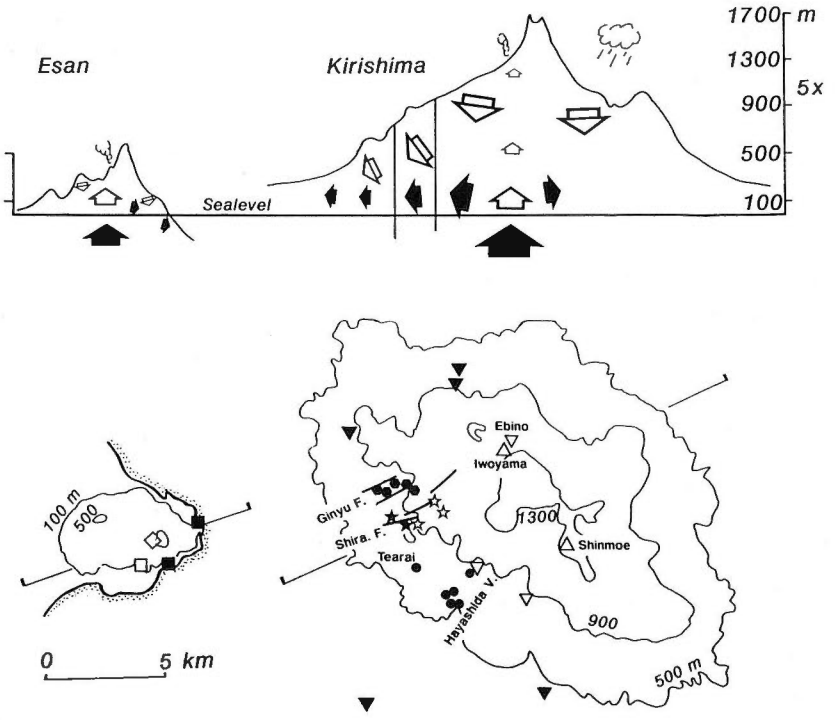

Fig. 1. Plan maps of Esan and Kirishima volcanoes, with contours every 400 m. Symbols for Figures 1 and 2 include: Fumaroles (◇, △), acid springs (□, ▽), and neutral pH hot springs (■, ▼) at Esan and Kirishima, respectively, plus neutral pH wells (●, ⬣, ★) at Hayashida, Ginyu and Shiramizugoe, respectively, and acid Shiramizugoe wells (☆). Cross-sections (5 X vertical exaggeration) show deduced schematic flow patterns. Open arrows are vapor, downward arrows are meteoric waters.

HCl.

At Kirishima, fumarolic discharges of 94 to 167°C occur at altitudes of 1300 m to about 900 m. The high altitude fumaroles at Iwoyama contain HCl (maximum of 170 mg/kg Cl, with condensate pH values of 2.5), and are the highest temperature. Lower altitude fumaroles are related to the geothermal system on the west flank of Kirishima. Ebino spring discharges acid (pH 2.3) chloride-sulfate water at an altitude of 1200 m.

Before geothermal development for hot spring baths in the Hayashida valley, neutral pH chloride springs discharged at altitudes of 800 m to 500 m; dilute chloride, bicarbonate-rich warm springs still discharge at altitudes to 200 m as far as 15 km from the summit. Steam-heated acid sulfate springs range in altitude from about 900 m to 700 m. Shallow wells reach chloride water at about 300 m altitude in the Hayashida valley where chloride springs once discharged. Several wells were drilled into two major faults for geothermal development. The wells penetrating the northern Ginyu Fault produce neutral pH waters; in contrast, the Shiramizugoe Fault has acid chloride-sulfate waters at elevations near sea level (Kodama and Nakajima, 1988). The acid waters have higher sulfate contents and higher temperatures than the neutral pH waters, and variable chloride contents.

Figure 2 shows the $\delta^{18}O$ and δD values of fumarolic condensates and hot spring waters at both locations. In addition to our sampling, we also summarize results for two Esan fumaroles analyzed by Matsubaya *et al.* (1978), a sample of Ebino spring collected in 1974 by Matsubaya *et al.* (1975), and the compositions of waters discharged from the Ginyu wells as well as meteoric waters local to the wells (Shimizu *et al.*, 1988). There are no isotopic (or metal) compositions available for the Shiramizugoe fluids.

We have analyzed all samples collected at Esan and Kirishima for major and minor elements, including trace metals. Some components of interest in the fumarole samples are reported as ranges of concentration in Figure 3, with the concentrations in high temperature fumaroles on Merapi volcano, Indonesia, included for comparison. In general, the concentrations of elements, particularly the base metals, are highest in the high temperature Merapi fumaroles, and lowest in the low temperature Kirishima vapors (different by several orders of magnitude), with HCl in the Kirishima fumaroles at least one and a half orders lower than at Merapi; Esan values are intermediate.

Discussion

Esan fumarole condensates lie on a simple isotopic mixing trend (Fig. 2) between local meteoric water and 900°C andesitic volcano discharges (Matsuo *et al.*, 1974). These results indicate less than a 50% meteoric component in the Esan fumarolic discharges. The ephemeral neutral pH and acid spring discharges are similar to local meteoric values, though they could have a small (<10%) component of magmatic water.

In contrast, the Kirishima features are dominated by meteoric water. Local meteoric δD ranges from −50 to −40 per mil with decreasing altitude (Shimizu *et al.*, 1988). Iwoyama HCl-bearing fumaroles, and the adjacent acid chloride-sulfate spring at Ebino (sampled in 1974), indicate a maximum of a 30% magmatic

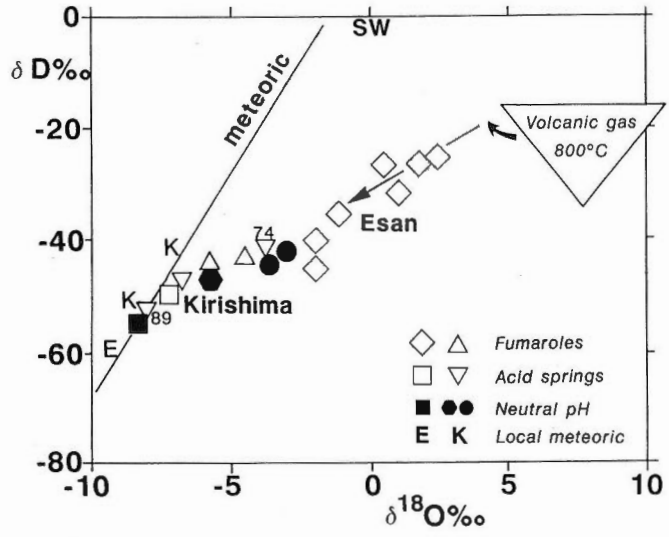

Fig. 2. δD-$\delta^{18}O$ diagram showing the magmatic-dominant signature of Esan fluids, and the meteoric-dominant signature of Kirishima fluids. Symbols as in Figure 1.

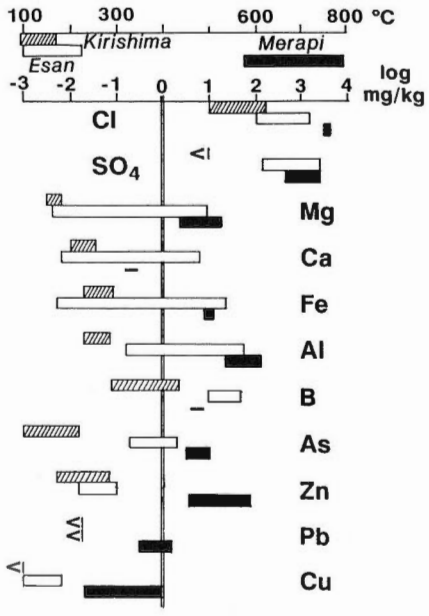

Fig. 3. Concentrations of selected components in volcanic fumarole condensates for Esan and Kirishima (this study), and for comparison, Merapi (Symonds *et al.*, 1987). No data (−) and below detection limit (<) are also noted.

component. The evidence for the magmatic shift from local meteoric δD values for these acid features comes from comparison with the Ebino sample collected in 1989, the day following 300 mm of rainfall; although still acid, the isotopic composition of the spring lies on the meteoric line 10 per mil lighter in δD than the 1974 sample. High chloride samples from wells in the Hayashida valley are also shifted a similar amount from local meteoric compositions of δ^{18}O and δD, with the shift lying along a magmatic mixing trend. The Ginyu waters, on the same trend, may also have a small magmatic component. Steam-heated acid sulfate hot springs all lie close to the meteoric line.

Based on our chemical and isotopic results, magmatic fluids reach the surface at Esan with a relatively small degree of interaction with meteoric waters (< 50%), though extensive cooling has occurred from the underlying magmatic system (degassing magma and/or magmatic brine). In contrast, fumarolic discharges at the summit of Kirishima, as well as geothermal discharges on its lower flanks, are dominated by meteoric waters, though with a minor magmatic component (possibly up to 30%; Fig. 2). We believe the difference is caused by the presence of a larger carapace of meteoric water at high levels in the Kirishima massif (Fig. 1, cross-section), which condenses the majority of magmatic volatiles and other components before they can discharge to the surface.

Implications for Mineralization in Volcanic Systems

Some mineralization in the volcanic environment is related to extensive leaching by an acid fluid, followed by deposition of copper and precious metals. Such epithermal mineralization is commonly termed "acid sulfate" (Heald *et al.*, 1987) or "high

sulfidation" (Hedenquist, 1987). Good examples are the Summitville, Colorado, deposit (Stoffregen, 1987) and the Nansatsu deposits of southern Kyushu (Hedenquist *et al.*, 1988). Detailed stable isotope studies of this environment (Rye *et al.*, 1989) indicate that magmatic fluids interact with meteoric waters during alteration and mineralization.

Much the same situation could be envisaged to be occurring at depth beneath Kirishima now, with magmatic volatiles and metals condensing into a hydrothermal system dominated by meteoric water; dissociation of the acids (HCl, H_2SO_4) will result in extensive leaching of the host rock. The acid composition of fluid from the Shiramizugoe wells indicates that such leaching is now occurring. Although there may also be acid condensates at depth at Esan, we have no direct evidence for their presence. If we assume that the deep, high temperature magmatic component at both Kirishima and Esan is relatively metal-rich (e.g., similar to Merapi; Fig. 3), it is clear that the lower temperature (and lower HCl) vapors at both volcanoes are less able to transport metals than chloride-rich vapors at 600°C+. However, the meteoric water dominance in the Kirishima hydrothermal system in comparison with that at Esan suggests that the extensive meteoric system at Kirishima serves as a "condenser" of magmatic volatiles and metals, thus accounting for the lower metal concentrations discharging to the surface. If true, then such meteoric interaction with magmatic discharges may be conducive to metal deposition, which if localised could produce ore.

Conclusions

1) Magmatic volatiles discharge to the surface at both Esan and Kirishima volcanoes, though the degree of magmatic contribution to the fumaroles (including water, gases and metals) is larger at Esan because of less meteoric interaction. At Kirishima, an extensive meteoric carapace is effective at condensing and diluting most of the magmatic components. In contrast, the hydrology of the Esan system, perhaps related to its much smaller catchment, precludes a large amount of meteoric interaction.

2) A hydrothermal system analogous to that present at Kirishima could be responsible for the extensive acid leaching and subsequent enargite and gold mineralization that occurs in the high sulfidation (acid and oxidizing) environment, in which some ore deposits throughout the Circum Pacific have formed. The interaction of magmatic volatiles and metals with an overlying meteoric system may be essential for mineralization. Where there is not extensive meteoric interaction, such as at Esan, the volatiles and metals exolved from a near surface (1-3 km deep?) magma largely degas to the surface rather than condensing at shallow (<1 km) depth. This model is consistent with the geology, alteration zonation, isotope signatures and fluid inclusion data from ore deposits deduced to have formed in this environment.

Acknowledgements

We thank Sachihiro Taguchi, Mike Thompson and Masami Watanabe for their help with field work, and Yukihiro Matsuhisa and Noel White for useful discussions.

References

Ando, S. (1974) Geology and petrology of Esan volcano, Hokkaido. *Japan Association of Petrology, Mine. and Econ. Geol.*, vol. 69, p. 302-312 (in Japanese).

Giggenbach, W.F. (1987) Redox processes governing the chemistry of fumarolic gas discharges from White Island, New Zealand. *Applied Geochemistry,* vol. 2, p. 143–161.

———, (1988) Geothermal solute equilibria. Derivation of Na–K–Mg–Ca geoindicators. *Geochimica et Cosmochimica Acta,* vol. 52, p. 2749–2765.

Heald, P., Hayba, D.O. and Foley, N.K. (1987) Comparative anatomy of volcanic-hosted epithermal deposits: acid-sulfate and adularia-sericite types. *Econ. Geol.,* vol. 82, p. 1–26.

Hedenquist, J.W. (1987) Mineralization associated with volcanic-related hydrothermal systems in the circum-Pacific Basin. In Horn, M.K., ed., Transactions of the Fourth Circum-Pacific Energy and Mineral Resources Conference, Singapore, 1986, p. 513–524.

———, Matsuhisa, Y., Izawa, E., Marumo, K., Aoki, M. and Sasaki, A. (1988) Epithermal gold mineralisation of acid leached rocks in the Nansatsu District of southern Kyushu, Japan. *Proceedings of Bicentennial Gold 88: Geol. Society of Australia, Extended Abstracts,* vol. 22, p. 183–190.

Kobayashi, T., Aramaki, S., Watanabe, T. and Kamada, M. (1981) Kirishima volcano. In Kubotera, A., ed., *Field Excursion Guide to Sakurajima, Kirishima and Aso Volcanoes,* Volcanological Society of Japan, Tokyo, p. 18–32.

Kodama, M. and Nakajima, T. (1988) Exploration and exploitation of the Kirishima geothermal field. *Chinetsu,* vol. 25, p. 1–30 (in Japanese).

Matsubaya, O., Ueda, A., Kasakabe, M., Matsuhisa, Y., Sakai, H. and Sasaki, A. (1975) An isotopic study of the volcanoes and the hot springs in Satsuma Iwojima and some areas in Kyushu. *Geol. Surv. Japan Bull.,* vol. 26, p. 375–392.

———, Sakai, H., Ueda, A., Tsutsumi, M., Kusakabe, M. and Sasaki, A. (1978) Stable isotope study of the hot springs and volcanoes of Hokkaido, Japan. *Papers of the Institute for Thermal Spring Research,* Okayama University, no. 47, p. 55–67.

Matsuo, S., Suzuoki, T., Kusakabe, M., Wada, H. and Suzuki, M. (1974) Isotopic and chemical compositions of volcanic gases from Satsuma-Iwojima, Japan. *Geochemical Journal,* vol. 8, p. 165–173.

Rye, R.O., Bethke, P.M. and Wasserman, M.D. (1989) Diverse origins of alunite and acid-sulfate alteration: Stable isotope systematics. *U.S. Geological Survey Open-File Report* 89–5, 33 p.

Shimizu, A., Misu, S. and Gokou, K. (1988) Geochemical studies of the Ginyu reservoir in the Kirishima geothermal field. In *Proceedings of the International Geothermal Conference, Kumamoto,* Geothermal Research Society Japan, p. 136–139.

Stoffregen, R. (1987) Genesis of acid sulfate alteration and Au–Cu mineralization at Summitville. *Econ. Geol.,* vol. 82, p. 1575–1591.

Symonds, R.B., Rose, W.I., Reed, M.N., Lichte, F.E. and Finnegan, D.K. (1987) Volatilization, transport, and sublimation of metallic and non-metallic elements in high temperature gases at Merapi volcano, Indonesia. *Geochimica et Cosmochimica Acta,* vol. 51, p. 2083–2101.

Taylor, H.P., Jr. (1979) Oxygen and hydrogen isotope relationships in hydrothermal mineral deposits. In Barnes, H.L., ed., *Geochemistry of Hydrothermal Ore Deposits,* vol. 2, John Wiley and Sons, New York, p. 236–277.

Comparative Study of Shallow and Deep Acid Alteration in the Otake and Hatchobaru Geothermal Systems, Kyushu, Japan

Sachihiro TAGUCHI

Faculty of Science, Fukuoka University
Nanakuma 8-19-1, Jonan-ku, Fukuoka, 814-01 Japan

The Otake and Hatchobaru geothermal fields are located on the north-western flank of Kujyu volcano in north Kyushu, Japan. They are 2 km apart and situated on two parallel NW-trending faults (Fig. 1).

In this area, the NW-trending faults play the most important role of hot fluid passage (Yamasaki *et al.*, 1970). Of these faults, the Komatsuike fault is believed to be the main passage for ascending hot fluid, because it is accompanied by many

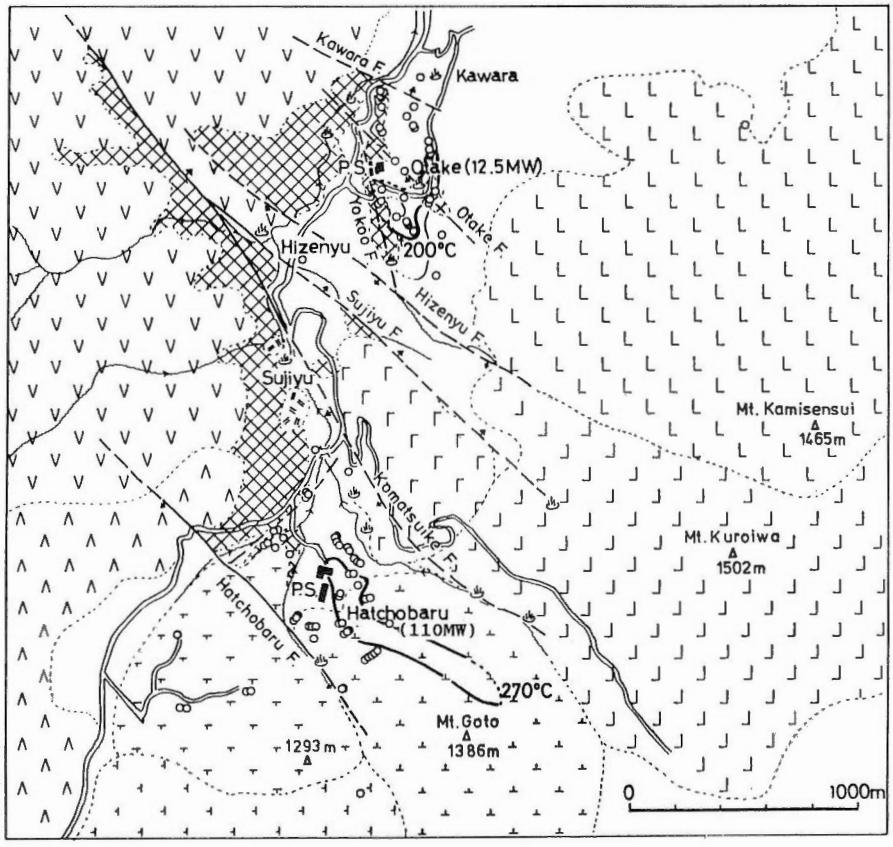

Fig. 1. Geologic map of the Otake-Hatchobaru geothermal area (modified from Hayashi *et al.*, 1985). Crosshatched area: early Pleistocene Hohi volcanic rocks, others: late Pleistocene Kujyu volcanic rocks.

Keywords : Otake geothermal field, Hatchobaru geothermal field, acid alteration, alunite zone, kaolin zone

thermal manifestations such as fumaroles, hot springs and advanced argillic alteration at the surface.

At Otake, acid alteration zones such as alunite and kaolin zones are mainly distributed at shallow levels. On the other hand, alunite and kaolin zones occur from the surface to a depth of about 1000 m at Hatchobaru, where deep fluids are composed of two types: acid and neutral to alkaline pH water.

Figure 2 shows a schematic model of the Otake geothermal system (Taguchi *et al.*, 1985). Alunite occurs only at shallow levels (less than 100 m) above the hot plume of neutral to alkaline water of 200 to 220°C. The kaolin zone occupies a position below and deeper than the alunite zone, and it also occurs at deeper levels surrounding the hot plume. That is, the neutral to alkaline hot plume is mantled by acid alteration minerals. Moreover, boiling phenomena of the ascending hot fluid are clearly observed in fluid inclusions at a depth of less than 200 m. All of these facts suggest that the acid fluid causing the formation of alunite and kaoline zones at Otake originated from acid sulphate steam heated water; it was formed in shallow meteoric water by oxidation of hydrogen sulphide, separated from ascending and boiling alkaline water.

Figure 3 shows the temperature distribution at the production level (about 1,000 m below surface) at Hatchobaru. A high temperature zone (above 270°C) is elongated almost 900 m, and is 100 m wide (Taguchi, in prep.). This high temperature zone is most likely related to the NW-trending Komatsuike fault (Taguchi *et al.*, 1986).

Figure 4 shows the chloride content of deep water before reinjection and the pH of discharged water (modified from Shimada *et al.*, 1985). The chloride content of deep water increases southward, indicating the source of ascending fluid. The pH values of discharged water are neutral to alkaline in the area of higher chloride content. A zone of acid water (pH = 3.4 to 5.0; Shimada *et al.*, 1985) surrounds the high temperature zone.

Figure 5 shows the distribution of temperature and alteration minerals on a NE cross section through Well H-4 (Taguchi, in prep.). Acid minerals (alunite and kaolin) occur from the surface to a depth of 1,000 m. At Well H-4, drilled in the central part of the high temperature zone, fluid inclusion data suggest the existence

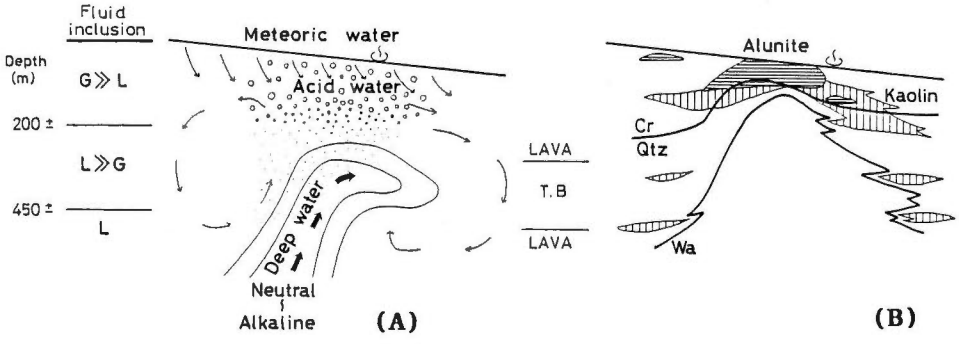

Fig. 2. Schematic model of the Otake geothermal system. A: Fluid conditions of ascending deep water, showing boiling and mixing with meteoric water. L and G are liquid- and gas-rich fluid inclusions, respectively. B: Distribution of alteration minerals. Solid line with Cr/Q indicates cristobalite-quartz transition, and the line labelled Wa indicates wairakite appearance below the line (Taguchi *et al.*, 1985).

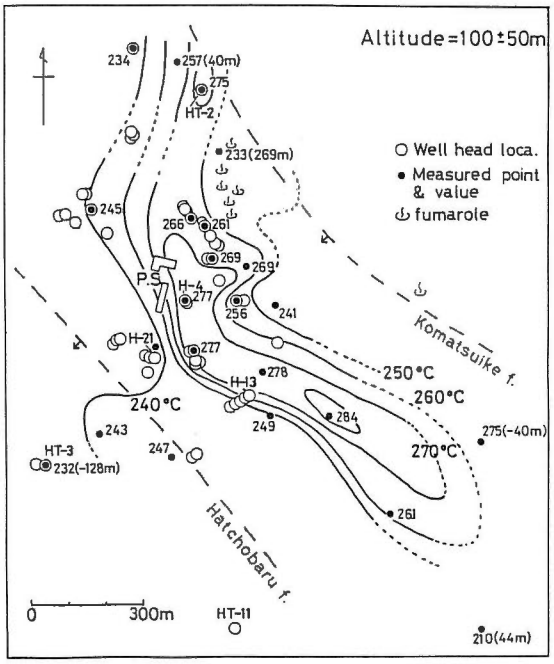

Fig. 3. Temperature distribution at production level (about 1,000 m below surface) in the Hatchobaru geothermal system (Taguchi, in prep.).

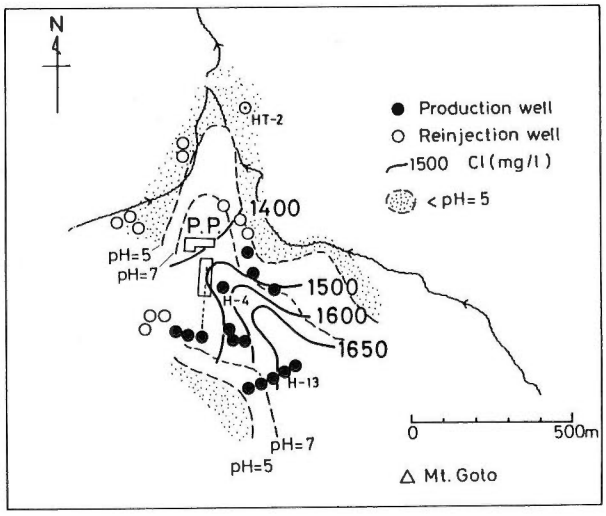

Fig. 4. Distribution of chloride concentration (mg/*l*) of deep water before reinjection started and pH of discharged water (modified from Shimada *et al.*, 1985).

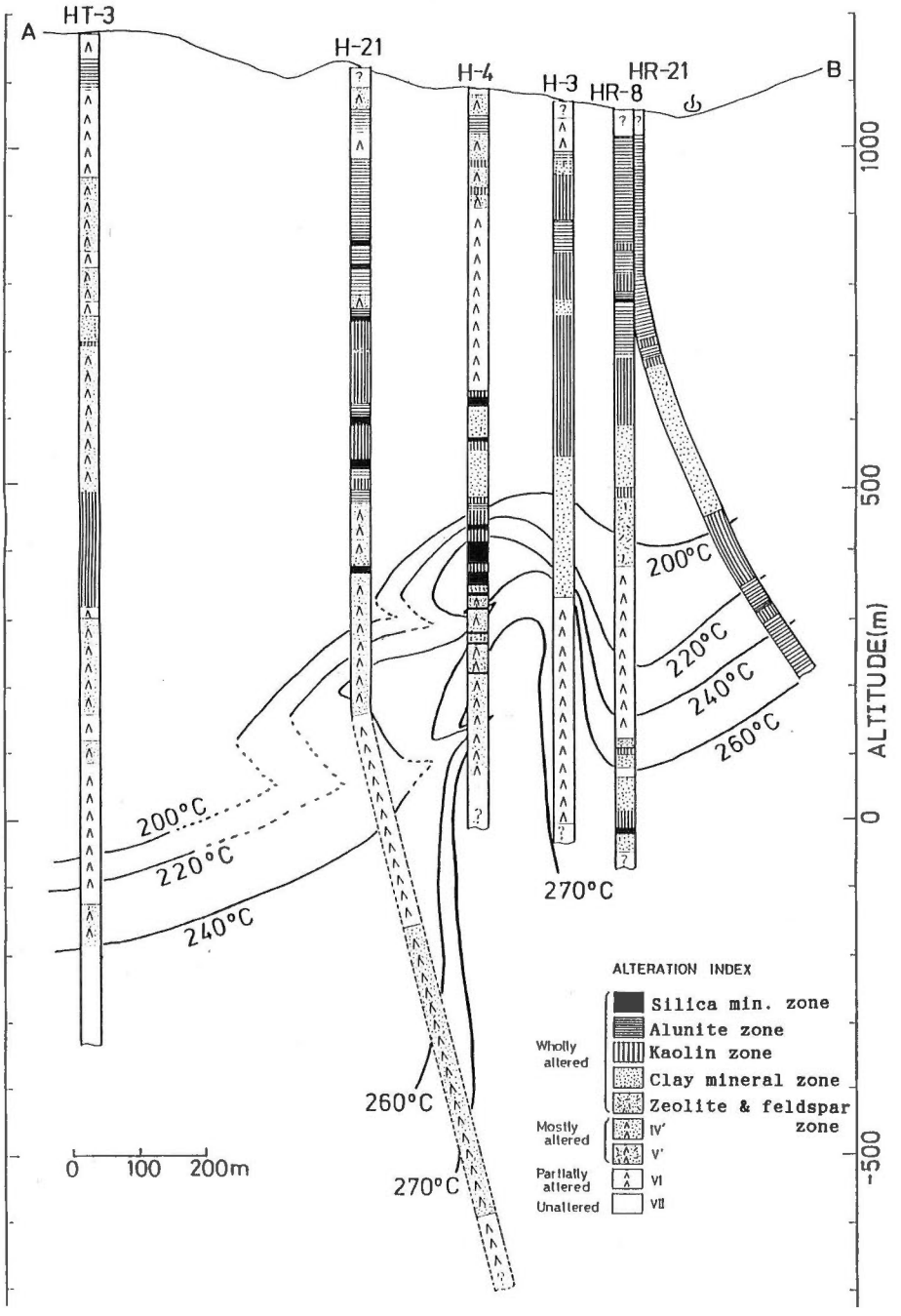

Fig. 5. Distribution of temperature and alteration minerals on a NE-SW cross section through Well H-4 at Hatchobaru (Taguchi, in prep.).

of boiling at a depth of 600 m, which corresponds nearly to the deepest acid alteration zones in this well. The relation of acid alteration and boiling depth at Hatchobaru is similar to that at Otake. Besides acid sulphate water near surface, Shimada *et al.* (1985) estimated two origins of deep acid waters at Hatchobaru, based on geochemical and geological data: reinjection of discharged water and hydrolysis of sulfur. They mentioned that the second process is the mechanism of acidification of natural water at the production level of Hatchobaru.

References

Hayashi, M., Watanabe, K. and Furutani, N. (1985) Faults and their stress fields at the Otake–Hatchobaru geothermal area. *Jour. Geotherm. Research Soc. Japan,* vol. 7, p. 383–399 (in Japanese with English abstract).

Shimada, K., Fujino, T., Koga, A. and Hirowatari, K. (1985) Acid hot water discharging from geothermal wells in the Hatchobaru geothermal field. *Jour. Japan. Geotherm. Energy Assoc.* vol. 22, p. 276–292 (in Japanese with English abstract).

Taguchi, S., Irie, A., Hayashi, M. and Takagi, H. (1985) Subsurface thermal structure revealed by fluid inclusion thermometer at the Otake geothermal field, Kyushu. *Jour. Geotherm. Research Soc. Japan,* vol. 7, p. 401–413 (in Japanese with English abstract).

———, Nakamura, M., Takagi, H., and Hayashi, M. (1986) Fracture control of fluid flow revealed by fluid inclusions at the Hatchobaru geothermal field. *GRC Transactions,* vol. 10, p. 199–202.

Yamasaki, T., Matsumoto, Y. and Hayashi, M. (1970) The geology and hydrothermal alteration of the Otake geothermal area, Kyushu, Japan. *Geothermics, Special Issue* 2, p. 197–207.

Geological Survey of Japan Report, No. 277, 1991, p. 83-90

Hydrothermal Systems and Associated Alteration in Iceland

Gudmundur Omar FRIDLEIFSSON

Orkustofnun, Geothermal Division
Grensasvegur 9, 108 Reykjavik, Iceland

Abstract

Hydrothermal systems in Iceland and their associated alteration is described. A twofold classification into high-T and low-T (temperature) hydrothermal systems has long been used, with reservoir temperature of 200°C as a dividing line. All the known systems are liquid dominated with fluids of metoric origin, while saline systems also occur. Rock alteration ranges from zeolite to greenschist facies, while amphibolite facies rocks, hedenbergite bearing iron-rich skarns and sanidinite facies metamorphic rocks are also known. The role of volcano-tectonic activity upon hydrothermal evolution of both low-T and high-T systems is the topic of the lecture.

Hydrothermal Systems

Traditionally the hydrothermal systems in Iceland have been classified into High-Temperature and Low-Temperature areas, where a reservoir temperature of 200°C has been used to distinguish between the two. The maximum fluid temperature at any depth in the open hydrothermal high-T systems is usually controlled by the boiling point curve of water (hydrostatic control). All the known systems are liquid dominated, some boiling, and most of them are fed by fluids of meteoric origin. While saline systems fed by the surrounding ocean exist, e.g. on the Reykjanes penninsula (Fig 1), most of the systems thrive on replenishing rainwater which affects the fluid composition. The annual preciptiation in Iceland ranges from 450-4500 mm/yr, lowest in the northeast but highest in the mountainous areas in the south and southeast. Most precipitation is returned to the ocean by rivers and groundwater runoff, but some enters the hydrothermal systems. The presently active high-temperature systems are confined to active volcanic zones while fossil analogs are common in the eroded Tertiary and Quaternary rocks, which host the presently active low-temperature systems.

As this abstract is presented at the Symposium on High-Temperature Acid Fluids and Associated Alteration, some attention to the acidity of the Icelandic systems seems appropriate. The average rainwater is slightly more acid (pH = 5.4) than local groundwaters in Iceland (pH 6-8), which reflects interaction with basic rocks, while the hydrothermal systems have pH-values ranging from 4-11. The commonest pH-values of the low-T systems are pH 6-9, while the reservoir fluids of the high-T systems usually show values between pH 5-7. Boiling of high-T water results in pH increasing to 8-9 of the effluent water, while fumaroles and mud pools on the surface commonly have values near pH 4. An extreme value of pH less than 2 was observed for a few weeks in the high-T well KG-4 in Krafla early in the Krafla volcanic rifting episode (Krafla files, 1975-1984). Another Krafla well (KG-12)

Keywords : Iceland, hydrothermal system, hydrothemal alteration, zeolite facies, greenschist facies, volcano-tectonic activity

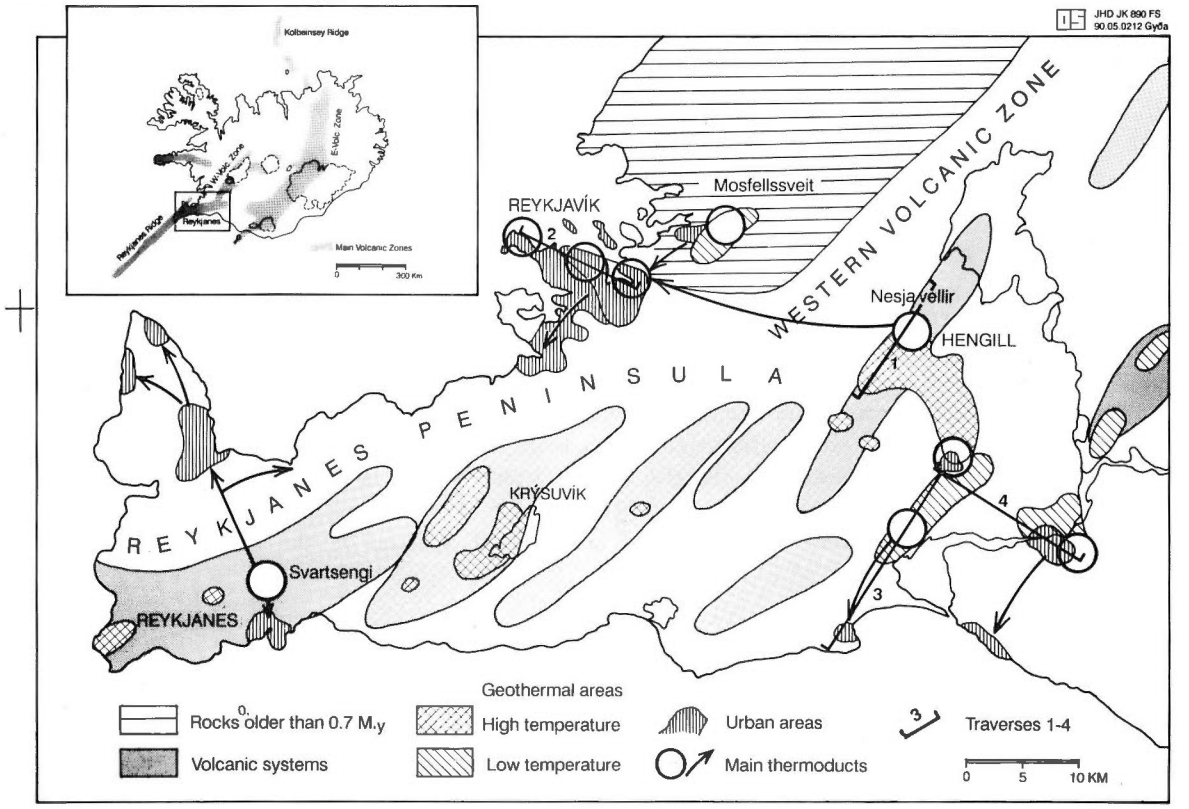

Fig. 1. Map of Iceland showing the active volcanic zones and the volcanic systems of Reykjanes peninsula (from F. Sigurdsson, Orkustofnun). The locations of traverses 1–4 in Figs. 2–5 are shown.

produced superheated vapour, and both SO_4^{2-} and Cl^- have been observed causing acidification of condensate water (Armannsson *et al.*, 1982, 1989; Truesdell *et al.*, 1989). The observation demonstrates that transient changes in acidity accompanying volcanic activity may be quite common in the reservoirs of the Icelandic high-T systems, on a local scale at least, the result of which would affect the secondary alteration pattern temporarily.

The salinity of the Icelandic fresh-water hydrothermal systems is extremely low, from 10–200 ppm chloride, while the saline systems on Reykjanes peninsula approach 20,000 ppm Cl, decreasing landwards. Accordingly, the content of dissolved solids in the thermal waters is quite variable, from 150–40,000 ppm (Kristmannsdottir and Olafsson, 1989). Except for chloride, the relative mobility of all other major elements in the thermal waters is largely governed by temperature-dependent mineral-solute equilibria (Arnorsson, 1979; Palmason *et al.*, 1979). The overall rock alteration is, however, more or less identical in the fresh water and saline systems, except for anhydrite which is common in the saline systems but rare in the others. Of particular interest with respect to precious metals are the generally lower pH values of 4.5–7 (compared to pH 6–7) and considerably higher metal concentration in the Reykjanes systems than in average sea water (Olafsson and Riley, 1978).

The lifetime of geothermal systems is quite variable, but is chiefly governed by the

volcano-tectonic situation within the volcanic rift systems of Iceland, part of the Mid-Atlandic-Ridge spreading system. In general, the high-T systems are relatively short-lived phenomena (0.2-1.0 m.y.). They are formed within active volcanic systems due to the accumulation in central volcanoes or fissure swarms of magma, which heat the surrounding groundwater. The high-temperature activity lasts as long as the magmatic heat sources. Upon spreading the volcanic systems drift out of the spreading zones and cool, while new ones replace them within the centre of the rift zones. Judging from the generally accepted fact that extinct central volcanoes within the Quaternary and Tertiary crust of Iceland are usually preserved as entities, it appears that the spreading axes shift positions every now and then within each spreading zone. A recent example of such a shift is possibly demonstrated by the progressively younger Hveragerdi→Hrodmundartindur→Hengill volcanic systems. Throughout the 16 m.y. history of Iceland the volcanic spreading zones themselves have even shifted position (Saemundsson, 1974). This has resulted in a variety of volcano-tectonic structures such as non-spreading flank zones, transform faults, crustal flexures and antiform structures. The complexity of the volcano-tectonic evolution inevitably affects the lifetime of high-temperature systems, as well as the low-temperature systems and their flow patterns, temperature distribution and hydrothermal history, which may span several million years.

With respect to distribution, for instance, the exploitable low-temperature hydrothermal systems are abundant on the west side of the presently active rift zone but scarce on the east side. From a simplistic point of view, this may be related to the above mentioned shift of the spreading zone from west to east and the resulting tectonic activity of the last 4-5 m.y. It appears that outside the areas where active fractures or fracture zones occur the permeability of the bedrock is sufficiently low to prevent the establishment of convective low-T systems, or in other words, that heat transfer through the crust is dominated by conduction. Therefore, the low-temperature systems of economic potential are better described as fracture controlled systems which derive heat from normal heat flow by active and localized convection in near vertical fractures or fracture zones (e.g. Flovenz and Saemundsson, 1990).

Hydrothermal Alteration

A form of low-temperature alteration in Iceland under non-convective conditions appears to be preserved by the classical zeolite zones of eastern Iceland, described by Walker (1960), where a close correlation was found to exist between the chemical composition of lavas and the types of zeolites. The regularity of the zeolite zones suggested that a relativley stagnant fluid system had existed in a regime of relatively low geothermal gradient within the Tertiary lavas, presumably for some million years. Heat transfer through the crust may have been dominated by conduction as discussed above. At the other extreme is the development of low-temperature convective systems which only last for a few years. Such a system has recently been discovered on Surtsey Island, which erupted from the seafloor just south of Iceland in 1963-1968. There a local hydrothermal system has formed in the cooling hyaloclastites, and has caused low-temperature zeolitization (Jakobsson and Moore, 1986). The alteration history of Pleistocene hyaloclastite formations in Iceland may range in age between such extremes in time. The overall effect of early zeolitization as well as other diagenetic processes (palagonitization) is to reduce the rock porosity and the permeability, which affects the flow patterns of later

hydrothermal activity if such is established. Early zeolitization, for instance, is found to have occurred within the later high-temperature systems at Nesjavellir, which is discussed below.

In general rock alteration within the active high-tempearture systems of Iceland ranges from zeolite facies to greenschist facies. A fourfold zonal division, based on index minerals, has been correlated with downhole temperatures and used to describe the hydrothermal systems (Kristmannsdottir and Tomasson, 1978; Kristmannsdottir, 1979, 1985; Palmason *et al.*, 1979). The zonal sequence basically involves a prograde transformation from smectite to chlorite, and then the additional appearance of actinolite. The discussion below on the relation between mineralogy and temperature is summarized from the above references. Most of the zeolites are formed at temperatures below 100°C (low-T zeolites). Between 100–120°C laumontite (lau) replaces other zeolites, except mordenite, which may persist to ca 200°C. At 180–200°C wairakite (wai) appears instead of laumontite, and persists at least up to 300°C. The thermal waters tend to be saturated with chalcedony at water temperatures below 180°C, but at higher temperatures equilibrium with quartz (qtz) is attained. Calcite (cc) is common at all temperatures below 300°C, disappearing from 260°C up. Smectite (Sm) is common at all temperatures below 200°C where it becomes interlayered with chlorite, the interlayering referred to as mixed layered clays (mlc). The temperatures at the boundaries between the low-T zeolite zone, the laumontite zone and the wairakite zone correspond to 120°C and 200°C, respectively.

The mineralogical transition from the low- to the high-temperature systems at approximately 200° is marked by the appearance of mlc, wai and qtz. At higher temperatures chlorite (chl) replaces the mixed layer clays, at temperatures somewhat arbitrarily fixed at 230–240°C. Epidote appears at similar temperatures in some areas while in others, like in Nesjavellir, its first appearance was at 260°C. A recent study of the smectite→chl transition from well NJ-15 at Nesjavellir, which is considered to be in a slight prograde state, implies that pure chlorite is first formed at 260°C (Schiffman and Fridleifsson, 1990). In all the above papers near-equilibrium conditions between fluids and minerals were assumed. The same applies to actinolite (act), the first appearance of which has been set at approximately 280°C, while actinolite becomes quite common at temperatures above 300°C. Andradite garnet (gt) has been found sporadically within the active high-T systems, assumed to be related to contact metamorphism, while in a fossil high-T system it has been found to have a cogenetic hydrothermal distribution with actinolite, presumably formed at temperatures above 300°C at low partial CO_2 pressures, as seen by the reactions: chl-cc-qtz→act, and mt-qtz-cc→gt, (Fridleifsson, 1983). While the first formation of some of the index minerals may have taken place at slightly lower temperatures than used below, it seems justifiable to set the temperatures at the zonal boundaries of the chlorite-epidote zone and the actinolite(-garnet)-zone at roughly 50°C intervals, or 250°C and 300°C, respectively. The mineral zones in Figs. 2–5 are sometimes marked by one index mineral only, in which case information on the others is incomplete.

While it has generally been assumed that hot magma is the ultimate heat source for the Icelandic high-temperature systems, mineralogical evidence for the heat transfer processes from the active systems has for obvious reason been somewhat meagre. The former heat sources, however, are quite accessible in the eroded Tertiary volcanoes. In one such extensively studied system clear mineralogical evidence for hot rock-fluid interactions was found at intrusive rock contacts. In the

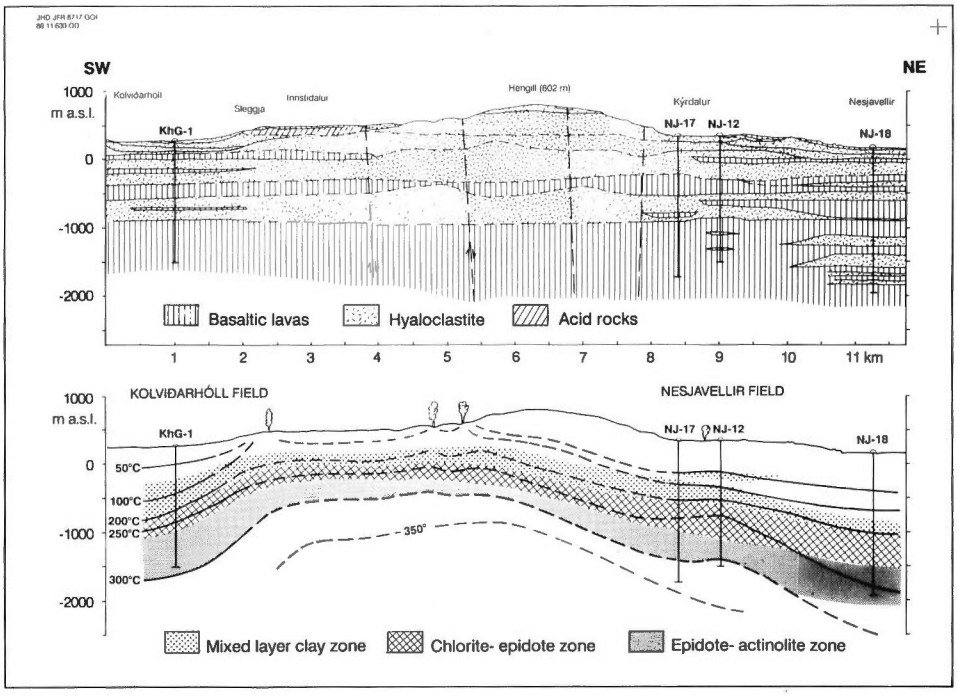

Fig. 2. Traverse 1: A cross section through the active high-temperature hydrothermal system in the Hengill Central Volcano.

case of large intrusive bodies like gabbros, inner aureoles of sanidinite facies metamorphic rocks had developed, enveloped by outer aureoles of hedenbergite–garnet–magnetite–bearing skarns. In another case, now involving thin sheeted dykes, actinolite–bearing assemblages were found within the dykes themselves at shallow levels far above an actinolite–garnet hydrothermal zone. Estimates of the P–T condition suggested that both supercritical and superheated hydrous fluids had existed locally within the otherwise hydrostatically controlled high–T system (Fridleifsson, 1984). Interestingly, such a situation was met in a drillhole at Nesjavellir just a year later, where a thermometer set at max–T of 380°C was permanently damaged (Steingrimsson *et al.*, 1990). A detailed study of drillcuttings from the well and a neighbouring one demonstrated that a transition from greenschist to amphibolite facies rock alteration had taken place, apparently in close proximity to a heat source (Hreggvidsdottir, 1987). Amphibolite–facies rocks, hedenbergite–bearing skarns and sanidinite facies contact metamorphic rocks represent the highest temperature alteration within the Icelandic high–T hydrothermal systems, bridging the gap from standard hydrothermal temperatures to magmatic temperatures.

Recent mineralogical studies at Orkustofnun have mainly focussed on linking the hydrothermal alteration sequences to the volcano–tectonic evolution of the geothermal systems concerned. Some examples are shown below.

The alteration patterns along traverses 1–4 in Fig. 1 are shown in Figs. 2–4. Traverse 1 (Fig. 2) shows a cross section through the active Hengill Central Volcano and its high–T system, while traverses 2, 3 and 4 depict cross sections through the low–T systems on both sides of the active spreading zone. Common to all the

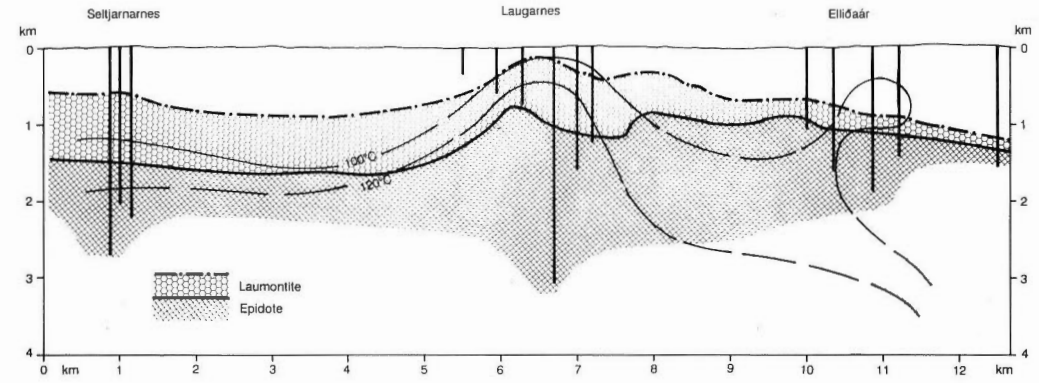

Fig. 3. Traverse 2: A cross-section through the low-temperature systems of Reykjavík, the capital of Iceland.

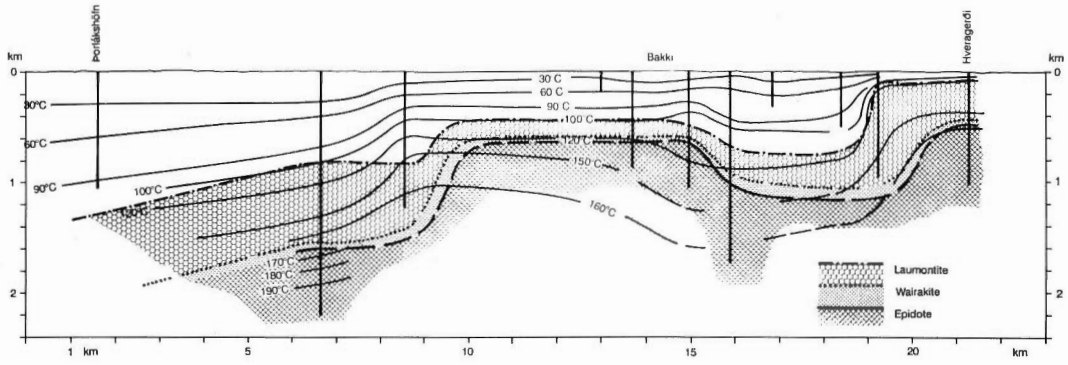

Fig. 4. Traverse 3: A cross-section through the low-temperature area in Ölfus, from Hveragerdi to Thorlákshöfn through the Bakki low-T field.

traverses is the presence of an epidote zone. A comparison between the above temperatures at the zonal boundaries and the present-day isotherms reveals cooling in all cases, but only to a subordinate degree within the active Hengill volcano.

The epidote zones within the Quaternary rocks (traverses 2, 3, 4) represent fossil high-T systems onto which low-T alteration is superimposed. Common to all the low-T systems is that they exist within fractured rocks. In the case of the Laugarnes system (Fig. 3) a fairly recent graben structure, perpendicular to the rift zone, may be responsible, while the south Iceland fracture zone is responsible for the permeability properties of the Bakki (Fig. 4) and Selfoss (Fig. 5) low-T systems. The fossil high-T system at Bakki is possibly a fossil analog of the Reykjanes high-T systems, while the others relate to extinct central volcanoes.

Acknowledgements

Thanks are due to Halldór Armannsson for critically reading this abstract and for providing data, and to Halldór, Kristján Saemundsson, Hrefna Kristmannsdóttir and other colleagues for inspiring discussion. Sincere thanks to Gyda Gudmundsdottir for masterly drawing the figures.

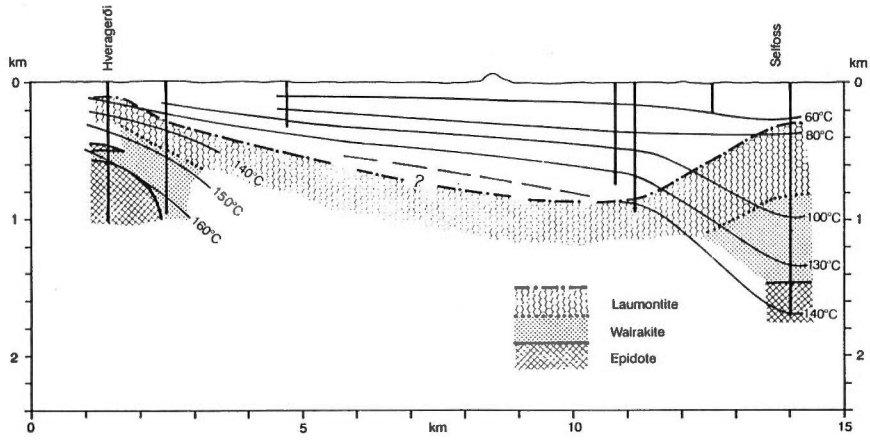

Fig. 5. Traverse 4: A cross-section through the low-temperature area in Ölfus, from Hveragerdi to Selfoss.

References

Armannsson, H., Gíslason, G. and Hauksson, T. (1982) Magmatic gases in well fluids aid the mapping of the flow pattern in a geothermal system. *Geochim. Cosmochim. Acta,* vol. 46, p. 167–177.

———, Benjaminsson, J. and Jeffrey, A.W.A. (1989) Gas changes in the Krafla geothermal system, Iceland. *Chemical Geology,* vol. 76, p. 175–196.

Arnórsson, S. (1979) Hydrochemistry in geothermal investigations in Iceland. *Techniques and applications. Nordic Hydrology,* 1979, p. 191–224.

Flóvenz, O.G. and Saemundsson, K. (1991) Geothermal Atlas of Europe. Explanatory Text for Iceland (in prep).

Fridleifsson, G.O. (1983) The geology and the alteration history of the Geitafell Central Volcano, SE-Iceland. PhD thesis. University of Edinburgh, 371 p.

——— (1984) Mineralogical evolution of a hydrothermal systems. Heat sources–fluid interactions. *Geotherm. Resources Council Trans,* vol. 8, p. 119–123.

Hreggvidsdottir, H. (1987) The greenschist to amphibolite facies transition in the Nesjavellir hydrothermal system, Southwest Iceland. MSc-thesis. Stanford University, 61 p.

Kristmannsdóttir, H. (1979) Alteration of basaltic rocks by hydrothermal activity at 100–300°C. In Mortland and Farmer, eds., *International Clay Conference 1978.* Elsevier Sci. Publ. Comp., p. 359–367.

——— (1985) Clay mineral zones in Icelandic geothermal fields. Abstracts, International Clay Conference 1985, p. 129.

——— and Tómasson, J. (1978) Zeolite zones in geothermal areas in Iceland. In Sand and Mumpton, eds., *Natural zeolites. Occurrence, Properties, Use,* Pergamon Press. p. 277–284.

——— and Olafsson, M. (1989) Manganese and iron in saline groundwater and geothermal brines in Iceland. Proceedings of the 6th Intl. Symposium on Water–Rock Interaction. p. 393–396.

Olafsson, J. and Riley, J.P. (1978) Geochemical studies on the thermal brine from Reykjanes (Iceland). *Chemical Geology,* vol. 21, p. 219–237.

Pálmason, G., Arnórsson, S., Fridleifsson, I.B., Kristmannsdóttir, H., Saemundsson, K., Stefánsson, V., Steingrímsson, B., Tómasson, J. and Kristjánsson, L. (1979) The Iceland crust: Evidence from drillhole data on structure and processes. In Talwani, Harrison and Hayes, eds., *Maurice Ewing Series 2. Deep drilling result in the Atlantic Ocean* Am. Geophys. Union, p. 43–65.

Saemundsson K. (1974) Evolution of the axial rift zone in northern Iceland and the Tjörnes fracture zone. *Bull. Geol. Soc. Am.,* vol. 85, p. 495–504.

Schiffman, P and Fridleifsson, G.O. (1991) The smectite to chlorite transition in drillhole NJ-15, Nesjavellir Geothermal Field, Iceland: XRD, BSE and electron microprobe investigation. *Special Issue of The Journal of Metamorphic Petrology,* (in press).

Steingrímsson, B., Gudmundsson, A., Franzson, H. and Gunnlaugsson, E. (1990) Evidence of a supercritical fluid at depth in the Nesjavellir field. 15th Workshop on Geothermal Reservoir Engineering. Stanford Geothermal Program.

Truesdell, A.H., Haizlip, J.R., Armannson, H. and d'Amore, F.D. (1989) Origin and transport of chloride in superheated geothermal steam. *Geothermics,* vol. 18, p. 295-304.

Walker, G.P.L. (1960) Zeolite zones and dyke distribution in relation to the structure of the basalts in eastern Iceland. *J. Geol.,* vol. 68, p. 515-528.

Redox Processes Accompanying the Deposition of Minerals in Volcanic-Magmatic-Hydrothermal Systems

Werner F. GIGGENBACH

DSIR Chemistry, Private Bag, Petone, New Zealand

The best known manifestations of waters produced through the interaction of initially magmatic vapors with groundwater are probably the highly acid, sulfate-chloride waters of volcanic crater lakes. The formation conditions and chemistry of these generally also highly mineralised waters are quite well understood (Giggenbach, 1975; Kiyosu and Kurahashi, 1983). The possible formation of such waters at depth and their involvement in the formation of ore deposits has recently attracted considerable attention (Sillitoe and Bonham, 1984; Hedenquist, 1987) and there exists a sufficient body of information to describe corresponding "high-sulfidation" ore deposits both geologically and mineralogically in quite some detail (Stoffregen *et al.*, 1989).

In attempts at unravelling underlying formation processes theoretically, major difficulties arise from the fact that the systems straddle a range of geochemically awkward conditions (highly gaseous and saline fluid mixtures at temperatures up to 500° and pH's below 2) not readily accessible to rigorous thermodynamic evaluation. The problems are largely due to the lack of thermodynamic information on vapor-liquid distribution coefficients and ion association constants in these "super-critical" solutions. Considerable headway, however, can be made by "bypassing" solution chemistry and evaluating fluid-rock interaction processes as long as possible in terms of reactions involving only gases and minerals. Their chemistry is generally much simpler and better known. Such an approach, however, has to be based on an accurate and quite detailed understanding of the hierarchy of processes likely to control the two major chemical variables: redox potential and acidity.

In a recent study of processes governing the chemistry of fumarolic gas discharges from White Island, New Zealand (Giggenbach, 1987), two endmember systems controlling the redox potential in volcanic-magmatic-hydrothermal systems were identified: one involving sulfur in its two oxidation states H_2S and SO_2 (gas buffer), the other involving Fe (II) and Fe (III) of the rock (rock buffer). Similarly, the acidity of any coexisting liquid phase was found to be determined by the degree of neutralisation of initially acid magmatic fluids containing, e.g., free HCl to metal chlorides through interaction with the oxide components of the rock phase (Giggenbach, 1988). The overall fluid-rock equilibration process within volcanic-magmatic-hydrothermal systems then corresponds essentially to the more or less successful conversion of SO_2 and HCl, as released under magmatic conditions, to their reduced (H_2S) and neutral (NaCl) counterparts, stable in equilibrium with lower temperature rock.

At high temperatures and in the absence of a liquid phase, the buffer action of the sulfur system is adequately described in terms of H_2S and SO_2. In lower temperature ($<400°C$) solutions, SO_2 is found to disproportionate into H_2S and the sulfate

Keywords: Volcanic-magmatic hydrothermal system, water-rock equilibration process, acid-base equilibrium, redox equilibrium, mineral deposition

species HSO_4^- or SO_4^{2-}. Any redox buffering in such solutions then is likely to be due to coexistence of H_2S with a sulfate species. The redox potentials expected for this buffer system, as shown in Fig. 1, were calculated by use of the reaction,

$$H_2S + 4H_2O\,(g) = H_nSO_4^{n-2} + 4H_2\,(g) + (2 - n)\,H^+ \qquad (1)$$

and

$$R_H = (L_1 + R_S + (2 - n)\,pH)/4, \qquad (2)$$

where L_1 is the logarithm of the equilibrium constant for reaction (1), calculated by use of data reported by Murray and Cubicciotti (1983), $R_H = \log (f_{H_2}/f_{H_2O})$ and $R_S = \log (a_{H_2S}/a_{H_nSO_4^{n-2}})$. Depending on the degree of neutralisation of the solutions, the H_2S–sulfate iso-activity lines move with increasing pH to higher R_H values. The double line marks optimum conditions for buffering of both redox potential and acidity by the sulfide–sulfate system. For solutions having attained full *acid–base* equilibrium with the rock matrix (Giggenbach, 1984), the only way to adjust also to full *redox* equilibrium with the (FeO) – ($FeO_{1.5}$) buffer consists of the conversion of SO_4 to H_2S shifting the $a_{H_2S}/a_{sulfate}$-ratios from the optimum buffer value of unity. This in turn implies that efficient action of the $H_2S - SO_4$ redox

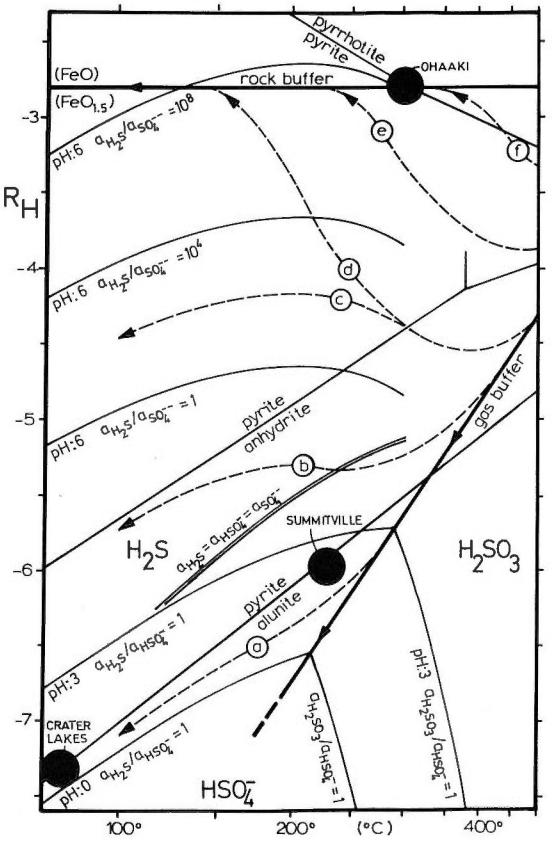

Fig. 1. Predominance diagram of sulfur species in aqueous solutions together with stability areas of sulfur containing minerals as a function of temperature and $R_H = \log (f_{H_2}/f_{H_2O})$.

buffer is limited to lower pH's. Based on this reasoning, it is possible to delineate a number of likely paths taken by fluid mixtures during their rise from an initially magmatic environment to the surface.

Assuming the vapor released from a magma to be cooled rapidly, e.g., when released at shallow levels to be absorbed into nearby groundwater without much interaction with rock, the redox potential of the fluid phase is determined by internal equilibration among H_2, H_2S and SO_2 and the system moves, in Fig. 1, well down the "gas buffer" line. At lower temperatures and in the presence of liquid water, H_2SO_3 tends to disproportionate into H_2S and a sulfate species, HSO_4^- at low, SO_4^{2-} at higher pH's. The positions of the HSO_4^- predominance boundaries vary as a function of the degree of neutralisation of the solution. The general direction of the buffer lines, however, remains unchanged and the path of the rising fluid is likely to change from the "gas buffer" line to one parallel to a $H_2S - HSO_4^-$ boundary, paths (a) to (c).

With decreasing temperature, the reactivity of the solutions with respect to rock alteration increases rapidly. The acidity of solutions formed through absorption of magmatic vapors into groundwater at shallow levels then may become high enough to cause complete rock destruction leaving only silica (quartz, chalcedony) as the alteration product, as observed at White Island (Giggenbach, 1987) and at Summitville (Stoffregen *et al.*, 1989). Following some neutralisation, the next major initial alteration product is alunite. Its stability boundary with respect to conversion to pyrite was evaluated on the basis of the reaction,

2 pyrite + 2 muscovite + 19 steam =
2 alunite + hematite + 6 chalcedony + 15 hydrogen (3)

or

$$R_H = (L_3 + 4F_{H_2O})/15, \quad (4)$$

where L_3 is the equilibrium constant for reaction (3) as obtained from data reported by Bowers *et al.* (1984) and F_{H_2O} the logarithm of the vapor pressure of brines as given by Giggenbach (1987). The pyrite–alunite boundary corresponds to a redox buffer only if alunite already pre-exists within the system. According to Fig. 1, formation of alunite is likely to be restricted to comparatively low temperatures ($< 350°C$). A typical example of a mineral deposit likely to have formed through absorption of magmatic fluids into comparatively shallow groundwater, following path (a), is that at Summitville as described by Stoffregen *et al.* (1989). Its probable position, together with that of obviously shallow volcanic crater lakes, is shown in Fig. 1.

A sulfate mineral potentially forming over a much wider range of conditions is anhydrite. The coexistence boundary with pyrite was calculated on the basis of the reaction,

2 pyrite + 4 Ca-Al_2-silicate + steam =
4 anhydrite + hematite + 4 Al_2-silicate + 15 hydrogen. (5)

Ca-Al_2-silicate represents the Ca-mineral least susceptible to acid alteration. It was taken to be laumontite at temperatures up to 240°C, followed by wairakite and anorthite above 370°C; Al_2-silicate is kaolinite to 240°C, then pyrophyllite (Giggenbach, 1984). Because of the involvement of Ca-Al_2-silicate, the pyrite–anhydrite boundary shown in Fig. 1 reflects conditions in an already quite neutral environment. Actual formation of anhydrite also requires access of the solutions to Ca-containing phases of the rock.

The redox potential of a solution formed through absorption of magmatic vapors into groundwater at higher temperatures would probably still be buffered by H_2S-SO_4^{2-}, as indicated by path (b). If the solution is able to interact with an adequate source for Ca, it would deposit anhydrite as the major secondary sulfur-containing mineral. In the absence of sufficient Ca, the major sulfur-containing alteration mineral remains pyrite.

Solutions forming at even higher temperatures, greater depth, and able to interact extensively with rock at temperatures $>400°C$, e.g., deeper within a volcanic structure, may still be affected by the H_2S-SO_4^{2-} redox buffer to follow path (c). Because of the reduced efficiency of this buffer, weakened by heavily reduced sulfate contents, the redox potential of the rising solutions can be expected to respond more readily to that dictated by the rock phase and the solution may follow path (d). The paths taken by geothermal waters originating from absorption of vapors released from very deep (>5 km) bodies of solidifying magma are likely to be presented by paths (e) and (f). In this case sulfides may be the only major secondary sulfur-containing minerals formed in the entire system, pyrrhotite down to about 300°C, then pyrite. The likely position of such a fully equilibrated, geothermal system is represented in Fig. 1 by Ohaaki (Broadlands), New Zealand.

The pattern of likely reaction paths of Fig. 1 may be superimposed on diagrams depicting stability relationships for other minerals. In Fig. 2 solubility contours of gold are shown. They were evaluated by assuming transport in these predominantly acid solutions as $AuSH^0$, rather than $Au(SH)_2^-$ likely to predominate in neutral solutions. The equilibrium constants of formation of this species were calculated from the experimental data reported by Seward (1973) and Shenberger and Barnes (1989). The average values obtained have a considerable uncertainty (± 2 log units). The lack of precision, however, affects the overall geometry only very little. The major effects of variations in the stability constants are parallel shifts of the contours in Fig. 2 to higher or lower values.

Another aspect affecting the validity of conclusions reached on the basis of Fig. 2, is the possible formation of Au-Cl complexes in the after all quite high Cl, volcanic-magmatic waters. At high temperatures, much of the Cl is likely to be present in associated form, HCl, NaCl or KCl (Ruaya and Seward, 1987) and therefore may not be able to compete with H_2S, also present in large amounts.

Accepting $AuSH^0$ to predominate, a saturated solution following path (a) would deposit 90% of any Au carried over comparatively narrow ranges of temperature of about 40°C. A solution following path (b) would deposit Au down to 350°C, but on further cooling would suddenly become undersaturated. Such a change in saturation over a small temperature interval may explain the close coexistence of gold-bearing and barren quartz veins in many mines. The existence of barren zones is also suggested by trajectories (c) and (d). Any solution, having deposited Au in an environment where sulfate minerals are present and following a H_2S-sulfate buffer line, would, on further cooling, become undersatured with respect to the deposition of Au and would remain so to quite low temperatures.

In the case of waters having formed at high temperatures and avoiding the formation of sulfate minerals, the rate of Au deposition with temperature is much "slower", but continuous. It would take a drop in temperature by 100°C to deposit 90% of any gold from a saturated solution. The differences in the theoretical rates and trends of Au precipitation with temperature may explain the different styles of ore formation in high and low sulfidation Au deposits.

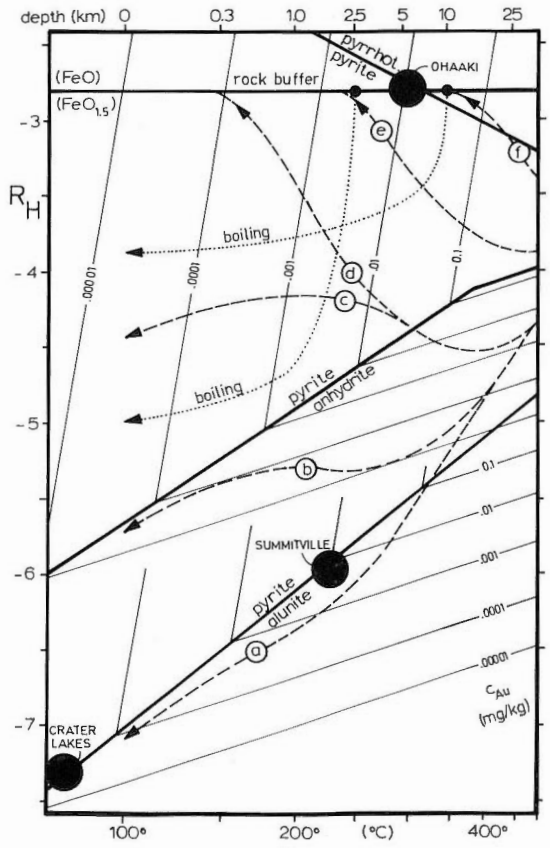

Fig. 2. The solubility of gold in aqueous solutions (in mg/kg), as $AuSH^0$, as a function of temperature and $R_H = \log (f_{H2}/f_{H2O})$.

Figure. 2 also contains two (dotted) lines showing the effects of closed system boiling on R_H values. For fully equilibrated solutions, starting to boil at temperatures of 350° and 250°C, R_H values drop initially very rapidly then much more slowly. For these systems, remaining in equilibrium with pyrite, boiling would actually delay Au deposition as solutions become undersaturated. Additional loss of H_2S to the vapor phase, however, may destabilise any Au–SH complex and Au would precipitate (Brown, 1989 ; Seward, 1989).

The effects of boiling on the solubility of Au would be quite drastic for more oxidised systems in equilibrium with a sulfate mineral. Boiling from 350° to 300° C would reduce saturation Au contents by four orders of magnitude. These acid systems, however, are likely to contain a free vapor phase throughout. In this case "boiling" is a continuous process and associated effects become much less important. Another process delaying the deposition of metallic Au in fully equilibrated, less acid systems is the conversion of $AuSH^0$ to more stable $Au(SH)_2^-$. Figure. 2 clearly shows that mineral deposition processes can be quite complex and depend strongly on the path taken by the rising fluids.

References

Bowers, T.S., Jackson, K.I. and Helgeson, H.C. (1984) Equilibrium activity diagrams.

Springer Verlag.
Brown, K.L. (1986) Gold deposition from geothermal discharges in New Zealand. *Econ. Geol.*, vol. 81, p. 979–983.
Giggenbach, W.F. (1975) The chemistry of Crater Lake, Mt Ruapehu (New Zealand) during and after the 1971 active period. *NZ J. Science*, vol. 17, p. 33–45.
——— (1984) Mass transfer in hydrothermal alteration systems. *Geochim. Cosmochim.* Acta, vol. 48, p. 2693–2711.
——— (1987) Redox processes governing the chemistry of fumarolic gas discharges from White Island, new Zealand. *Appl. Geochem.*, vol. 2, p. 143–161.
——— (1988) The interplay of magmatic and hydrothermal processes in the formation of volcanic and geothermal fluid discharges. Proc. Kagoshima Int. Conf. on Volcanoes, p. 843–846.
Hedenquist, J.W. (1989) Mineralisation associated with volcanic-related hydrothermal systems in the Circum-Pacific Basin. Trans. 4th Circum-Pacific Energy and Mineral Resources Conference, Singapore, 1986, p. 513–524.
Kiyosu, Y. and Kurahashi, M. (1983) Origin of sulfur species in acid sulfate-chloride thermal waters, NE Japan. *Geochim. Cosmochim. Acta*, vol. 47, p. 1237–1245.
Murray, R.C. and Cubicciotti, D. (1983) Thermodynamics of aqueous sulfur species to 300° and potential-pH diagrams. *J. Electrochem. Soc.*, vol. 130, p. 863–869.
Ruaya, J.R. and Seward, T.M. (1987) The ion-pair constant and other thermodynamic properties of HCl up to 350°. *Geochim. Cosmochim. Acta*, vol. 51, p. 121–130.
Seward, T.M. (1973) Thio complexes of gold and the transport of gold in hydrothermal ore solutions. *Geochim. Cosmochim. Acta*, vol. 37, p. 379–399.
——— (1989) The hydrothermal chemistry of gold and its implications for ore formation: boiling and conductive cooling as examples. *Econ. Geol. Monogrq* vol. 6, p. 398–405.
Shenberger, D.M. and Barnes, H.L. (1989) Solubility of gold in agueous sulfide solutions from 150–350°C. *Geochim. Cosmochim. Acta*, vol. 53, p. 269–278.
Sillitoe, R.H. and Bonham, H.F. (1984) Volcanic landforms and ore deposits. *Econ. Geol.*, vol. 79, p. 1286–1298.
Stoffregen, R.E., Rye, R.O. and Bethke, P.M. (1989) Relationship between magmatic and hydrothermal processes in the Summitville, Colorado, gold deposit. Abstr. IAVCEI Gen. Ass., Santa Fe. *New Mexico Bur. Mines Min. Res., Bull.* vol. 131, p. 256.

Geological Survey of Japan Report, No. 277, 1991, p. 97-99

Pressure Dependence of Water/Rock Reaction and Control of HCl/NaCl Ratio

Hiroshi SHINOHARA

Geological Survey of Japan, Higashi 1-1-3, Tsukuba, Ibaraki, 305 Japan

Introduction

There have been a number of experimental studies on mineral-water reaction equilibrium. Temperature dependence investigations of equilibrium constants were conducted in wide range of temperature from 200 to more than 1000°C, which exhibited the importance of the temperatures dependence. On the other hand, the studied pressure range is rather limited to from 1 to 2 kb, and the pressure dependence of equilibrium constants has been generally regarded as less important than the temperature dependence. The number of the pressure dependence study is, however, limited, and most of the experiments were carried out in the pressure range from 1 kb to larger pressure.

The pressure dependence of the equilibrium constant is controlled by partial molar volumes of the reactants and products. Under the conditions of the upper crust, the molar volumes of minerals are almost constant. In contrast with the minerals, the partial molar volumes of the components in the aqueous phase are strongly pressure-dependent, especially at low pressure. Dehydration reactions may be good examples to show the importance of the pressure dependence in the low pressure range where the molar volume of water is much larger than at higher pressure. As the aqueous phase is much less dense at lower pressure, the partial molar volumes of solutes may also be strongly affected by the pressure. In this short report, I will discuss the pressure dependence of water/rock reactions which control the HCl/NaCl ratio in the aqueous phase, with an example of the experimental study of the andalusite-quartz-albite-water-NaCl-HCl system.

Experimental

The equilibrium constants of the following reaction were experimentally obtained at temperature of 600°C and in the pressure range from 400 to 2000 bars (Shinohara and Fujimoto, 1988),

$$1/2Al_2SiO_5 + 5/2SiO_2 + 1/2H_2O + NaCl = NaAlSi_3O_8 + HCl.$$
(Andalusite) (Quartz) aq aq (Albite) aq

Since each solid phase is pure, the equilibrium constant of the reaction can be expressed with activities of the components in the aqueous phase, as follows,

$$K = a_{HCl}/[a_{NaCl} \times (a_{water})^{1/2}].$$

The equilibrium constants were obtained for dilute solutions in this study. With the assumption of unit activity coefficients and unit activity of water, the equilibrium constant can be reduced to the following form,

$$K = C_{HCl}/C_{NaCl}.$$

Keywords: water-rock reaction, pressure dependence, equilibrium constant, HCl/NaCl ratio, partial molar volume

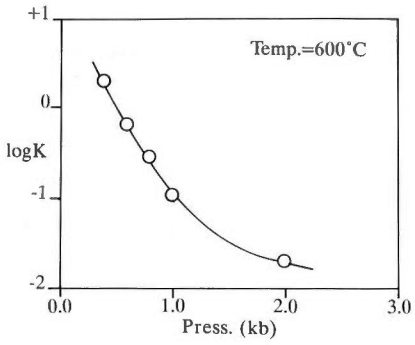

Fig. 1. Variation of the equilibrium constant with pressure.

The equilibrium constants obtained are plotted against pressure in Fig. 1. There is a strong negative pressure dependence of the equilibrium constant, especially in the lower pressure range.

Discussion

The pressure dependence of the equilibrium constant is expressed by the change in the molar volume by the reaction as follows,

$$(\partial \ln K/\partial P)_T = -\Delta V/RT,$$

where ΔV is the change in the molar volume by the reaction, and R is the gas constant. For the above reaction, ΔV is expressed as follows,

$$\begin{aligned}\Delta V &= (V_{Ab} - 0.5V_{And} - 2.5V_{Qtz})_s + (V_{HCl} - V_{NaCl} - 0.5V_{water})_{aq} \\ &= \Delta V_s + \Delta V_{aq},\end{aligned}$$

where s and aq indicate the solid phase and the aqueous phase, respectively.

The ΔV can be calculated from the obtained pressure dependence. The molar volumes of albite, andalusite, and quartz are 100, 52, and 23 (cm^3/mol), respectively (Robie *et al.*, 1978), and these molar volumes are taken to be invariant in the studied pressure range. Since the aqueous phase is dilute, the molar volume of pure water at each condition is applied. With the volume data given by Burnham *et al.* (1969), the difference in the partial molar volumes of HCl and NaCl in the aqueous phase can be calculated, and the results are listed in Table 1.

As seen in Table 1, the difference in the partial molar volumes of HCl and NaCl in the dilute aqueous phase is calculated to have very large values. The ΔV_s, the molar volume change in the solid phase, is calculated to be 17 (cm^3/mol), which is almost negligible in comparison with the V_w and $(V_{HCl} - V_{NaCl})$. Although the V_w, the molar volume of water, is known to have a large value at high temperature and low pressure, the effect of V_w on ΔV is found to be much less than that of $(V_{HCl} - V_{NaCl})$. And it can be concluded that the large negative pressure dependence of the reaction is due to the large ΔV, which is mainly controlled by the $(V_{HCl} - V_{NaCl})$.

Concluding Remarks

The experimental study of Ab–And–Qtz–NaCl–HCl–H_2O system illustrated the strong pressure dependence of the equilibrium constant at 600°C, which will provide the aqueous solution with a higher HCl/NaCl ratio at lower pressure. As the large

Table 1 List of pressure, equilibrium constant, ΔV, V_{Water}, and $(V_{HCl}-V_{NaCl})$.

Press. (kb)	lnK	$\left(\frac{\partial \ln K}{\partial P}\right)$	ΔV	V_w	$V_{HCl}-V_{NaCl}$
0.4	0.7				
		>-5.5	400	117	440 ± 140
0.6	-0.4				
		>-4.0	290	74	310 ± 140
0.8	-1.2				
		>-5.5	400	55	410 ± 140
1.0	-2.3				
		>-1.6	120	39	120 ± 30
2.0	-3.9				

V is in cm^3/mol.
The uncertainty in $(V_{HCl}-V_{NaCl})$ is due to the uncertainty in K ($\pm10\%$).

pressure dependence of the equilibrium constant is due to the large $(V_{HCl} - V_{NaCl})$, the equilibrium constant of the following general reaction is also expected to show a large pressure dependence,

$$Rock + NaCl + 1/2H_2O = Rock^* + HCl,$$

and

$$\Delta V = (V_{Rock} - V_{Rock^*}) + (V_{HCl} - V_{NaCl} - 0.5V_{water}).$$

The $(V_{Rock} - V_{Rock^*})$ is expected to be negligible and ΔV is mainly controlled by $(V_{HCl} - V_{NaCl})$. As the equilibrium constant of the above reaction will show a large negative pressure dependence, the HCl/NaCl ratio in the aqueous phase, which is in equilibrium with common host rocks, is always expected to increase with a decrease in pressure at constant temperature.

References

Burnham C.W., Holloway J.R. and Davis N.F. (1969) Thermodynamic properties of water to 1,000°C and 10,000 bars. *Geol. Soc. Am. Special Paper* no. 132, p 96.

Robie R.A., Hemingway B.S. and Fisher J.M. (1978) Thermodynamic properties of minerals and related substances at 298.15 K and 1 bar (10^5 Pascals) pressure and at high temperatures. *Geol. Survey Bull.* 1452. p 455.

Shinohara H. and Fujimoto K. (1988) Pressure dependence of mineral-water reaction equilibrium in the low pressure range. Proc. 6th Int. Symp. Water-Rock Interaction, p. 635-638.

Generation of HCl by High Temperature Hydrolysis of NaCl

Kohei KAZAHAYA and Hiroshi SHINOHARA

Geological Survey of Japan, Higashi 1-1-3, Tsukuba, Ibaraki, 305 Japan

Introduction

It is ambiguously thought that high temperature acid fluids originally relate to a magma. But, as some workers have pointed out, the hydrolysis process will generate HCl in the system NaCl-H_2O at high temperatures, implying the possibility of the generation of non-magmatic acid fluids. Concerning the behavior of acid fluids in magmatic hydrothermal systems, we must investigate, at first, whether or not the origin of the acid fluids is magmatic. Both magmatic and non-magmatic acid fluids may exist in the natural system. We will show possible processes for the generation of the acid fluids by the hydrolysis of halite or brine, which is thought to be formed near the magmatic heat source.

Hydrolysis Reaction

The high temperature experiment for the hydrolysis of solid and molten NaCl was firstly performed by Hanf and Sole (1970). They found a greater generation of HCl than otherwise expected, because the activity of NaOH was much less than unity. This reaction with the addition of silicates has been applied for producing cheap silicates for the glass industry, or for producing "HCl".

The reaction of NaCl hydrolysis and the equilibrium constant $K_r(1)$ are written as;

$$NaCl\ (s, l) + H_2O\ (g) = NaOH\ (s, l) + HCl\ (g) \quad (1)$$
$$K_r\ (1) = a_{NaOH}P_{HCl}/a_{NaCl}P_{H_2O}.$$

The P_{HCl}/P_{H_2O} ratio is proportional to the a_{NaOH}. A smaller a_{NaOH} yields a higher P_{HCl}. The activity of NaOH may be reduced by other acid gases such as CO_2 and SO_2. A typical reaction that controls the a_{NaOH} can be written as ;

$$NaOH\ (s, 1) + 1/2\ CO_2\ (g) = 1/2\ Na_2CO_3\ (s, l) + 1/2\ H_2O\ (g). \quad (2)$$

By analogy with the industrial processes for producing economical amounts of HCl, silicates may also be important substances for reducing a_{NaOH}.

Quantitative Discussions

Minimum estimates on C_{HCl} or P_{HCl}/P_{H_2O} of the evolved gas can be obtained by treating reaction (1). A simple flow system as shown in Fig. 1 is considered for calculating the C_{HCl} value. In this model, high temperature halite or brine is continuously depositing near the intruded magma.

The model flow system is discussed using the terms listed below.

n_i : number of moles of species i produced in time t,

F : flow rate of H_2O,

P_i : equilibrium partial pressure of species i,

g : activity coefficient of NaOH in NaCl,

Keywords : Hydrolysys, acid fluid, HCl, NaCl, brine

r_i : (species i)/H_2O mole ratio of the supplied solution.
The rates of HCl production (= NaOH production) and NaCl deposition are,

$$dn_{HCl}/dt = FP_{HCl}/P_{H_2O}, \quad (3)$$

and

$$dn_{NaCl}/dt = Fr_{NaCl}. \quad (4)$$

Since, $a_{NaOH} = gn_{HCl}/n_{NaCl}$ with $a_{NaCl} = 1$, assuming equilibrium, the equilibrium constant $K_r(1)$ is,

$$K_r(1) = gn_{HCl} P_{HCl}/n_{NaCl} P_{H_2O}. \quad (5)$$

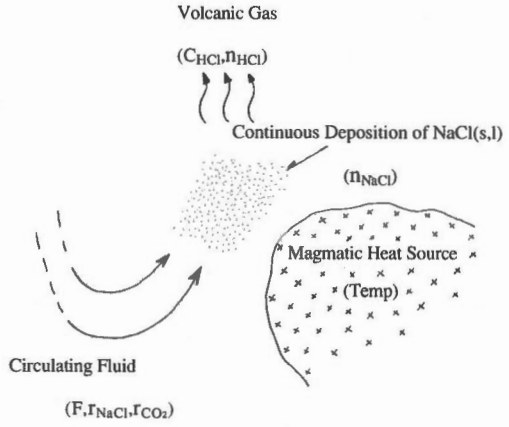

Fig. 1. Schematic view of a simple model flow system used for calculating HCl concentration in vapor phase.

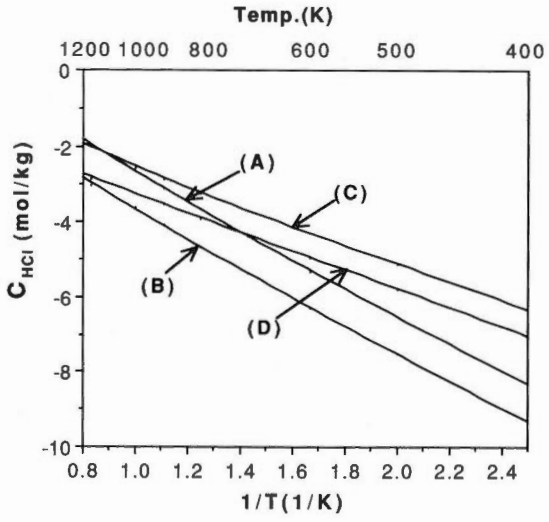

Fig. 2. Relationship between C_{HCl} and temperature. (A) and (B) are the results for the binary system ($NaCl$-H_2O), and (C) and (D) for the ternary system ($NaCl$-H_2O-CO_2). (A): $r_{NaCl} = 0.01$, (B): $r_{NaCl} = 0.0001$, (C): $r_{NaCl} = 0.01$, $r_{CO2} = 0.01$, (D): $r_{NaCl} = 0.0001$, $r_{CO2} = 0.01$.

From eqs (3), (4) and (5), integration yields,

$$n_{HCl} = (r_{NaCl} K_r (1)/g)^{1/2} \, Ft. \quad (6)$$

Thus, C_{HCl} is,

$$C_{HCl} = 55.5 n_{HCl}/Ft = 55.5 (r_{NaCl} K_r (1)/g)^{1/2}. \quad (7)$$

Obviously, C_{HCl} is independent of time, but is dependent on temperature and r_{NaCl}. The relationship between C_{HCl} and temperature is plotted in Fig. 2. At temperature conditions higher than 800 K, vapor with relatively high HCl concentration can be generated during the NaCl deposition process. In the figure, the result in the ternary NaCl–H_2O–CO_2 system using eqs. (1) and (2) with the same approach as that of NaCl–H_2O system is also plotted for comparison. The presence of CO_2 gives a slight higher C_{HCl} value in the vapor phase.

In natural systems, there are many other components or reactive materials that may reduce a_{NaOH} or increase C_{HCl}, such as SO_2, HF and silicates. The silicate behavior during NaCl hydrolysis is of interest; however, the abilities on buffering the a_{NaOH} have not been clearly established. Further experiments are necessary to discuss more complex systems. In conclusion, we must consider the possibility of the generation of acid gas from a non-magmatic source in the study of magmatic hydrothermal systems.

Reference

Hanf, N.W. and Sole, M.J. (1970) High-temperature hydrolysis of sodium chloride. *Trans. Faraday Soc.*, vol. 66, p. 3065–3074.

Three End-members of Hydrothermal Fluid Related to the Izu Oshima Volcanic Eruption: Magmatic, Sea Water and Meteoric

Masaaki TAKAHASHI, Kikuo ABE, Tetsuro NODA,
Kohei KAZAHAYA and Naoyuki ANDO

Geological Survey of Japan, Higashi 1-1-3, Tsukuba, Ibaraki, 305 Japan

Introduction

A groundwater temperature increase of >40°C was observed in the northwestern part of Izu Oshima Island since June, 1987, seven months after the 1986 eruption of Izu Oshima Volcano. Only two other observations of temperature increase of groundwater or hot spring water around volcanoes after volcanic activities have been reported in Japan. One is Toyako hot spring, discovered after the 1910 eruption of Usu Volcano, northern Japan (Soya *et al*,. 1981) and another is Gora hot spring, where a temperature increase of about 20°C was observed about a year after the 1966 activity (swarm earthquake) of Hakone Volcano, central Japan (Oki *et al.*, 1968). We present mechanisms of thermal water formation which caused the remarkable temperature increase of groundwater in Izu Oshima Island, from observations of temperature, chemical concentrations and isotopic compositions of groundwater.

The Geologic Setting of Izu Oshima Volcano

Izu Oshima Island is located in Sagami Bay of the Pacific, about 120 km SSW of Tokyo and about 40 km E of the Izu Peninsula (Fig. 1). Izu Oshima Volcano is an active basaltic volcano overlying highly dissected remnants of three old volcanoes.

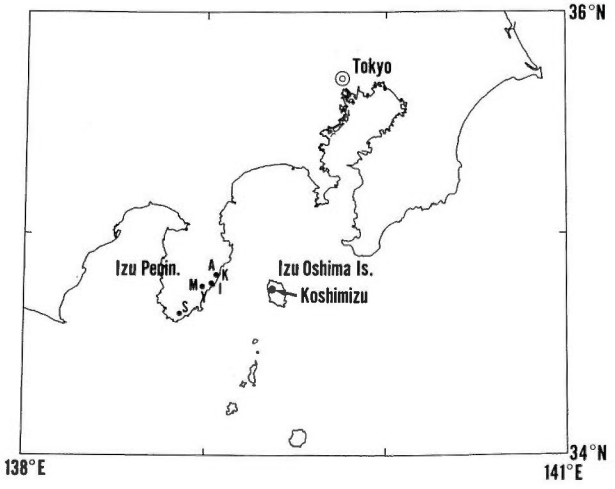

Fig. 1. Locality map of Izu Oshima Island.
S: Shimogamo hot spring, a typical hot spring formed by the interaction between sea water and rock (Mizutani and Hamasuna, 1972).

Keywords : Izu Oshima, volcanic eruption, thermal water, magmatic water, sea-water, meteoric water, chemical composition, isotopic composition

The present Izu Oshima Volcano began its eruptive activities a few tens of thousands years ago and large-scale eruptions from a summit crater occurred repeatedly every 100–200 years to form a pre-caldera stratovolcano. At the top of the volcano, there is a gourd (cocoon)-shaped caldera (4.5 km × 3.5 km) formed about 1500 years ago. In the southwestern part of the caldera, a post-caldera cinder cone, called Mihara Yama (Mt. Mihara), formed about 200 years ago (Nakamura, 1964). This volcano started to erupt from the central crater of Mt. Mihara on November 15, 1986. On November 21, fissure eruptions began violently on the caldera floor and outside the caldera rim NNW to NW of Mt. Mihara (GSJ, 1987). The activity of Izu Oshima Island has been relatively calm after the eruptions of December 18, 1986, and November 16 and 18, 1987.

Groundwater in Izu Oshima Island

In oceanic islands, there are generally two types of groundwater systems (Macdonald and Abbott, 1970). One is the Ghyben-Herzberg's (fresh water) lens, floating on a saline (sea) water layer due to the difference of their densities. The shape of the fresh water body is like a lens, which thickens inland. The other groundwater system is perched water. The distribution of this water is restricted by several types of impermeable layers, buried old soil, volcanic ash and dikes. All wells in the northwestern part of this island, where noticeable groundwater temperature increase has been observed, penetrate the fresh water body of the Ghyben-Herzberg's lens. The chemical and isotopic compositions of the Ghyben-Herzberg's lens are caused by a single mixture of meteoric water and sea water.

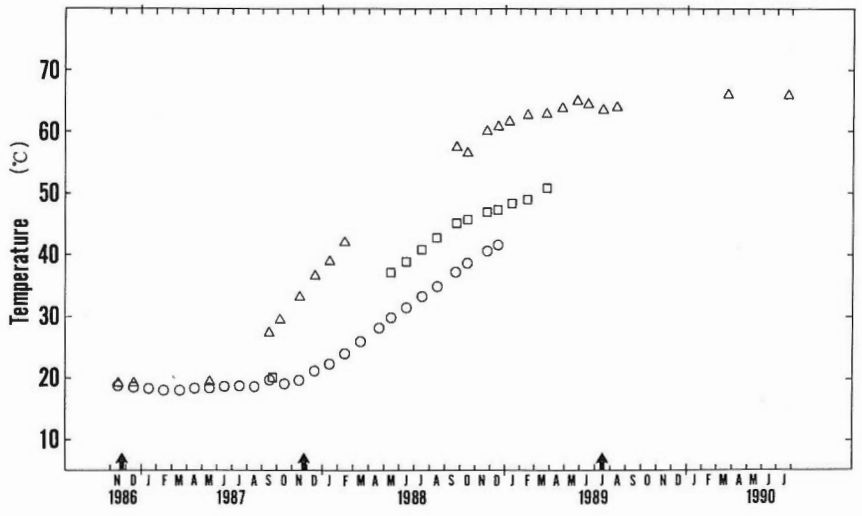

Fig. 2. Monthly changes of water temperature at Koshimizu well (△), Dai-ichi Junior High School well (□) and Otsu well (○). Koshimizu well is located 5 km NW of Mt. Mihara and 1 km WNW of the nearest craters of the fissure eruption outside the caldera rim.
Dai-ichi Junior High School well is located 20 km WSW and Otsu well is 300 m SW of Koshimizu well, respectively. ⬆ shows the 1986 and 1987 eruptions of Izu Oshima Volcano, and the 1989 submarine eruption off eastern Izu Peninsula, respectively.

Results and Discussion

The temperature of groundwater probably started to increase in the northwestern part of the island in June, 1987, seven months after the 1986 eruption. However, temperature measurements were not made until September at Koshimizu well, the closest observation well to one of the volcanic fissures. The temperature increase has now been observed in wells in a radius of 1000 m from the Koshimizu well. For the first several months, the rate of temperature increase was 3°C/month at the Koshimizu well, but has gradually become smaller, as shown in Fig. 2. The monthly changes of Cl^- and total CO_2 concentrations are shown in Figs. 3 and 4, and the correlation between Cl^- concentration and $\delta^{18}O$ values in Fig. 5. The monthly

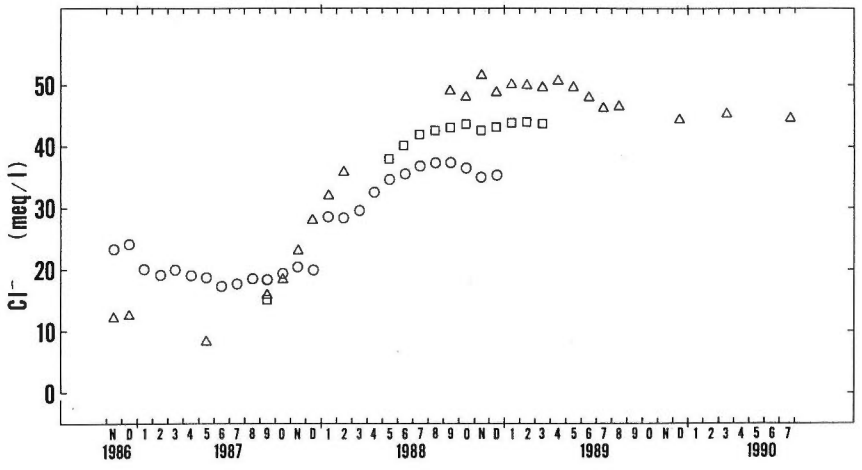

Fig. 3. Monthly changes of Cl^- concentration at Koshimizu, Dai-ichi Junior High School and Otsu wells. Cl^- concentration of sea water is about 535 meq/l.

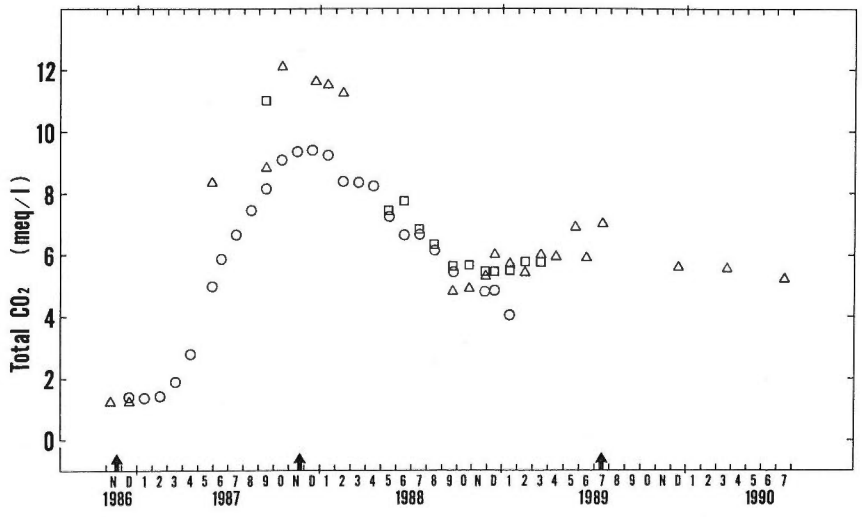

Fig. 4. Monthly changes of total CO_2 concentration at Koshimizu, Dai-ichi Junior High School and Otsu wells.

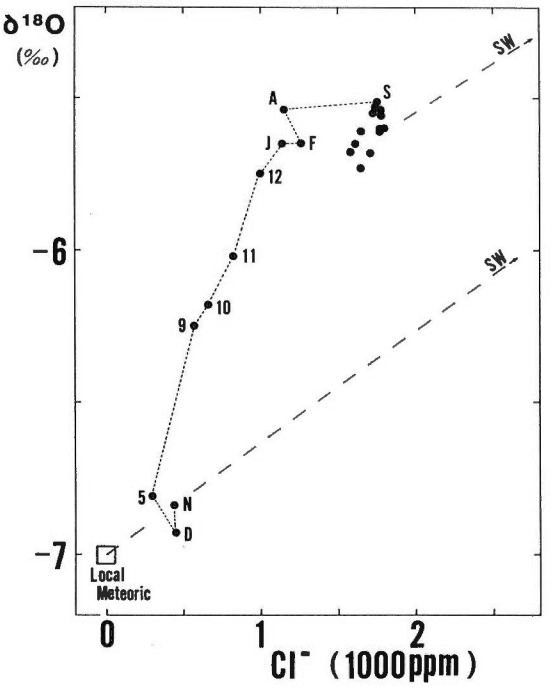

Fig. 5. Correlation between Cl^- concentrations and $\delta^{18}O$ values of water obtained from Koshimizu well. N and D: November and December, 1986. 5 to 12: May to December, 1987. J to S: January to September, 1988. After September, 1988, compositions cluster near the S value. To avoid congestion, only September, 1988 is labeled. The upper dashed line trends towards sea water. The lower dashed line is a mixing line between sea water and local meteoric water ($Cl^- \fallingdotseq 0$ ppm and $\delta^{18}O \fallingdotseq -7$ ‰). Compositions of water from other areas on Izu Oshima Island plot near the mixing line of sea water and local meteoric water. From May, 1987, to April, 1988, the correlation between Cl^- and $\delta^{18}O$ at Koshimizu well trends toward relatively ^{18}O-rich water (thermal water), and after April, 1988, the trend is toward the composition of sea water.

changes of Na^+ and K^+ concentrations are similar in style to that of Cl^-, while Mg^{2+} is similar in change to total CO_2. The monthly change of Ca^{2+} concentration was first related to variation of total CO_2 concentration, but then varied with the Cl^- concentration.

Monthly changes of temperature, chemical concentrations and isotopic compositions in the Koshimizu well are divided into the following four periods, according to these observations.

(1) From January to June, 1987, Cl^- concentration decreased from that observed before the 1986 eruption, while total CO_2 increased. $\delta^{13}C$ values of the total CO_2 were about -5‰, consistent with a magmatic source. The influence of sea water decreased and simultaneously that of volcanic gases, especially CO_2 gas, increased.

(2) From June to November, 1987, water temperature and chemical compositions (except SO_4^{2-}) increased. The change in δD and $\delta^{18}O$ values trended toward sea water, but with a shift due to a component of high temperature volcanic gas (see

Fig. 6) as measured for Izu Oshima fumaroles (which have an envelope of compositions if mixed with local groundwater). $\delta^{34}S$ values of SO_4^{2-} decreased to 10 to 13‰ from values similar to sea water, as observed before the 1986 eruption. The influence of sea water had decreased at this stage, and thermal water intruded into the Ghyben-Herzberg's lens.

(3) From November, 1987 to September, 1988, water temperature and Cl^- concentrations increased and total CO_2 decreased. The correlation between Cl^- and $\delta^{18}O$ values trended toward sea water (see Fig. 5). The influence of volcanic gas had been replaced by the influence of sea water.

(4) After September, 1988, water temperature, chemical concentrations and isotopic compositions have been almost constant.

From the correlation between Cl^- and other major ion concentrations, depletion of Na^+, Mg^{2+} and SO_4^{2-} and enrichment of K^+ and Ca^{2+} are apparent. These phenomena indicate the interaction between sea water and rock, as observed in hot springs near the sea shore like Shimogamo hot spring, Izu Peninsula (see Fig. 1)

Conclusions

The mechanisms of thermal water formation may be deduced as follows. A schematic diagram of the mechanisms is shown in Fig. 7.

(1) Fluid pressure increase in the volcano occurred after the 1986 eruption, originating from the ascent of volcanic gases (magmatic emanations). As the permeation of sea water into the island was restricted by the pressure increment, the degree of mixing of saline water into the Ghyben-Herzberg's lens decreased. Subsequently, the salinity of the Ghyben-Herzberg's lens became relatively low.

(2) Volcanic gases rose in the northwestern part of Izu Oshima Island through

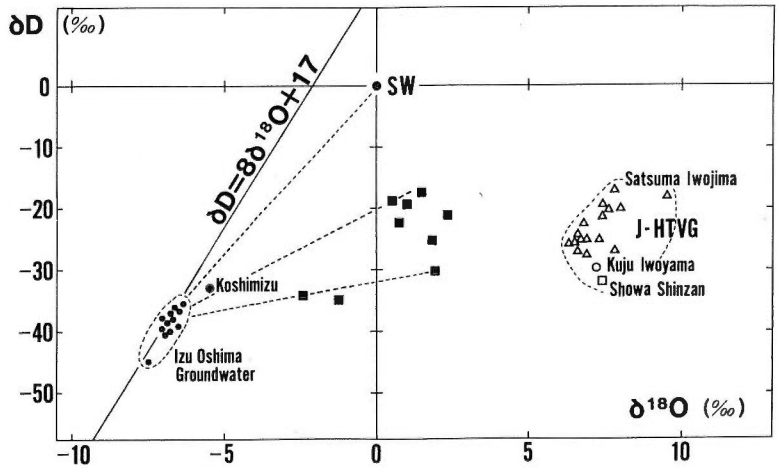

Fig. 6. Correlation between $\delta^{18}O$ and δ D values of water.
The Koshimizu well sample was collected in September, 1988. ■: Condensed waters obtained from fumaroles near the central crater of Mt. Mihara. J-HTVG: High temperature volcanic gas obtained from several fumaroles near active volcanoes in Japan. SW: Sea water. $\delta^{18}O$ and δD values of groundwater around the Koshimizu well are about -7‰ and -39 ‰, respectively. In Izu Oshima Island, the compositions of water sampled from the Ghyben-Herzberg's lens plot near the mixing line between sea water and groundwater.

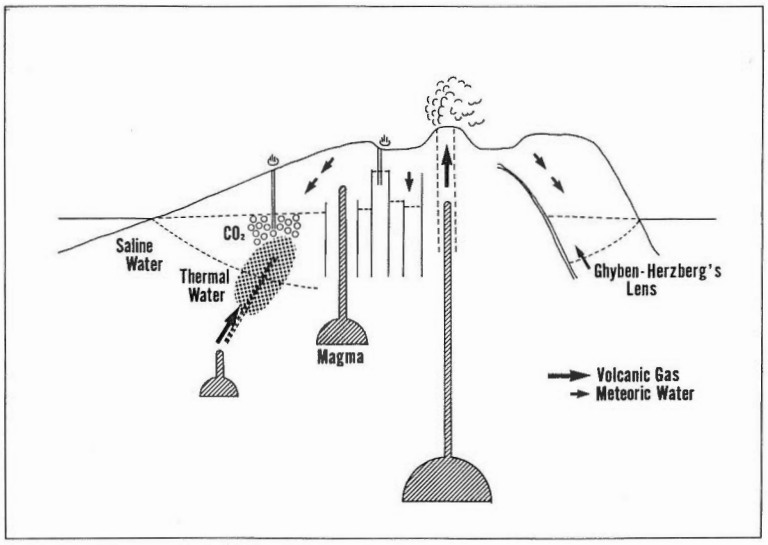

Fig. 7. A schematic diagram showing the mechanisms of thermal water formation which caused the large temperature increase of groundwater in the northwestern part of Izu Oshima Island.

fractures formed during the 1986 eruption. At first, only CO_2 gas reached the Ghyben-Herzberg's lens, because the solubility of CO_2 gas in the deeper water was lower than other acid gases, like HCl and SO_2. Leaching of Mg^{2+} and Ca^{2+} then occurred.

(3) Boiling of a mixture of saline water and volcanic gases, or boiling of sea water itself, then occurred. Condensed water and condensates of volcanic gases reacted with wall rocks and formed thermal water. This thermal water then ascended to the Ghyben-Herzberg's lens.

(4) The thermal water warmed the surrounding saline water layer and convection occurred in the layer.

(5) At present, the remnants of thermal water and heated sea water maintain a nearly constant condition.

References

Geological Survey of Japan (1987) The 1986 eruption of Izu Oshima Volcano. Sakaguchi, K., Okumura, K., Soya, T. and Ono, K. eds. 8 p. (in Japanese).

Macdonald, G.A. and Abbott, A.T. (1970) Volcanos in the sea. Univ. Hawaii Press, Honolulu, 441 p.

Mizutani, Y. and Hamasuna, T. (1972) Origin of the Shimogamo geothermal brine, Izu. *Bull. Volcan. Soc. Japan,* vol. 17, p. 123–134 (in Japanese).

Nakamura, K. (1964) Volcano-stratigraphic study of Oshima Volcano, Izu. *Bull. Earthq. Res. Inst. Univ. Tokyo,* vol. 42, p. 649–728.

Oki, Y., Ogino, K., Hirano, T., Hirota, S., Ohguchi, T. and Morita, M. (1968) Anomalous temperature encountered in the Gora hydrothermal system of Hakone Volcano and its hydrological explanation. *Bull. Hot Spring Inst. Kanagawa Pref.,* no. 6, p. 1–20 (in Japanese).

Soya, T., Katsui, Y., Niida, K. and Sakai, K. (1981) Geologic map of Usu Volcano. Geol. Surv. Japan. 10 p. (in Japanese).

地 質 調 査 所 報 告

第 271 号
矢野雄策・須田芳朗・玉生志郎編：日本の地熱調査における坑井データ　その 1　コア測定データ—物性，地質層序，年代，化学組成—，1989

第 272 号
Sato, Y.: Paleontological study of molluscan assemblages of the Miocene Moniwa Formation, Northeast Japan and description of their Pectinidae, 1991

第 273 号
須田芳朗・矢野雄策：日本の地熱調査における坑井データ　その 2　検層データおよび地質柱状図データ，1991

第 274 号
鹿野和彦・加藤碵一・柳沢幸夫・吉田史郎：日本の新生界層序と地史，1991

第 275 号
玉生志郎編：日本の地熱資源評価に関する研究，1991

第 276 号
村田泰章・須田芳朗・菊地恒夫：日本の岩石物性値　—密度，磁性，P 波速度，有効空隙率—，1991

REPORT, GEOLOGICAL SURVEY OF JAPAN

No. 271
Yano, Y., Suda, Y. and Tamanyu, S. eds.: Well data compiled from Japanese Nation-Wide geothermal surveys, Part 1 Core sample data, 1989 (in Japanese with English abstract)

No. 272
Sato, Y.: Paleontological study of molluscan assemblages of the Miocene Moniwa Formation, Northeast Japan and description of their Pectinidae, 1991 (in English)

No. 273
Suda, Y. and Yano, Y.: Well data compiled from Japanese Nation-Wide geothermal surveys, Part 2 Logging data geologic columnsdata, 1991 (in Japanese with English abstract)

No. 274
Kano, K., Kato H., Yanagisawa, Y. and Yosida, F.: Stratigraphy and geologic history of the Cenozoic of Japan, 1991 (in Japanese with English abstract)

No. 275
Tamanyu, S. ed.: Research on the geothermal resource assessment in Japan, 1991 (in Japanese with English abstract)

No. 276
Murata, Y., Suda, Y. and Kikuchi, T.: Rock Physical Properties of Japan —Density, Magnetism, P-wave Velocity, Porosity, Thermal Conductivity—, 1991 (in Japanese with English abstract)

平成3年11月26日　印刷
平成3年11月30日　発行

通商産業省工業技術院　地質調査所

〒305　茨城県つくば市東1丁目1-3

印刷所　創文印刷工業株式会社

〒116　東京都荒川区西尾久7-12-16

地　調　報　告
Rept. Geol. Surv. Japan
No. 277, 1991